Université Libanaise
École Doctorale
Sciences et Technologies
Doyen

PHD Thesis

Submitted for the degree of

Doctor of Philosophy

Lille University

Lebanese University

Specialty: Civil Engineering

Presented by

ATTOUE Nivine

The 13th of May 2019

Use of Smart Technology for heating energy optimization in buildings: Experimental and numerical developments for indoor temperature forecasting.

Members of Jury

Mr. Hussein Mroueh, Prof., Lille University, France	Director
Mr. Rafic Younes, Prof., Lebanese University, Lebanon	Co-director
Mr. Yacin Fahjan, Prof., Gebze Institute of Technologie, Turkey	Reporter – President
Mrs. Nesserine Ghaddar, Prof., American University of Beirut, Lebanon	Reporter
Mr. Isam Shahrour, Prof., Lille University, France	Member
Mrs. Ariane Abou Chakra, MCF, Insa Toulouse University, France	Member
Mr. Oussama Ibrahim, Prof., Lebanese University, Lebanon	Member
Mrs. Chantale Maatouk, MCF, Saint Joseph University, Lebanon	Member

Acknowledgement

Undertaking this PhD has been a truly life-changing experience, and it would not have been possible to do without the support and guidance that I received from many people.

I would like to express my sincere gratitude to Prof. Isam Shahrour for the continuous support of my PhD study and research, for his patience, motivation, enthusiasm, and immense knowledge.

I would like to acknowledge my supervisors Prof. Hussein Mroueh and Prof. Rafic Younes for their support and encouragement during this thesis.

A very special thanks goes to all jury members: Prof. Yacin Fahjan, Prof. Nesrin Ghaddar, Prof. Oussama Ibrahim, Dr. Ariane Abou Chakra, Dr. Chantale Maatouk and Prof. Fadi Hage Chehadeh for their insightful comments and remarks.

I would like to thank my lab mates and friends for their continued support. Moreover, I am thankful to Dr. Ammar Aljer and Marine Loriot for their collaboration and contribution in the experimental study of this thesis. I am also grateful to Dr. Shaker Zabada and Dr. Ola Hajj Hassan for their valuable guidance.

Thanks, are also due to the AUF (Agence universitaire de la francophonie), CNRS – L. (National council for scientific research in Lebanon) and Lille University for their financial support.

I would like to thank my parents Abed El Hadi and Ghada, my sister Lamise and my brothers Ahmad, Bassem and Ali for their endless support and warm love.

Finally, last but no means least, I would like to express my deepest gratitude to my husband Ali and my baby Mohamad. This dissertation would not have been possible without their warm love, continued patience and endless emotional support.

Abstract

With the highly developing concerns about the future of energy resources, the optimization of energy consumption becomes a must in all sectors. A lot of research was dedicated to buildings regarding that they constitute the highest energy consuming sector mainly because of their heating needs. Technologies have been improved and several methods are proposed for energy consumption optimization. Energy saving procedures can be applied through innovative control and management strategies.

The objective of this thesis is to introduce the smart concept in the building system to reduce the energy consumption, as well as to improve comfort conditions and users' satisfaction. The study aims to develop a model that makes it possible to predict thermal behavior of buildings.
The thesis proposes a methodology based on the selection of pertinent input parameters, after a relevance analysis of a large set of input parameters, for the development of a simplified artificial neural network (ANN) model, used for indoor temperature forecasting. This model can be easily used in the optimal regulation of buildings' energy devices. Results shows that indoor temperature can be well predicted considering only the indoor façade temperature.

The smart domain needs an automated process to understand the buildings' dynamics and to describe its characteristics. Such strategies are well described using reduced thermal models. Thus, the thesis presents a preliminary study for the generation of an automated process to determine short term indoor temperature prediction, heating control and buildings characteristics based on grey-box modeling. This study is based on a methodology capable of finding the most reliable set of data that describes the best the building's dynamics. The study shows that the most performant order for reduced models is governed by the dynamics of the collected data used.
By applying a control approach based on grey box modeling important energy savings were performed.

Keywords: Smart technology; artificial neural network (ANN); indoor temperature; façade temperature; forecasting; sensors; grey-box models; performance; input parameters; control.

Résumé

L'inquiétude croissante concernant le futur des ressources énergétiques a fait de l'optimisation énergétique une priorité dans tous les secteurs. De nombreux sujets de recherche se sont focalisés sur celui du bâtiment étant le principal consommateur d'énergie, en particulier à cause de ses besoins en chauffage. Les technologies se sont évoluées et plusieurs méthodes sont proposées pour l'optimisation de la consommation d'énergie. L'application des stratégies de contrôle et de gestion innovantes peuvent contribuer à des économies d'énergie.

L'objectif de cette thèse est d'introduire le concept intelligent dans les bâtiments pour réduire la consommation d'énergie, ainsi que pour améliorer les conditions de confort et assurer la satisfaction des utilisateurs. L'étude vise à développer un modèle permettant de prédire le comportement thermique des bâtiments.
La thèse propose une méthodologie basée sur la sélection des paramètres d'entrée pertinents, après une analyse de pertinence d'un grand nombre de paramètres d'entrée, pour développer un modèle simplifié de réseau de neurones artificiel (ANN), utilisé pour la prévision de température intérieure. Ce modèle peut être facilement utilisé dans la régulation optimale des dispositifs énergétiques des bâtiments. Les résultats indiquent que la température interne peut être prédite en considérant seulement la température interne de la façade.

Le domaine intelligent nécessite un processus automatisé pour comprendre la dynamique des bâtiments et décrire ses caractéristiques. L'utilisation des modèles thermiques réduits convient pour de telles stratégies. Ainsi, la thèse présente une étude préliminaire pour la génération d'un processus automatisé pour déterminer la prévision de température intérieure à court terme, le contrôle du chauffage et les caractéristiques des bâtiments basées sur la modélisation en boîte grise. Cette étude est basée sur une méthodologie capable de trouver l'ensemble de données le plus fiable qui décrit le mieux la dynamique du bâtiment. L'étude montre que l'ordre le plus performant pour les modèles réduits est régi par la dynamique des données collectées utilisées.
En appliquant une méthode de contrôle basée sur la modélisation en boîte grise, une amélioration de la consommation énergétique a été déduite.

Mots-clés : technologie intelligente ; réseau de neurones artificiels (ANN); température intérieure température de façade; prévision; capteurs; modèles en boîte grise; performance; paramètres d'entrée ; contrôle.

Table of contents

List of figures

List of tables

List of flow charts

Chapter 0: General introduction

In recent years, energy consumption has been receiving huge public and political attention due to a mix of increasing energy prices, the wish of independence from some energy supplying countries, and last but not least alarming reports about the impacts of CO_2 emissions on the global climate. This is while the global energy demand is still increasing - a development expected to continue for years to come due to rapidly growing economies.

In industrialized countries, the building sector is one of the biggest consumers of energy whose needs are constantly increasing due to demographic change and the improvement of living's standards. At present, since the Rio Summit (1992) and the Kyoto Protocol (2005) more attention is being paid to reduce and control energy consumption, which is an economic and environmental necessity. European and particularly French efforts are reflected in the application of various thermal regulations and quality labels. The objective being to play on the building's construction features to reduce energy requirements.

The consumed energy in buildings is affected by several factors such as the insulation, the environment and the heating regulation etc.… In order to reduce this consumption, a better understanding of the building performance as well as regulation methods is needed. Static and dynamical relationships are needed for many important purposes such as control of heating and ventilation with respect to indoor comfort. If reliable models of the heat dynamics of buildings can be obtained, the thermal mass in buildings provides an energy storage that may be used to shift some of the energy demand away from demand at peak hours.

The design of an environmentally friendly building requires mastery and knowledge of energy and bioclimatic aspects. This implies taking into consideration of all the elements that make up the building and the way in which the energy exchange occurs between these elements. These couplings involve a fundamental reflection to allow an optimal functioning of the building, both in winter and in summer. The study of these energy interactions requires the most often well-adapted models.

Hence, the Laboratory of Civil Engineering and Geo-Environment (LGCgE) at Lille 1 University and his partners have undertaken a project of great magnitude, that of to build on the campus of Lille 1 university a demonstrator of the smart and durable city (project SunRise). The work of this thesis constitutes a part of this project.

The aim of this study is to introduce the smart concept in the building system in order to reduce the energy consumption, as well as to improve comfort conditions and users' satisfaction. Using smart technologies (sensors) allows following the indoor and outdoor conditions of the building to understand its thermal behavior. The study is applied on tertiary buildings at the school of engineering 'Polytech'Lille' and at the research building "A4" in France. An advanced monitoring system was installed in many buildings for modeling purpose in order to study buildings' thermal behavior. The objective of the thesis is therefore to develop a model that makes it possible to predict thermal behavior of buildings. The model must be generalizable, and a minimum information should be necessary for its implementation. In addition, it must allow the establishment of energy optimization strategies.

In chapter one, we will present increasing energy consumption of buildings and their environmental impact. We focused on the solutions to achieve low energy buildings concerning building regulations and codes. However, this is not enough to achieve the expected goal in 2020. We noted that, improving building performance required a total understanding of their thermal behavior and thus modeling the thermal dynamic system is needed. Different prevision models are identified within a bibliographic analysis.

Chapter two presents a detailed description of the monitoring system installed in Lille 1 university with a deep analysis of the distribution of the measured indoor and outdoor parameters and general conclusions. A set of experimentation with its analysis is described too. This investigation allows the determination of the major factors influencing the indoor temperature for better forecasting and optimization of the heating energy.

The next chapter introduces a black box methodology 'Artificial Neural Network' and presents a data-based model for indoor and façade temperature forecasting, which could be used for the optimization of energy device use. This study proposed a methodology for the development of a simplified ANN-based model for forecasting indoor temperature.

Chapter four describes another grey box methodology to predict the indoor temperature and building characteristics. It presents a study of the influence of the data's dynamics on the prediction of the indoor temperature. The impact of building's parameters is determined through a sensitivity analysis.

The last chapter presents an empirical on/off control method to minimize the energy consumption. It completes the work of the previous chapter. This study describes the proposed control methodology and analyzes several applications to confirm the effectivity of the control method.

Chapter 1: State of the Art

1.1 Introduction

Energy is the most precious resource among all resources and its demand is rapidly growing. There could be two possible ways to tackle this problem: (1) production of additional energy and exploration of alternate resources and (2) more efficient utilization of existing resources. The first approach is highly expensive, time consuming, and costly, and the second one is inexpensive, more proficient and highly recommended as the efficient utilization of energy avoids the need to produce new energy. Technologies have been improved and several methods are proposed for energy consumption optimization. Energy saving procedures can be applied through innovative control and management strategies. The research issue around the necessity to integrate supply and demand sides has produced important developments, leading to new research purposes based on the system thinking in design and management of buildings. Hence, this thesis concerns the use of the Smart Technology for the optimization of the heating/cooling consumption in buildings.
The use of this technology requires forecasting of the indoor temperature for the regulation of energy devices to ensure occupant comfort, as well as for energy optimization. Thus, the use of models for sustainability assessment of intelligent buildings was a key strategy to quantify the improvement of energy efficiency and occupants' satisfaction. Several models were proposed in this work.
In this chapter we will present the challenges of buildings heating/cooling with some data, proposed models for the optimization of the heating consumption, and smart technology for heating optimization.

1.2 Challenges and motivation

In Europe, the energy consumption increases on average by 1.5% per year, due to the economic development, the expansion of the construction sector and energy services used. With a consumption greater than 40% and more than 20% of CO_2 emissions (figure 1.1), the building sector is in first position before those of industry and transport [1]. Because of this observation and pushed by its membership, the Kyoto Protocol and by the public will, Europe is now moving towards buildings with very low energy consumption. In France, the French Environment and Energy Management Agency (ADEME) estimated that the building was also the largest consumer of energy in 2015 with 45% of total energy consumed and 25% of Greenhouse Gas emissions (GHG) [2]. In 2015, the Observation and Statistics Service (SOeS), which is part of the General Commission for Sustainable Development always attributed more than 45% energy consumption in the building sector (Figure 1.2) and in contrast to other industrial sectors, emissions from the residential /tertiary sectors and transport continues to grow.

During the last thirty years, despite the drop of more than a third of the consumption per square meter, consumption increased by almost a quarter [3]. This consumption is based essentially on fossil fuels. Existing buildings account for half of the energy consumption of this sector.

Following the Rio Earth Summit in 1992 and the Kyoto Protocol in 1997, France became committed in 2002 to respect the directives of the European Union "Energy Efficiency" with the goal of reducing greenhouse gas emissions. The Climate Plan was launched in 2004, which consists of setting short- and medium-term goals:

- Divide by four greenhouse gas emissions by 2050;
- Increase the production of thermal renewable energy by 50% by 2015;
- Increase the production of renewable electricity by 25% by 2015.

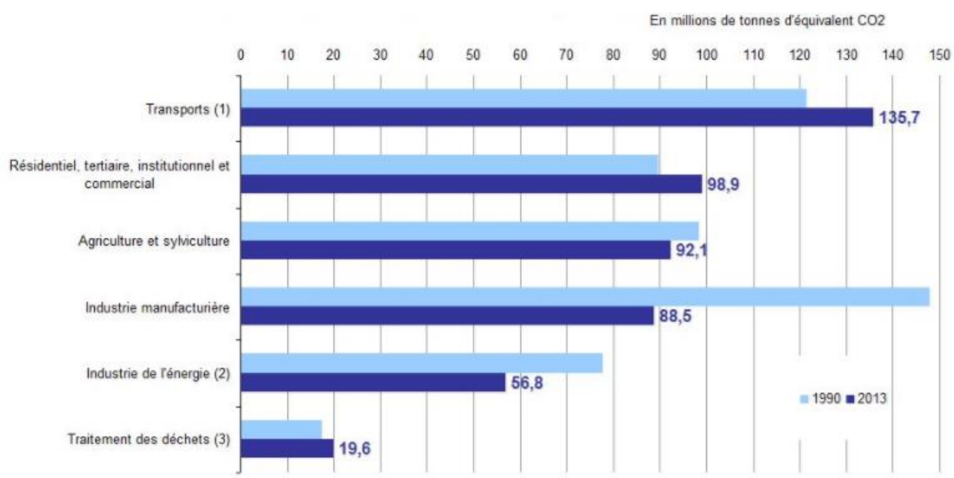

Figure 1.1: CO_2 emission in France per sector. [2]

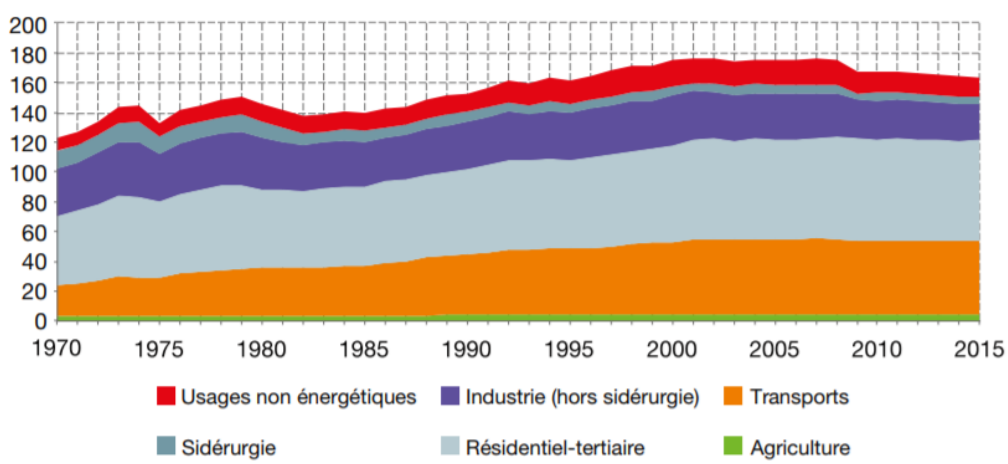

Figure 1.2: Final energy consumption per sector. [2]

Faced with this challenge, the Grenelle Environment Forum set objectives to create favorable conditions to the emergence of a new French deal in favor of the ecology and sustainable development [4]. The High Environmental Quality (HQE) approach was created to meet these objectives and to respect the regulations in the building sector.

Following the perspective of 2004 Climate Plan, a passage from the regulation thermal 2000 to 2005 was carried out. RT2005 is applied to all building permits since September 1, 2006 in the residential and tertiary sectors. It strengthens 15% the energy performance requirements of new buildings compared to the RT2000 [4]. To ensure this continuity in improving energy performance, RT2012 has seen then the day. This regulation must be applied to the new residential buildings from the end of 2012 and tertiary buildings from the end of 2010. It increases the level of regulatory requirements to consume less than 50 kWh / m² / year in primary energy (figure 3).

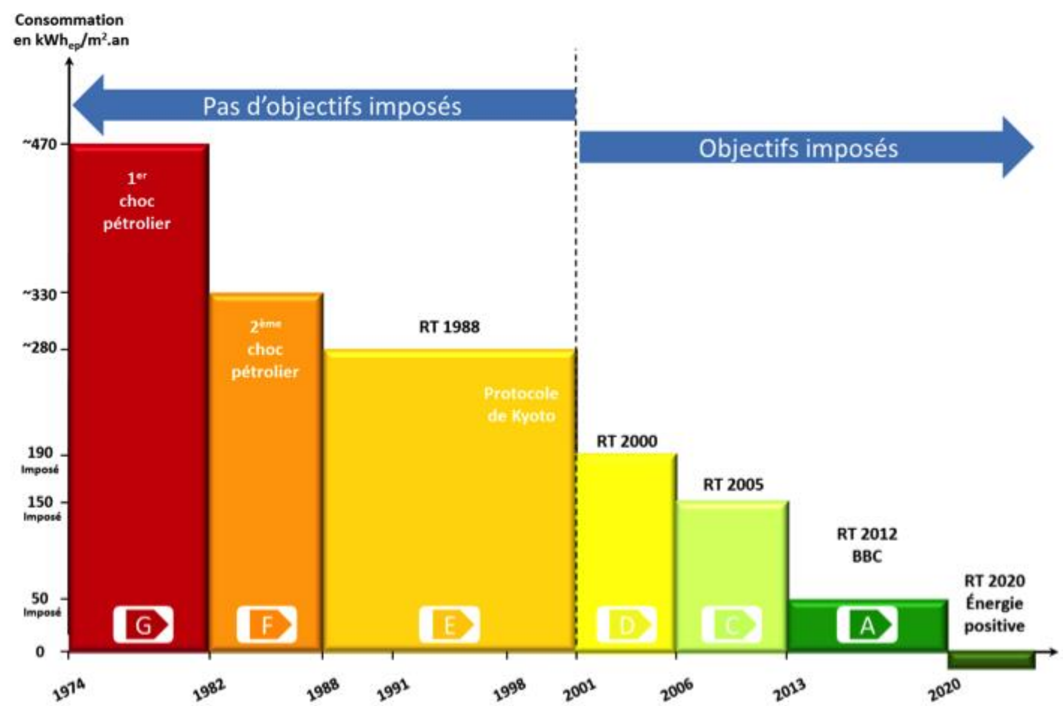

Figure 1.3: Evolution of energy consumption according to several French regulations. [http://www.cfbp.fr/gpl-maitrise-de-l-energie/reglementation-thermique-n261]

Building conception is a principal factor that affects the energy consumption and the comfort in the building. In the European context, this is one of the most important challenges to be worked out. Many facilities were put in action with tools to ameliorate the building energy behavior from the conception phase as mentioned before. However, this is not enough since the rehabilitation of the existing mass of buildings can be very expensive with a very long investment cycle. Moreover, there are other factors that can affect this behavior such as the technical as well as economical and regulatory issues to be integrated.

Heating and cooling loads represent the largest consumption (more than 60% of total consumption) (figure 1.4) [5] for the building sector. Better management of climatization (heating and cooling) consumption becomes an emergency, especially in a rapidly evolving economy and increased awareness of environmental constraints. Understanding the building heating/ cooling system is challenging as well. The type of the heating/cooling system and its design affects enormously the energy consumption. Buildings with central systems consume totally differently from those with individual systems. The same thing applies for the nature of the heating/cooling system (gas, electricity....). Furthermore, the regulation and planning of the climatization system is highly important and can affect the energy consumption (use of building inertia, occupation planning, sun, energy pricing…).

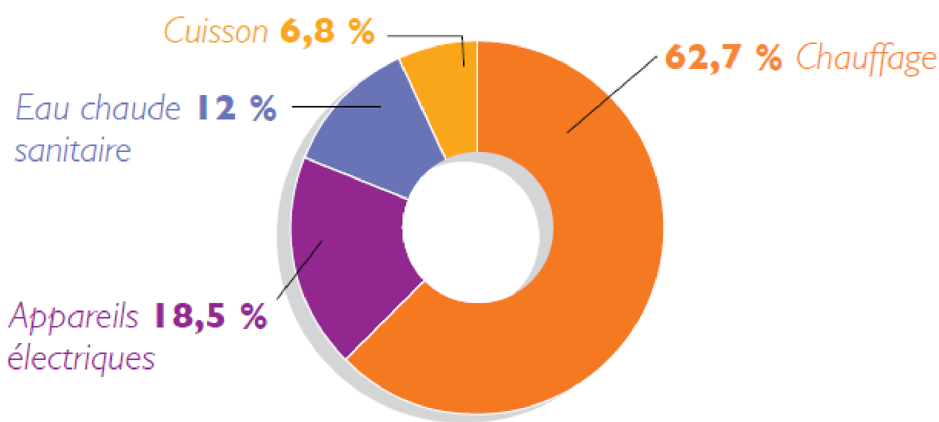

Source : CEREN, Les chiffres du bâtiment, 2011, ADEME

Figure 1.4: Distribution of building energy consumption in France.

Concretely, it would be a question of choosing a facility well adapted to the needs (management demand for energy) and to ensure that the building is properly insulated, whether existing or under construction. A good knowledge of the thermal behavior of the building (residential, tertiary, industrial) helps to improve the management of the energy demand of heating/cooling system. The marketer uses this information to propose energy service offers such as building diagnosis and recommendations for improving the structure of the building, or replacement of the electric heating system. For the customer, a better knowledge of the behavior of his building is necessary to modify his energetic behavior, to reduce its bill or to improve its comfort.

Achieving the energy performance levels already mentioned requires a special attention to the "elements" constituting the building: reducing thermal losses through the envelope, minimizing thermal bridges, choosing a system of ventilation that limits heat loss through air exchange, using phase change, etc. Achieving energy savings is also substituting conventional energy equipment system and strategies with smart ones. Therefore, promoting low-energy buildings requires integration of smart technologies to improve their performance.

1.3 Buildings' models

As one of the ways to enhance building energy performance, thermal analyses of building systems should be carried out. The building system includes envelopes of a building and its inner sub-systems, such as HVAC and electrical equipment.

For obtaining a complete understanding of thermal behavior of a building system, the characteristics of the following components must be known:

- Outdoor conditions : orientation, location, climate, etc.
- Physical properties: structure, materials, thermal capacitance, thermal resistance, etc.
- Energy efficiency of inner sub-systems: HVAC, lighting, electrical appliances, renewable energy source installation, etc.
- Occupancy
- Geometry of building
- Window to wall ratio

Figure 1.5: Dynamic interaction of building's components.

These characteristics are dynamically interacting with each other (Figure 1.5). It requires a more detailed study of the above characteristics of the building system to assess its energy performance [6]. In order to obtain a more accurate data, each component of the building system has to be rigorously studied. Furthermore, since the thermal characteristics of the building system are closely related to the energy consumption, thermal modeling of each component of the building system is the most important task to do for analyzing the building energy performance.

Interest in the building as a system that interacts dynamically with a set of climatic data and conditioned by the behavior of the occupant (heat input due to the presence of people, domestic appliances, heating management, etc.) is relatively new. Indeed, the first studies go back to the end of the years 70 and faced three major difficulties:

- Lack of detailed information on the constitution of the building.
- Uncertainty about occupant use and behavior.
- Limited capacities of the means of calculation and experimentation of the building.

Two approaches were adopted to model the building. The first was about a simplified modeling to overcome the limitations of the calculation. The proposed models are of a reduced order and the parameters are derived from on-site surveys (electrical power, indoor temperature, etc.). The second was interested in understanding the heat exchange phenomena in the building for simulation purposes. Existing models can be classified into two families according to the adopted approach, a static approach and a dynamic approach. The choice of the method is essentially related to the simplicity of the adopted model and the time interval chosen.

1.3.1 Static models

Static models are dedicated to the modeling of the steady state of the building (the interior temperature is equal to the set point at every moment and the demands are constant in time). This regime results in a thermal balance, ensured at every moment, between foreign exchange (mainly weather) and domestic (heating input parameters) of the envelope of the building. As a result, the static models are designed to express the heating load as a function of the external stresses (for example outside temperature, sunshine, etc.) according to the heat balance equation [7]:

$$Q = U\,(T_{ind} - T_{out}) - SI + \varepsilon \tag{1.1}$$

where:

- Q is the energy needed to maintain the set temperature;
- T_{ind} is the average indoor temperature in the building (°C);
- T_{out} is the average outdoor temperature (°C);
- U is the coefficient of the global static losses (W/°C);
- S is the equivalent south surface (m^2);
- I is the global south vertical radiation (W/m^2);
- ε is a factor that depending on the start and end time of the observation period and it is weighted by the inverse of the measurement time step (W).

The difference between the proposed models is related to the choice of the number and the assumptions made on the excitations of the studied system. Equation 1.1 can be adapted according to the precision needed and the data available. The term ε can be further developed by taking into consideration more gains to have better precision of calculations. It can be as well further simplified by ignoring ε and even the sun radiation and calculating the heat load as a function of the temperature difference between indoor and outdoor.

The most famous application of this concept is the energetic signature (figure 1.6). This method has been designed to analyze heating consumption in the absence of detailed measurements of thermal magnitudes of the building. Here, the goal is to express the heating/cooling load according to the outside temperature. Equation 1.1 can then be simplified in equation 1.2 called building signature.

$$Q = \alpha + \beta T_{out} \tag{1.2}$$

The coefficients α and β can be calculated by linear regression using some registered measures of the studied building.

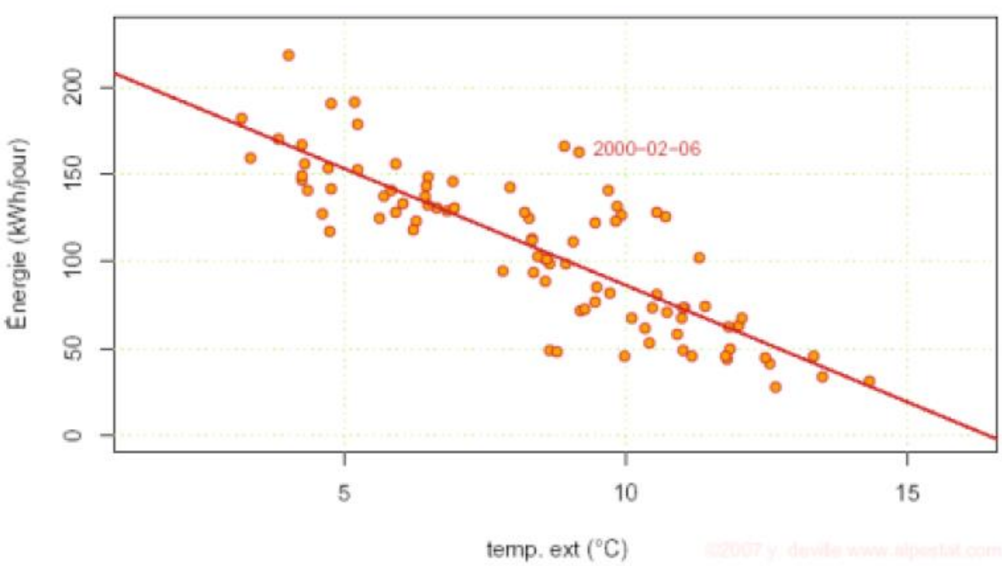

Figure 1.6: Example of building energy signature.

It can also be interesting to compare buildings in different climatic zones or to evaluate their heating/cooling needs not for a given outside temperature but according to the severity of the climate using the Degree Day concept (DJ). For a given location, the Degree Day is a value representative of the gap between the temperature of a given day and a pre-established temperature threshold (18 or 19°C per example). It is typically used to estimate energy consumption for heating or cooling [9].

These static models are simple. They offer the possibility of having a first characterization of the building (for the diagnosis for example) through the estimation of its static gain. But they present the three following limitations:

- they require a relatively long observation period
- they do not consider the transient behavior of the building
- These models do not make it possible to account for the regulation of heating/cooling.

From where appeared the necessity of dynamic thermal models.

1.3.2 Dynamic models

The transient-state method, called "dynamic" analysis, requires various information and computational calculations in order to provide more detailed and accurate results. This method treats dynamic thermal behavior of building systems, including steady and transient-states. It allows the analysis of temporal and spatial performances within building systems. For example, the gradient of temperature and the diffusion of heat flux inside the building can be described by this method. Furthermore, it is possible to analyze the whole building system that contains the building envelopes and its sub-systems.

Given the multitude of methodologies, it is interesting to perform a classification to determine the degree of precision and adaptation of each method. This classification will not be perfect, as the boundary between two levels of modeling is usually not well marked. We will group them into three approaches white box, black box and grey box (figure 1.7).

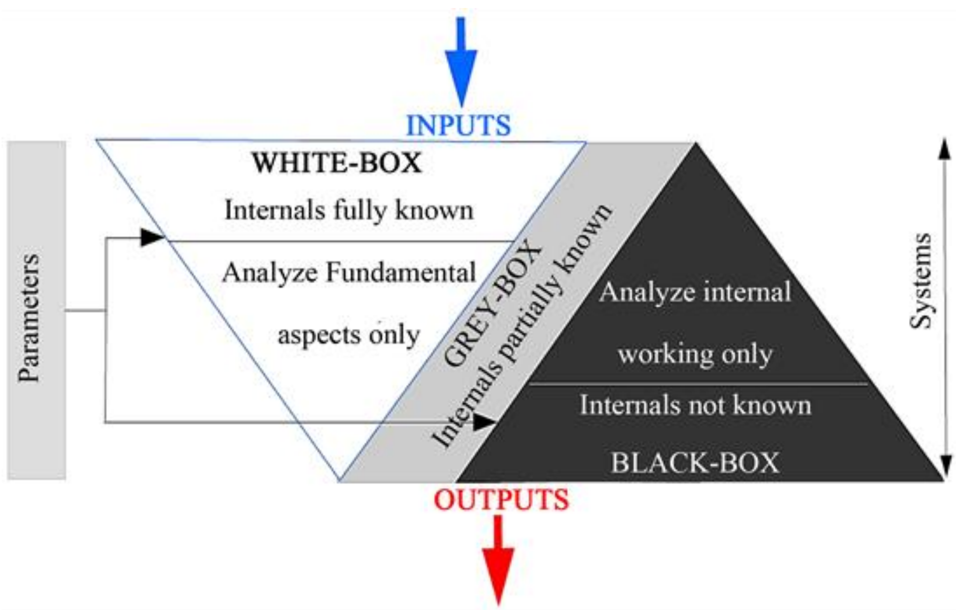

Figure 2.7: Different methodologies for dynamic modeling.

1.3.2.1 White box approach

The complete modeling of a building ("white box") allows to predict its thermal needs. This requires a precise knowledge of the composition of walls and measurements [10], which is not always easily accessible. In addition, it is often necessary to group the parts in homogeneous thermal zones, which makes it necessary to take strong assumptions and to have good knowledge of the thermal behavior of the building. Even with such a precise model of the building, the simulated thermal requirements are distance from reality, which makes it necessary to calibrate certain buildings' parameters to better represent the reality [11]. Once the "white box" model of the building is completed, it is possible to predict the thermal needs of the building by simulation. Moreover, the model will have the possibility to predict the input parameters such as climate data (temperature, sunshine) and occupation profiles. Three main thermal building models are currently used [12]:

- CFD 'Computational fluid dynamics': Microscopic approach of the thermal transfer model detailing the flow field. It is based on the decomposition of buildings' zone in many control volumes with global mesh.

- Zonal approach: First degree of simplification of the CFD technique. It consists in dividing each building zone into several cells. One cell corresponds to a small part of a room.

- Multizone or nodal approach: Considers each building zone as a homogeneous volume characterized by uniform state variables approximated to a node that is described by a unique temperature, pressure, concentration, etc.

Even in the most complete models, some phenomena are neglected (for example, the variation in air infiltration rate as a function of external and internal pressures) which can create a bias in load forecasts. Another negative point of the "white box" models is the calculation time. We know that it will be necessary to execute several hundred simulations for the implementation of optimization strategies and this represents an important calculation cost.

Physical modeling of the "white box" type is not retained as a solution adapted to the issue of load forecasting and optimization of air conditioning, because it is not generalizable (deployment to many buildings in a short time) and has too important cost of calculation [13, 14]. This method has been applied to several building energy simulation tools, such as DOE-2 [15], HVACSIM+ [16], TRNSYS [17], BLAST [18], and EnergyPlus [19].

1.3.2.2 Black Box approach

Internal operation of the building is not described. This type of model simply allows a numerical resolution of the problem without providing a physical interpretation. The method of resolution is based on empirical relationships that link the input and output parameters (figure 1.8). These relationships are the result of a regression analysis that requires experimental measurements. In addition, this approach procures a very simple model and accurate results in a reduced calculation time.

From existing literature on prediction model where data-driven modelling techniques have been used, it is evident that nonlinear models are more effective than linear models for prediction [20-22].

Figure 3.8: Representation of the black-Box modeling.

The simplest building model is linear regression as a function of the outdoor temperature. This static modeling works mainly in heating and on old buildings (few windows, poorly insulated and without temperature reduction). Since the first thermal regulation (RT 88 for non-residential) and following numerous energy savings (Grenelle I & II, Law n ° 2010-788), this case tends to disappear. Rabl [23] shows, on a case study (air-conditioned shopping center), that adding a variable occupancy (in addition to the outside temperature) significantly increases the accuracy of the model. He is one of the first authors to use multiple linear regression to predict the consumption of a building. MISO linear regression models (Multi Input Single Output) are available in several formulations [24]:

- ARX model 'Autoregressive with exogenous input' where noise is directly coupled to the dynamics of the model. It is efficient if the noise ratio on signal is weak.

$$Ay = Bu + e \qquad (1.3)$$

- OE 'Output error' allows an independent modeling of the dynamic and noise.

$$Ay = \frac{B}{F}u + e \qquad (1.4)$$

- ARMAX 'Autoregressive moving average with exogenous input', where the dynamics of the model and the noise are coupled, but they may be different for each entry.

$$Ay = Bu + Ce \qquad (1.5)$$

- BJ or ARIMA 'Box-Jenkins' or 'Autoregressive integrated moving average'. Very flexible model, it allows to set independently the dynamics and the noise, whether at input or output.

$$Ay = \frac{B}{F}u + \frac{C}{D}e \qquad (1.6)$$

Where y and u are respectively the model output and input, e represents the white noise that consider the unmeasured disturbances in the studied system and A, B, C, D and F are matrices to identify in the learning phase.

Different data-driven non-linear modelling techniques were used by many authors [25-28]. We can mention:

- ANN 'Artificial Neural Network': Learning technique inspired by the biological neurons used as an approximation tool of the complex relationships between models' input and output.

- SVM 'Support Vector Machines' techniques developed on the concept of decision hyperplanes (nonlinear function). The derived concept is based on finding the largest deviation from the obtained target.

- RF 'Random Forest': An ensemble learning methodology where the performance of several weak learners is boosted via a voting scheme.

- GA 'Genetic algorithm': Optimization technique deduced from an analogy with the evolution theory of Darwin. It is based on the faculty of a given species to adapt itself to a natural environment and to survive extreme conditions.

Each of these statistical techniques has his own advantages and drawbacks and the choice of the method depends mainly on the user and on what he expects at the end of the study.

Black box models 'data-driven approach' have shown their limitations as to the need for measurements which require significant resources. Moreover, the optimization study is not based on a physical understanding of the phenomena.

1.3.2.3 Grey Box approach

Located midway between the black box models and the white box models, the grey box models combine the physical sense and the spirit of simple patterns. The principle of "grey box" modeling is to use a simplified physical representation of the studied system and identify models' parameters to minimize errors of forecast. Buildings can be modeled by simple dynamic differential equations representing the phenomena of conduction, convection and capacitive phenomena. These equations have been widely studied in the literature, notably by Laret and Roux [29-30].

Indeed, this approach requires computing resources less heavy than those required by white box models and have better flexibility. Its main advantages revolve around the following points:

- Compactness and simplicity of construction of the model given the reduced number of settings;
- More practical sensitivity analysis;
- Better flexibility that makes it easy to manipulate the model;
- Minimization of parameters' number while keeping an important level of precision.

Several applications are available for this hybrid approach. A first strategy consists in using machine learning techniques (black box) as physical parameters estimator. A second application is to implement a learning model using statistics to describe the building behavior. This learning model is built from a physical approach. A third strategy consists in using statistical method in fields where physical models are not effective and accurate enough. (end uses consideration, heat behavior in multiple zones...)

From the mid-1980s, the thermal network method, based on the grey box approach, using the thermal-electrical analogy has been used in order to simplify the building modeling. The thermal network method is based on the energy balance equation. The heat transfer phenomena of building systems are described by their corresponding electrical components. The supplementary heat gain/loss due to solar radiation, metabolic heat of occupants, infiltration/ventilation, and electrical equipment and appliances can be expressed by current sources. It permits the analysis of thermal behavior of building systems during steady and transient-states. Briefly, the thermal models of building systems are represented by electrical circuits, including electrical components and electrical sources. The thermal dynamics of the building systems are analyzed in accordance with the electrical dynamics of the corresponding electric circuits (table 1.1). The choice of the number of resistances and capacities depends on the available data and priorities of modeling process. There are several possible choices according to the use. In the bibliography, models with the forms (RC, R2C2, R3C2, R4C2, ...etc.) were found [31-32].

Some drawbacks own to each technique (white and black box) remain in the hybrid method as the free parameters for statistical tool or the computation time needing for both physical or statistical codes.

Table 1.1: Representation of building thermal factors in an electrical circuit.

In the building	In the circuit
Heat flow	Electric current
Supplied heat flow	Current Generator
Thermal conductance	Electrical conductance
Set temperature	Tension generator
Thermal capacity	Electrical Condenser

1.4 Smart technologies

Buildings can save energy by using advanced sensors and automated controls in HVAC, plug loads, lighting, and window shading technologies, as well as advanced building automation and data analytics. Buildings that have advanced controls and sensors along with automation, communication, and analytic capabilities are known as smart buildings. In a fully-fledged smart building, the building systems are interconnected using information communications technologies (ICT) to communicate and share information about their operations. Smart building technologies can provide facilities operators with the tools to anticipate and proactively respond to maintenance, comfort, and energy performance issues, resulting in better equipment maintenance, higher occupant satisfaction, and reduced energy consumption and costs.

Smart buildings include efficient technologies with automated controls, networked sensors and meters, advanced building automation, data analytics software, energy management and information systems. In the following, we will mention these key building systems and technologies and we will discuss the smart technologies of HVAC systems.

Systems that can use smart technologies in buildings are: HVAC systems, plug loads, Lighting, Window shading, Automated system optimization, Human operation and Connected distributed generation and power. Figure 1.9 gives an overview of these interconnected systems.

1.4.1 HVAC systems

It takes an enormous amount of energy to condition air and then distribute it throughout a building. Using controls to properly manage HVAC operation is an essential part of saving energy in a building. However, building operators frequently manage HVAC operations through trial-and-error adjustments in reaction to occupant comfort feedback—sometimes relegating energy savings to a much lower priority.
Smart HVAC systems have the potential to greatly reduce energy consumption while maintaining or even improving occupant comfort. Smart building software interprets information from a variety of HVAC sensor points and maintains that information in real time, in a cloud-based system that

is remotely accessible. Engineers develop algorithms within the smart building software that use the database information to optimize the monitoring and control of HVAC systems. These advanced controls can limit HVAC consumption in unoccupied building zones, detect and diagnose faults, and reduce HVAC usage during times of peak energy demand.

One of the largest energy efficiency benefits of smart building HVAC controls is found through optimizing the amount of conditioned (i.e., heated or cooled) air supplied throughout a building. Although it may seem like a simple concept, this goal can be achieved in several ways. Smart controls can optimize airflow using data provided by occupancy, temperature, humidity, duct static pressure, and air quality sensors.

Smart HVAC systems can also support sophisticated data analysis. Armed with smart building data analytics, building operators can review historical building occupancy and usage on a granular level, receive performance data in real time and fine-tune the HVAC controls, accordingly, thereby avoiding wasted HVAC usage.

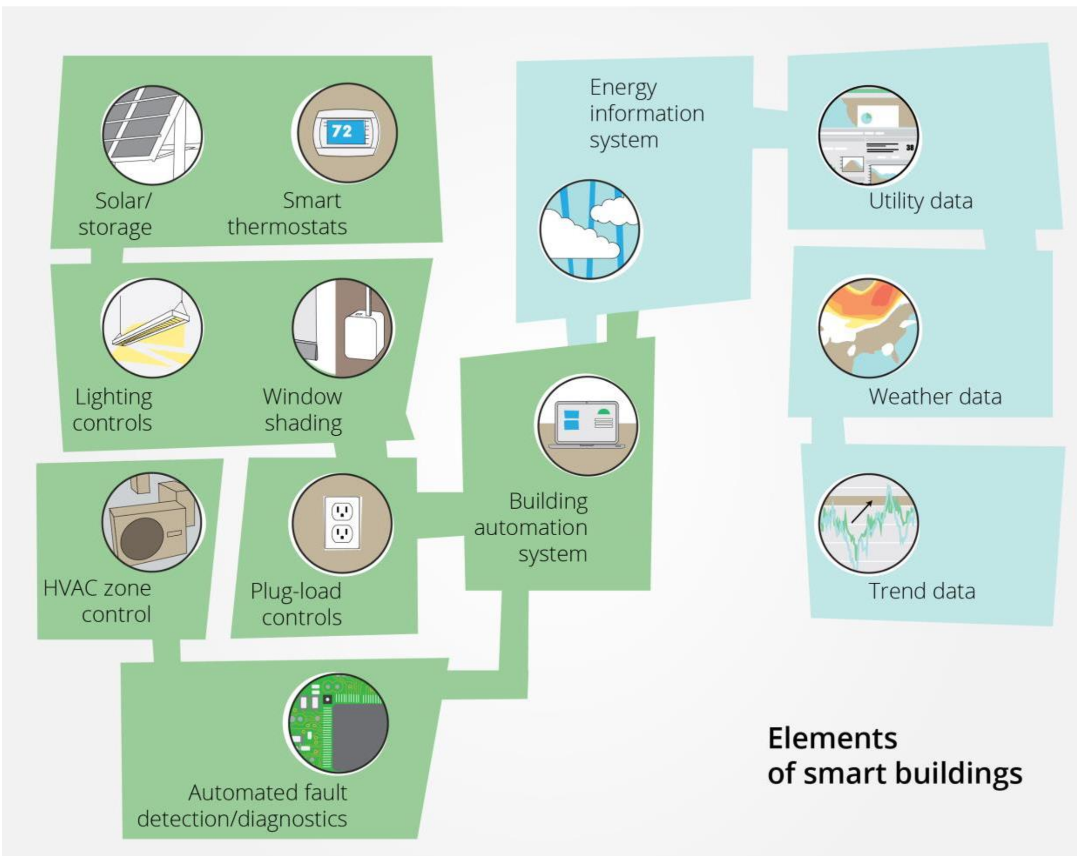

Figure 4.9: Overview of smart building technologies.

1.5 Conclusion

This chapter included a state-of-the-art synthesis on the problematic related to buildings energy consumption reduction with a particular focus on models used for the building thermal modelling. Analysis showed that this issue is very complex and still requires effort to build models which could be easily used by professional.

The recent development in smart technology offers new opportunity to collect comprehensive data about the building environment and use. These data could be used to build data-based models, which could be easily calibrated and used in indoor temperature forecasting, which constitutes a major step in the optimal thermal management of buildings.

In the following chapters we will present the use of this method for the development of two classes of models: Artificial Neural Network model and Grey models.

Chapter 2: Experimental developments

Introduction

In this chapter, an intensive and advanced monitoring system will be presented. It was designed to follow the indoor and outdoor conditions of a building. Experimentation were executed at Lille 1 university in the North of France. Monitoring system was installed in three locations at the university campus: an occupied office at the first floor of the school of engineering ‘Polytech’Lille’, four unoccupied classrooms at the fourth floor of the same building and a research building ‘A4’.

Furthermore, the chapter presents a preliminary study for each experimentation. It includes a homogeneity investigation of the indoor parameters in order to understand their distribution. Several experimental scenarios were performed to explore the importance of some parameters on the energy consumption. This preliminary analysis is indispensable for the numerical modeling presented in the next chapters. It indicates major parameters that should be considered for heating energy optimization.

Flow chart 2.1 presents the planned monitoring of different spaces and its objective.

2.1 Instrumentation system

2.1.1 Design

A new monitoring system was designed to study the temperature and relative humidity distributions. Before the design and construction of the system, the determination of its specification was established. This study is a part of the ‘sunrise project’ whose goal was to transform Lille1 university campus into a demonstrator of a smart and durable city. The building monitoring required the design of an innovative monitoring system to follow fluids consumption (water and energy), comfort conditions (temperature, humidity, air quality, lightening, noise) and state of windows and doors (open/closed). The system stores data and allow analysis of historical data. It includes a friendly graphic interface and guarantee tenants’ or researchers’ privacy. The system should also be robust, based on wireless low energy consumption technology and low-cost.

The new system is composed of a central unit, wireless sensors and friendly users’ interface (figure 2.1).

The central unit with a free and open software communicates with sensors using radio frequency (RF) protocol ensuring the management of the monitoring system. It is formed of a small computer without screen or keyboard, a ‘Raspberry Pi’, which hosts the free and open source Linux operating system for data storage, analysis and display (figure 2.2). A local Wi-Fi network is created by this unit enabling access to stored data and information.

Flow chart 2.1: Different monitored spaces and its objectives.

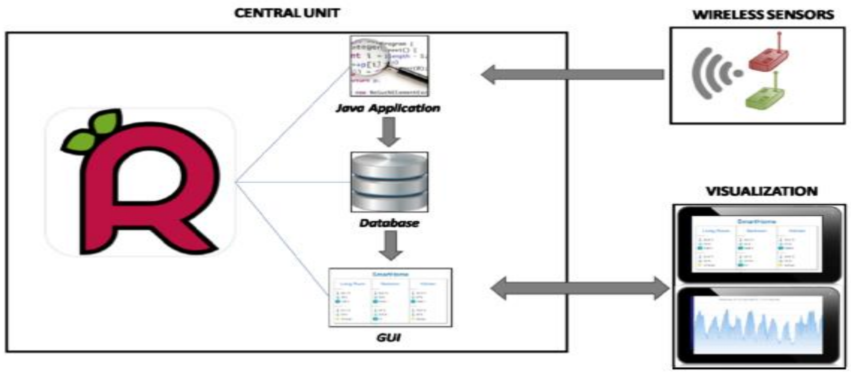

Figure 2.1: Architecture of the monitoring system.

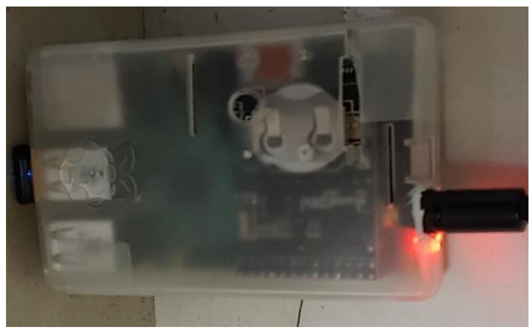

Figure 2.2: Central unit.

Several parameters were tracked at a chosen time interval using the wireless sensors that are connected to the central unit. The main function of these sensors is the pursuit of indoor comfort parameters (temperature, relative humidity and lighting) and the control of doors/windows (open or closed). These parameters are monitored in a multi-parameters smart card and sent using a communication system. Sensors used in our experimentation are associated with PanStamp and Inodesign programmable modules.

A web friendly interface was designed to enable users to access easily to all the information concerning the indoor environment [33].

2.1.2 Sensors

All the sensors, associated with a PanStamp, are programmable low-power wireless board (module), especially conceived for Internet of Things applications, with an Atmega328p micro-controller and a CC1100 RF transceiver. It consumes only 1 µA in sleep mode and 2.5 mA in transmitting mode. It could be programmed with the Arduino Environment. Izar Pulse I, magnetic contact and current transformer sensors are associated with a PanStamp Battery-Board, which includes a card with the Panstamp wireless module, powered by an AA battery. It provides analog and numeric input to get sensors signal and to transmit it with RF to the central unit. Temperature and relative humidity are measured using SI7021 sensors. The temperature is measured in the temperature interval -10 to 85°C with max 0.4°C precision, while the relative humidity is measured in the interval 0 to 80% with max 3% precision.

Other sensors, associated with Inodesign programs, are formed of SX1211 single-chip transceiver operating in the frequency ranges from 863-870, 902-928 MHz and 950-960 MHz (figure 2.3). The SX1211 is optimized for very low power consumption (3mA in receiver mode). Its highly integrated architecture allows for minimum external component count while maintaining design flexibility. All major RF communication parameters are programmable and most of them may be dynamically set [34]. Temperature and relative humidity are measured using SI7020 sensors. The temperature is measured in the temperature interval -10 to 85°C with max 0.4°C precision, while the relative humidity is measured in the interval 0 to 80% with max 4% precision.

Figure 2.3: Inodesign sensor.

2.1.3 Communication protocol

The PanStamp Wireless module uses the open-source Simple Wireless Abstract Protocol (SWAP). It can use the 868MHz free Industrial, Scientific and Medical (ISM) frequency bands. It works within an open area of around 200 meters distance.
Incoming SWAP packets are listened and parsed by the SWAP software stack. It ensures their transmitting or responding to their queries or command, management of registers, sending updated data and managing power.
For each sensor, the SWAP unit with a unique identifier stores the configuration parameters and data as a register. The frequency at which each register is updated and sent with RF can be chosen or the update is triggered by event. Different sensors data can be included in one register as its size can reach 55 bytes.
The addresses of the destination and source devices hop counter, security options, security nonce, function of the packet, address and identifier of the register and finally the register value which is the payload are included in the SWAP frame. The Raspberry Pi is equipped with a PanStamp wireless board to follow the incoming SWAP packets.

2.1.4 Visualization

The central unit contains an Apache web server, which permits users to access via a friendly web interface to real-time and historical data using graphic interface (Figure 2.4).

The web interface is implemented in HTML, CSS and JavaScript with Bootstrap and High charts libraries to allow the design of interactive charts. PHP is used to communicate with the database to get the sensors' values.
The web server is accessible via a local Wi-Fi network using smartphones, tablets and Smart TV.

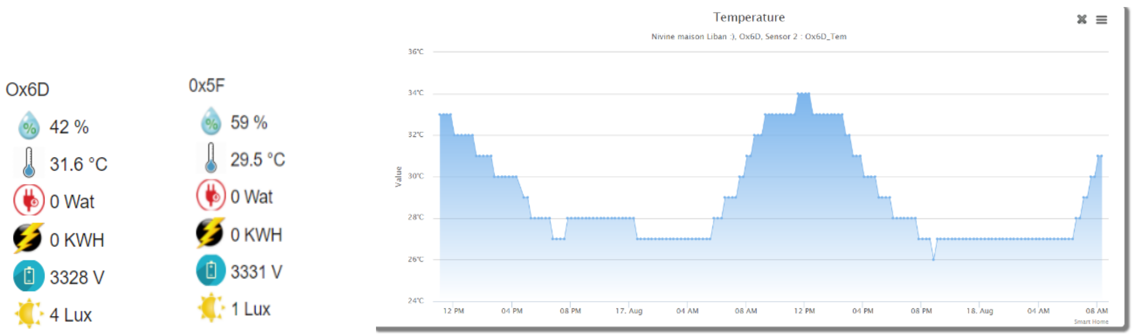

Figure 2.4: Example of user's interface.

2.2 Study of the occupied office

2.2.1 Experimental Setup

The study is conducted on an occupied office room in building D at the first floor of the school of engineering Polytech'Lille in the North of France (figure 2.5). Two-month measurement series were recorded with intensive monitoring of both temperature and relative humidity. Experimentation was executed from May 2017 to July 2017. Heating system was off for this period.

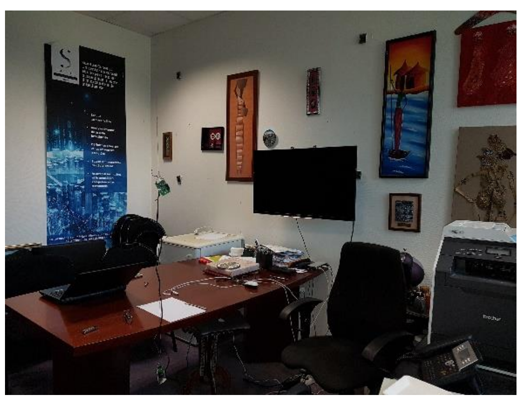
Figure 2.5: Experimented office – First floor.

At first, around 90 sensors were installed to follow the thermal conditions inside the room. Some were placed at the same location to explore the reliability of the monitoring system, others were installed at the three walls, facade, at the center (air) and outside (exterior parameters). The facade is formed of well insulated, two double glazing windows. The left wall, adjacent to the facade, was equipped by three levels of sensors (top, middle and bottom) and by three other spots, for each level, each one with a certain distance from the facade (nine sensors at this wall in total). The sensors at top level were installed at 238cm height from the ground, others at the middle were at

144cm height from the ground and the last level was at 50cm from the ground. For the horizontal distance from the facade, the first sport (1) was at 512cm, the other one (2) at 300cm, and the last one (3) at 87cm. Figure 2.6 illustrates this monitoring system.

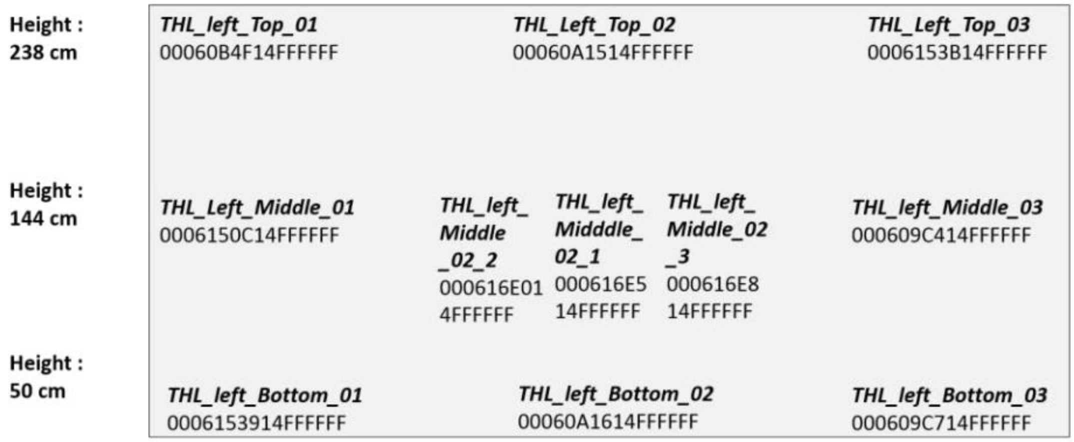

Figure 2.6: Monitoring plan for the left wall.

After one month of monitoring, a database was built with a time series measurement having an interval of five minutes. Analyzing these preliminary data allowed us to follow indoor parameter distribution in order to understand the building thermal behavior.

2.2.2 Homogeneity of indoor parameters

2.2.2.1 Bibliographic analysis

The temperature and humidity distribution are two important indexes often used to evaluate the indoor environmental conditions and to assess the human thermal comfort or building management [35]. Many studies discussing this topic.

Some experimental studies have been conducted to investigate the air flow field, temperature distribution and uniformity, and the thermal comfort problems inside the finite room. For thermal comfort improvements and energy savings, Zhang et al. [36] studied the air flow and temperature fields inside a passenger compartment. Zingano [37] evaluated, by experimental studies, the importance of the humidity to thermal comfort temperatures.

Manzan and Saro [38] performed numerical simulations of flow field, temperature field and distribution of water vapor within the duct for thermal performance evaluation purposes. Chow and Holdo [39] carried out further study of accurate thermal boundary conditions on the simulation accuracy of the air field inside an indoor room. Thermal re-distribution by surface heat radiation was determined.

By both experimental method and simulation, Ding et al. [40] examined the flow fields, temperature field and uniformity inside a chamber of two kinds of refrigerators. Antonio et al. [41]

measured the temperature values in a commercial household and compared the measurement results with that from two different simulation methods.

Other authors have studied the relations between temperature and humidity under certain conditions. Liu et al. [42] investigated the heat and moisture transfer between the free water surface and surrounding air by experimental tests and CFD simulation. Sureshkumar et al. [43, 44] evaluated, through experimental and simulation studies, heat and mass transfer processes between a water spray and ambient air under different conditions.

Traditionally, indoor air environments are considered uniform, and therefore, in several energy programs the modeling phase entails the subdivision of the building into zones in which the temperature can be considered uniform [45, 46]. Usually rooms and thermal zones coincide but in some cases one room must be subdivided into more than one thermal zone. However, there are few studies focusing on the investigation of humidity and temperature heterogeneity in indoor environments. The indoor temperature and humidity monitoring constitute an important procedure to study room parameters distribution. Indoor temperature and humidity differ within a room at a given instant. Nevertheless, several monitoring studies adopt one single sensor to record the room temperature or humidity [47], meaning that indoor parameters have been considered homogenous. The research should define the precision level required, prior monitoring process, to study indoor thermal uniformity. A standard methodology for monitoring cannot be found in the scientific literature, therefore, the sensors' number and positions and the recording frequency is often omitted since based on empirical approaches.

Thus, this chapter aims to study the distribution of indoor parameters (temperature and humidity) within one room through an advanced monitoring. The number and position of installed sensors enable the determination of parameters non-uniformity and maximize the accuracy of the monitoring system. The study will be done on the occupied office.

2.2.2.2 Sensors' reliability

At first, the reliability of the monitoring system was checked by the comparison of data recorded by sensors located at the same position. These tests showed that the recorded data are very closed (Figure 2.7). The maximum temperature difference (0.2°C) between sensors do not exceed the precision range of 0.4°C (Figure 2.8). Similar for relative humidity difference, the maximum (1%) do not exceed sensors' precision range (3%). These results confirmed the reliability of the monitoring system. Analyses were then conducted to study the variation of the temperature and relative humidity in the room in normal operating conditions.

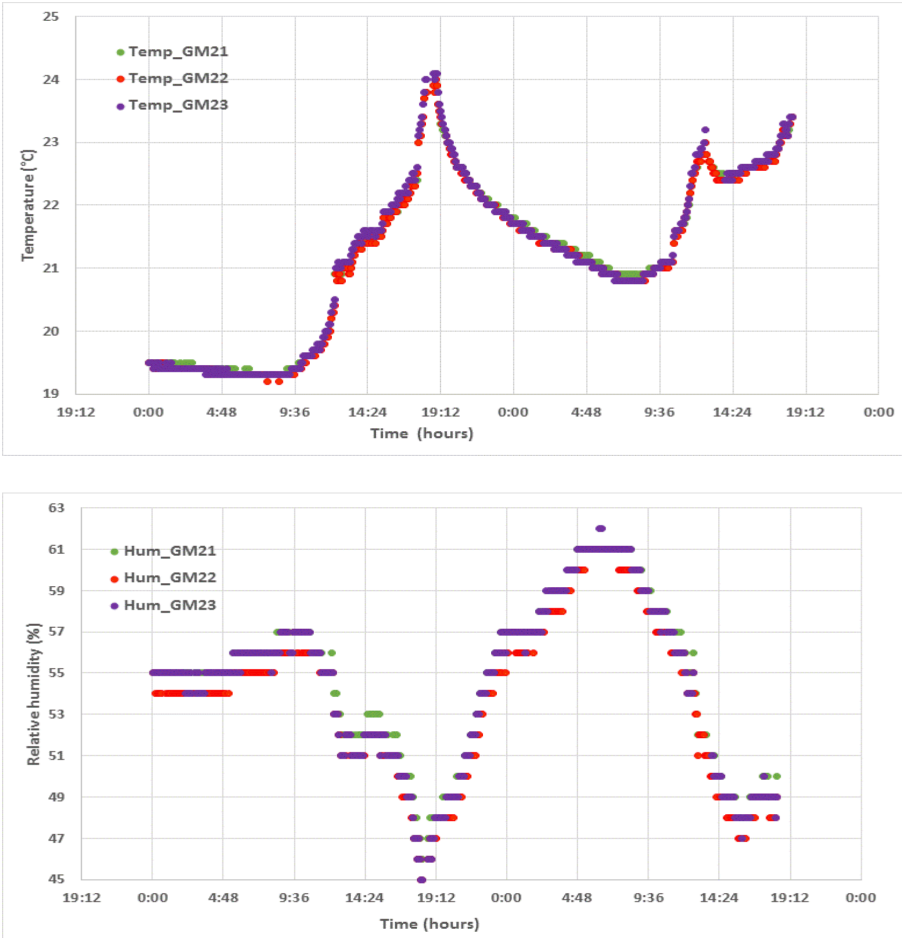

Figure 2.7: Recorded data by the sensors located at the same position on the left wall.

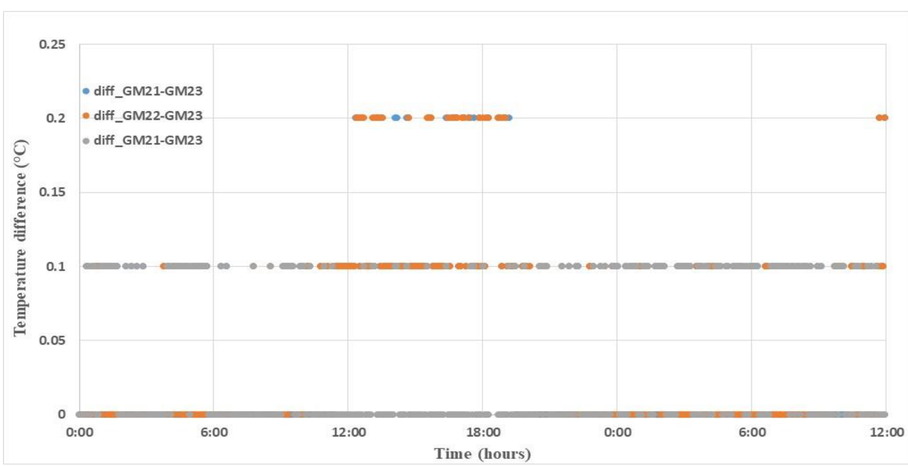

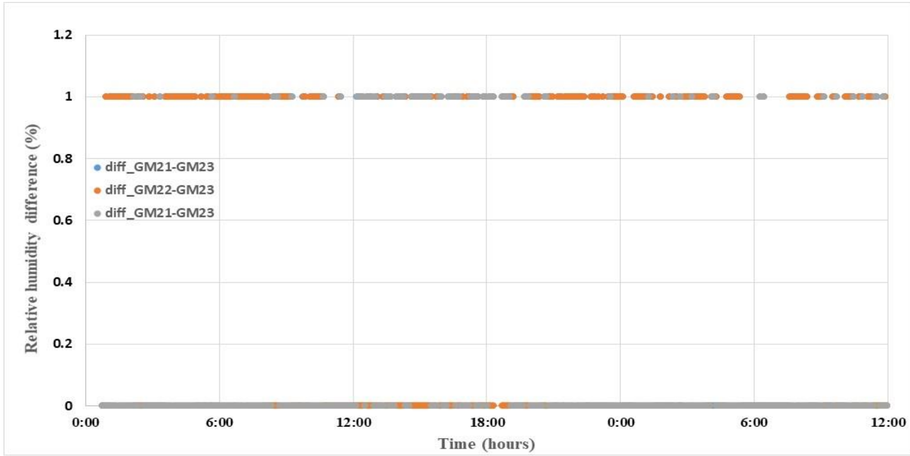

Figure 2.8: Temperature and relative humidity difference for the sensors located at the same positions.

2.2.2.3 Parameters distribution analysis for the room

Comparing the temperature at different walls for one week showed that the facade was the most influenced by the outside condition with a difference of 2°C in average compared to the wall temperature which has the least impact from exterior as we can see in the figure 2.9. The average difference between the wall and the air temperatures was 1°C. The external temperature varied between 17.5 °C and 34 °C, while the facade indoor temperature varied between 21°C and 25.5°C. The temperatures at the center of the office and the center of the lateral wall varied between 22°C and 24.2°C.

Same comparison was made for relative humidity, similar to the temperature variation, the facade was the most influenced by the outside. Relative humidity for the center and the left wall were almost very close with a difference in average of 5% from the facade (figure 2.10).

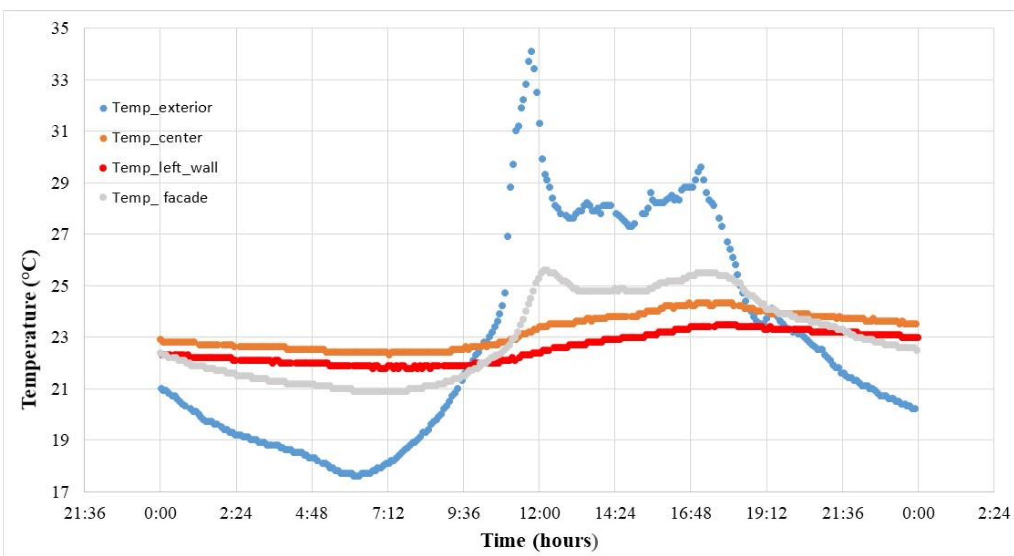

Figure 2.9: Temperature variation for wall, facade and air.

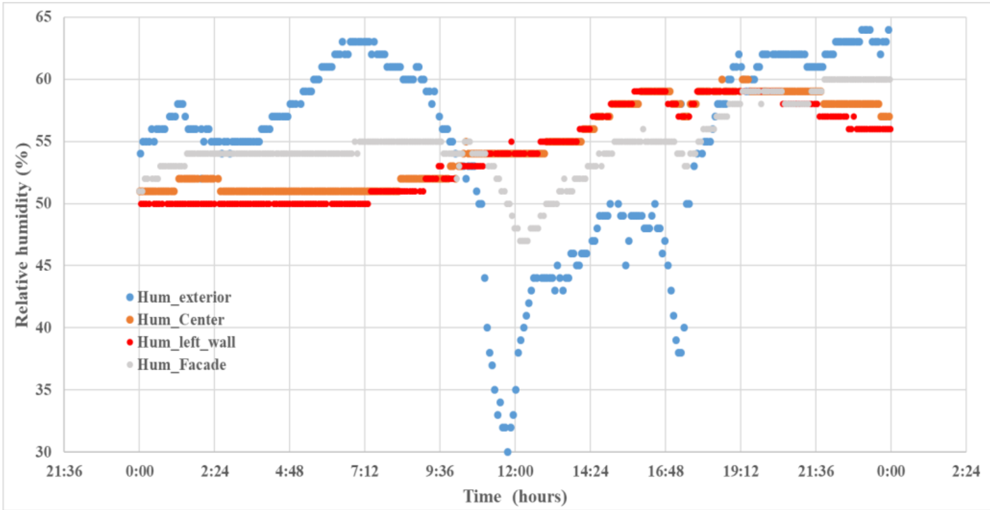

Figure 2.10: Relative humidity variation for wall, facade and air.

Figure 2.10 indicates that relative humidity variation for the center and the wall do not always keep the same variation as the outdoor relative humidity. Hence, we compare this variation to the internal temperature variation (figure 2.11), it indicates that this relative humidity variation is similar to that of the internal temperature.

These analyses indicate that the temperature and the relative humidity within a room are not homogeneous. In the following, we present analysis of indoor condition along the left wall.

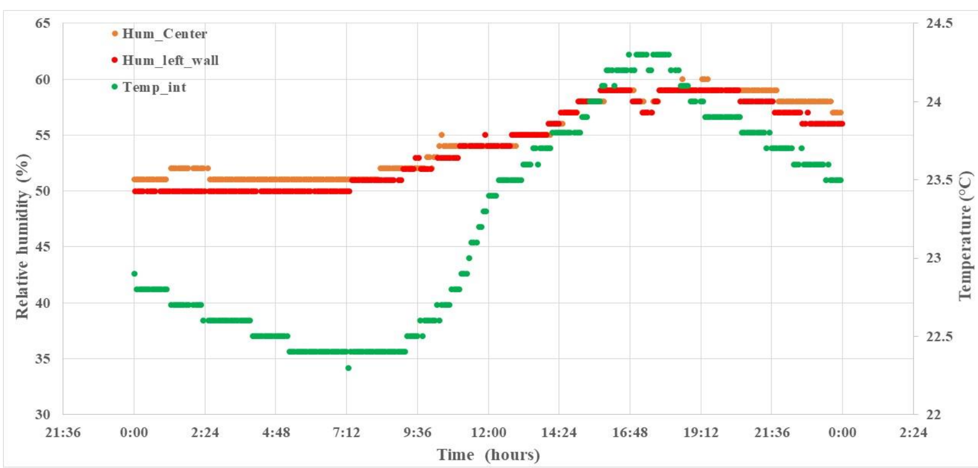

Figure 2.11: Relative humidity and internal temperature variation.

2.2.2.4 Parameters distribution at the left wall

For the three positions (1, 2 and 3), we compare the temperature of the bottom and top levels to the middle one. Figure 2.12 presents the difference between the middle level temperatures with the top land the bottom levels. We noticed a difference between the top and the bottom levels of 0.5°C in average for the three positions. Furthermore, analysis indicates that the temperature increases with height. In order to verify this result, we compare the temperature at the center of the room for three different heights. This analysis confirms the previous result, but we can clearly observe the difference of the temperature distribution between the wall and the center of the room. The middle level at the center of the room has the most elevated temperature, this is related to occupation.

Same comparison was made for the relative humidity variation, a difference of 5% in average was noticed between the top and the bottom levels of the left wall for the three positions. However, relative humidity distribution along the wall was not uniform to determine a certain relation with the height. This may be explained by the dependency of the relative humidity distribution on the internal temperature variation. Moreover, we compare the relative humidity variation at the center of three levels, different distribution from the left wall was observed with keeping the same difference of 5% in average between top and bottom levels (figure 2.13).

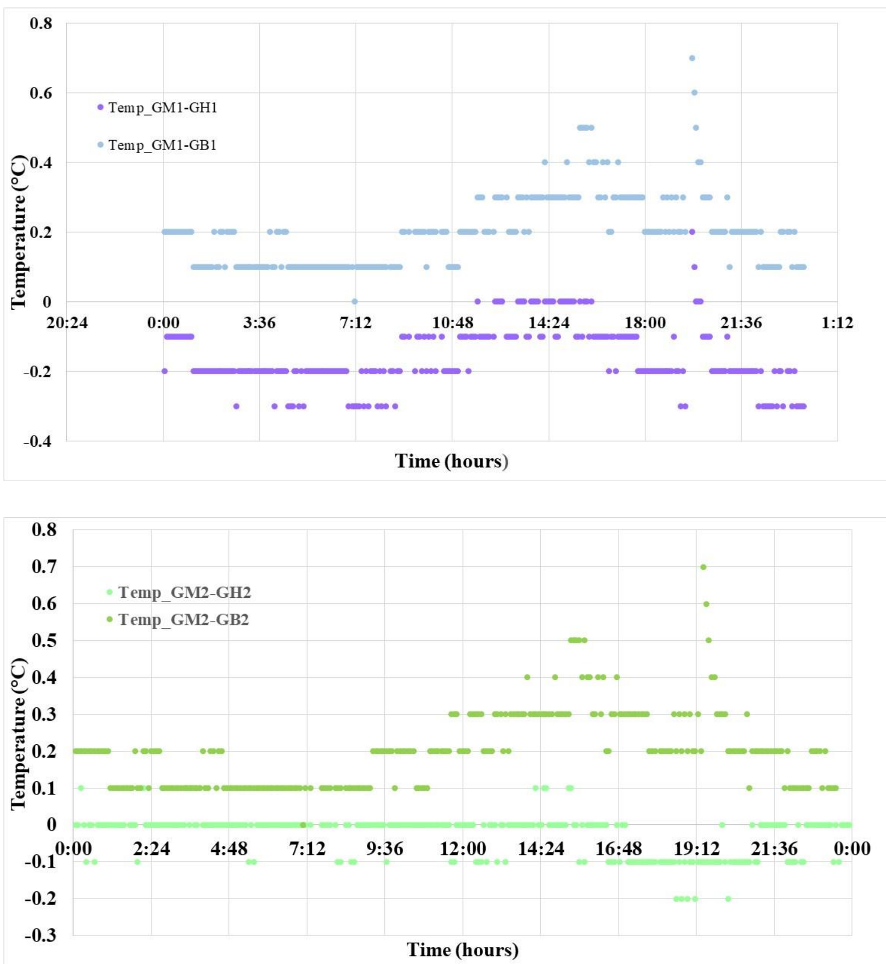

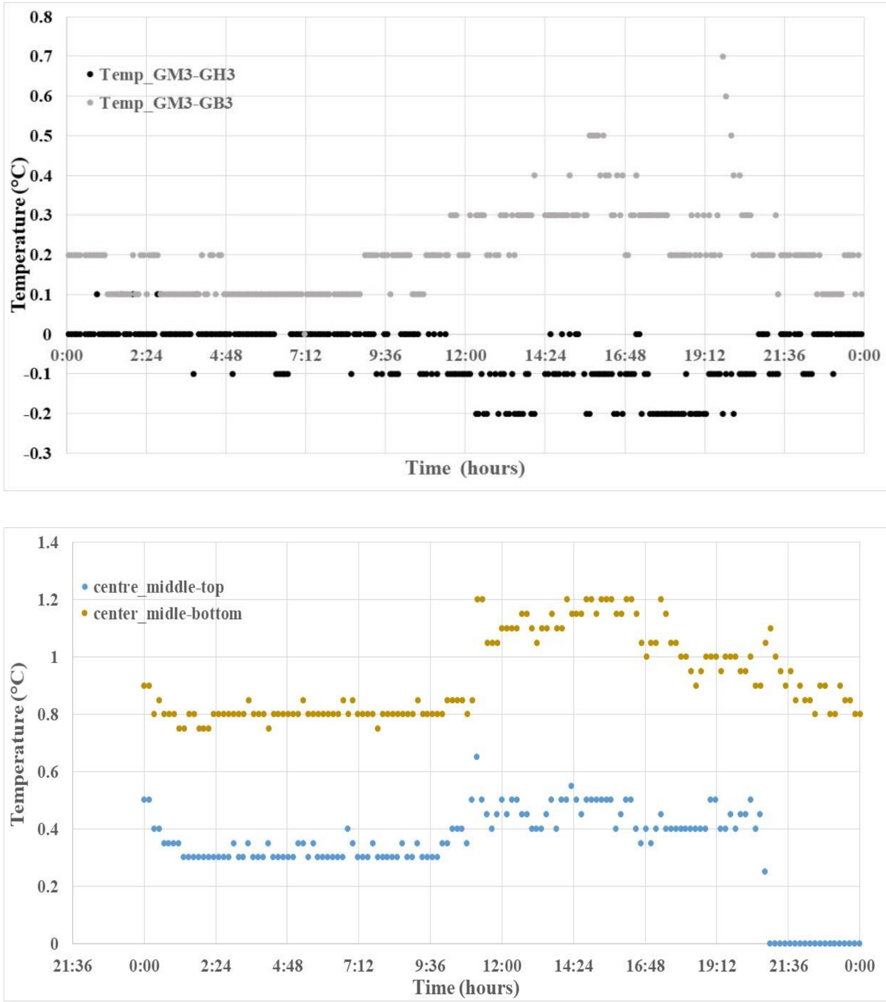

Figure 2.12: Temperature variations along the height of the left wall and the center of the room.

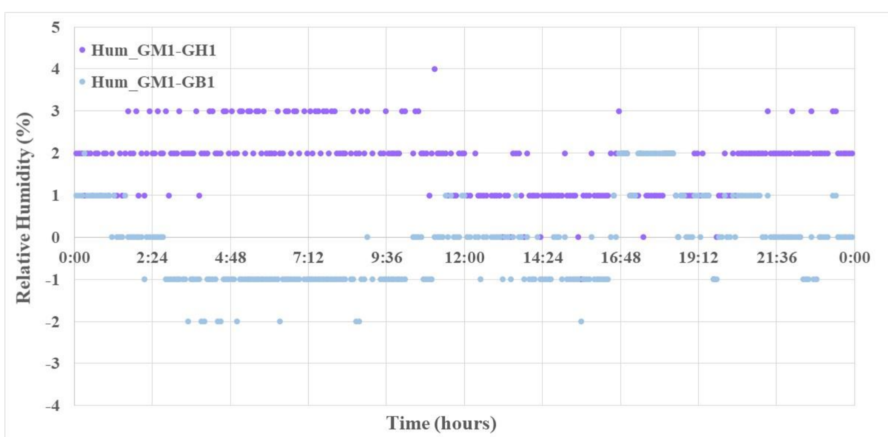

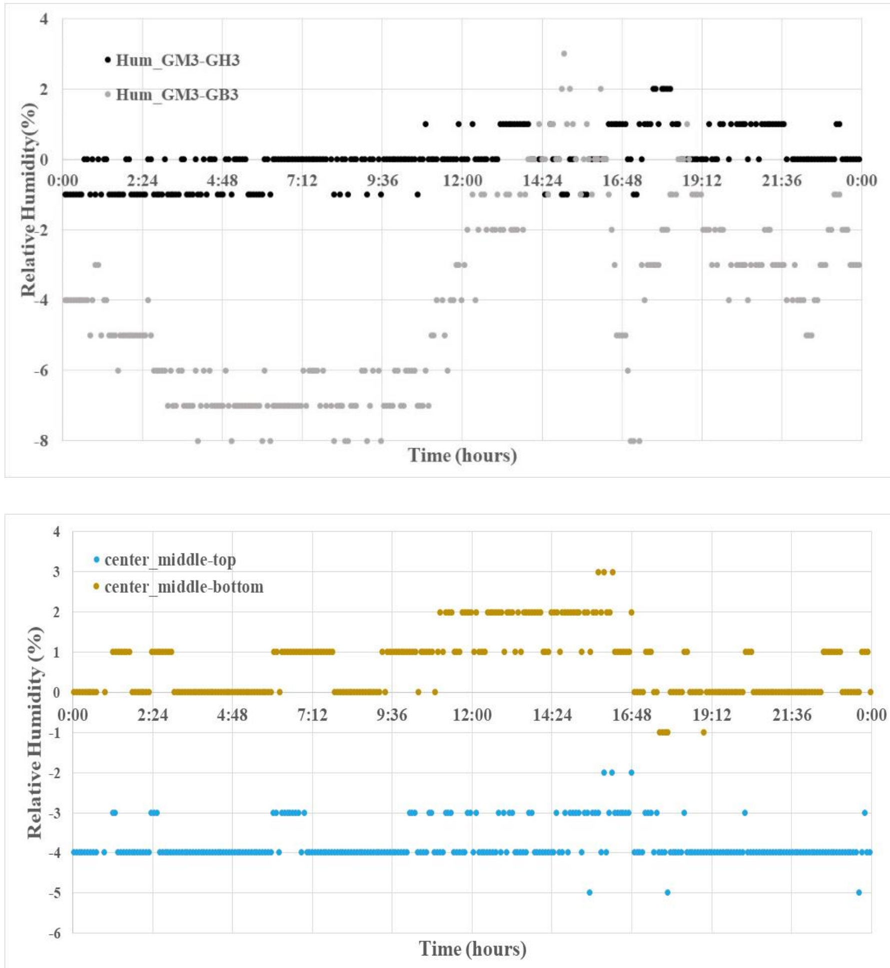

Figure 2.13: Relative humidity variations along the height of the left wall and the center of the room.

The previous analysis shows the heterogeneity of the temperature and the relative humidity distributions within the room. Now, we will study the effect of varying the distance from the facade on the uniformity of the indoor parameters.

We studied the temperature variation for the three levels (top, middle and bottom) by changing sensors' distance from the facade. Upon comparing the results, we noticed that by approaching the facade, the extremum of the temperature (maximum or minimum) are more influenced by external conditions. Figure 2.14 indicates that the temperature at position 3 is the most affected by the external variation and that temperature variation is almost close for positions 1 and 2 for the two top and middle levels. Furthermore, the temperature difference at the bottom level constitutes the most heterogeneous distribution along the length of the wall.

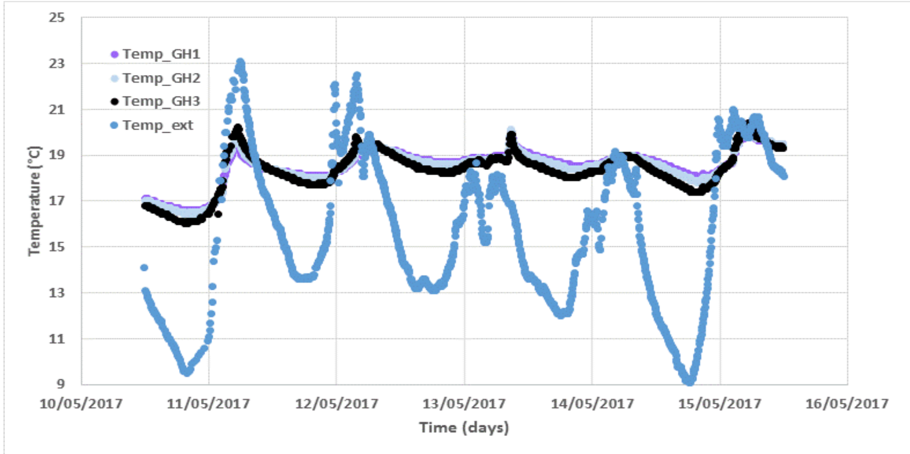
Temp_GH1
Temp_GH2
Temp_GH3
Temp_ext
Temperature (°C)
Time (days)
25
23
21
19
17
15
13
11
9
10/05/2017
11/05/2017
12/05/2017
13/05/2017
14/05/2017
15/05/2017
16/05/2017

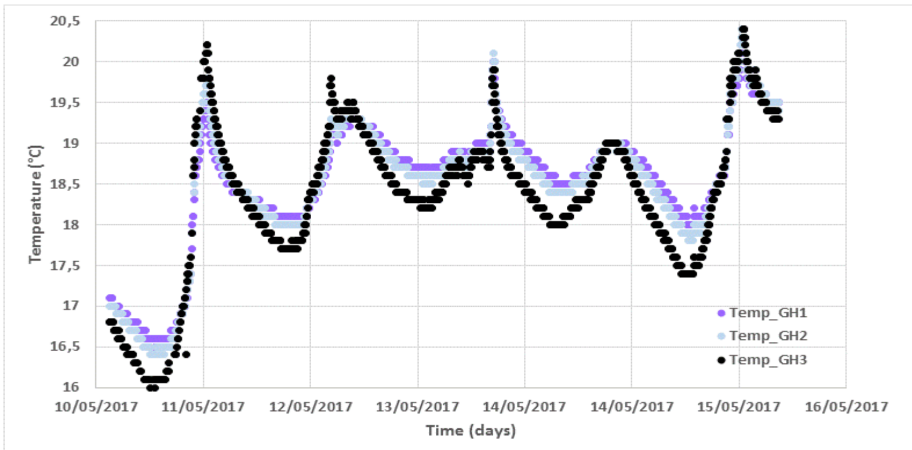
Temp_GH1
Temp_GH2
Temp_GH3
Temperature (°C)
Time (days)
20,5
20
19,5
19
18,5
18
17,5
17
16,5
16
10/05/2017
11/05/2017
12/05/2017
13/05/2017
14/05/2017
14/05/2017
15/05/2017
16/05/2017

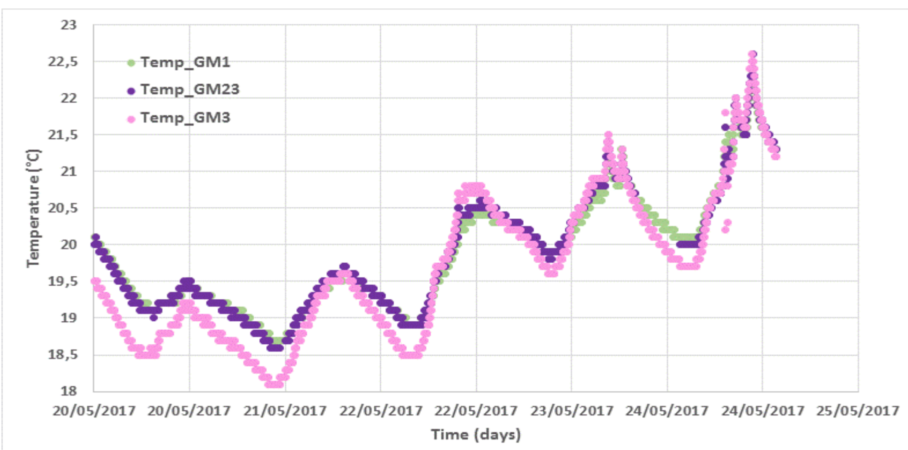
Temp_GM1
Temp_GM23
Temp_GM3
Temperature (°C)
Time (days)
23
22,5
22
21,5
21
20,5
20
19,5
19
18,5
18
20/05/2017
20/05/2017
21/05/2017
22/05/2017
22/05/2017
23/05/2017
24/05/2017
24/05/2017
25/05/2017

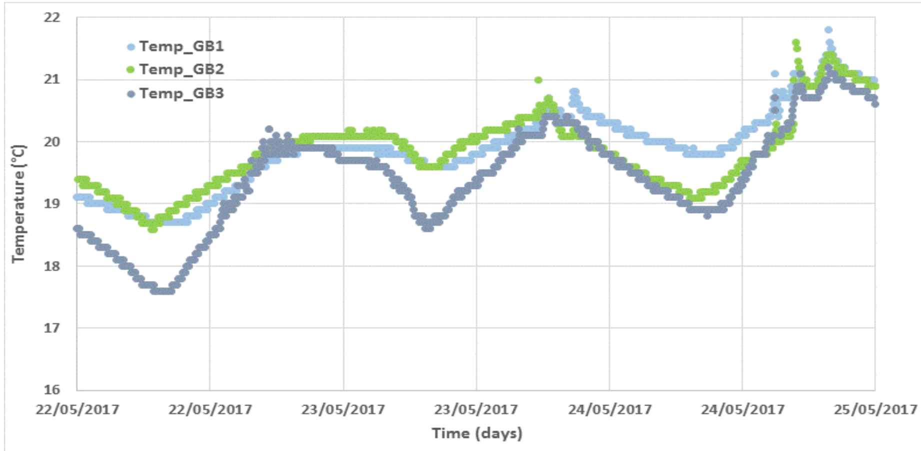

Figure 2.14: Temperature variations for different distances from the facade.

Same procedure is applied for the relative humidity distribution. Studying its variation along the length of the left wall shows that the distribution is nearly the same for the three levels (figure 2.15) and that the difference is almost negligible, within the accuracy interval of sensors (3%). This indicates that the relative humidity is not affected by the distance from the facade and that can be related as before to the temperature distribution within the room.

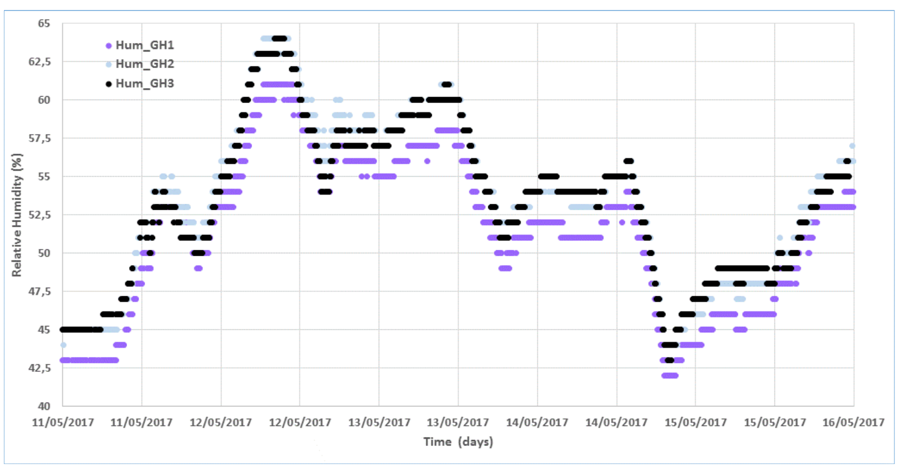

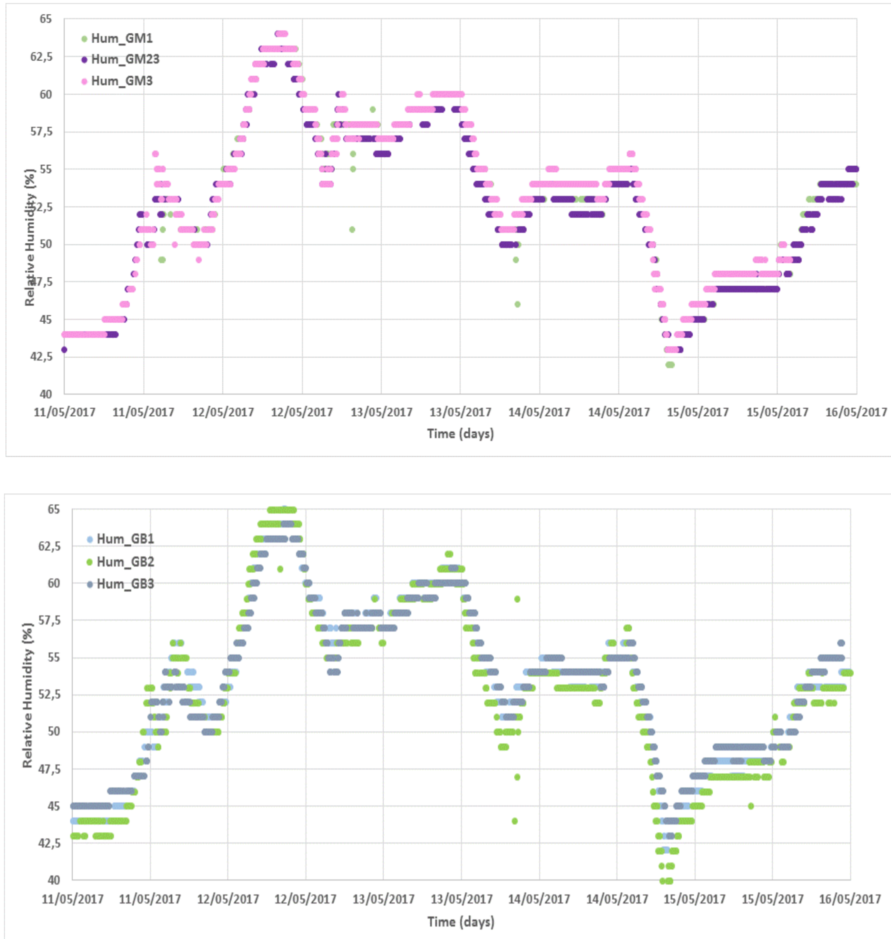

Figure 2.15: Relative humidity variations for different distances from the facade.

2.2.3 Usage conditions analysis

After one month of monitoring the occupied office, a database was built with a time series measurement having an interval of five minutes. Preliminary analysis allowed us to understand the distribution of the indoor parameters. Then, two sets of scenarios were executed to study the impact of occupants' behavior. An air conditioner with an adjustable temperature and a power meter was used during these experimentations. It has a coefficient of performance COP = 2.6 and a cooling power of 1200 Btu/h. The first set of testing was executed on a temperature of 17°C, the other one on 20°C.

For the first one, an air conditioner was launched at 17°C for four days. We opened the windows, located at a south orientation, for 24h, then analyzed the consumption needed. By comparing the energy consumption for closed and opened windows (Figure 2.16), we noticed an increase by 33% in average. This is illustrated by figure 2.17 where the energy for the two scenarios were represented with the sum of the exterior temperature.

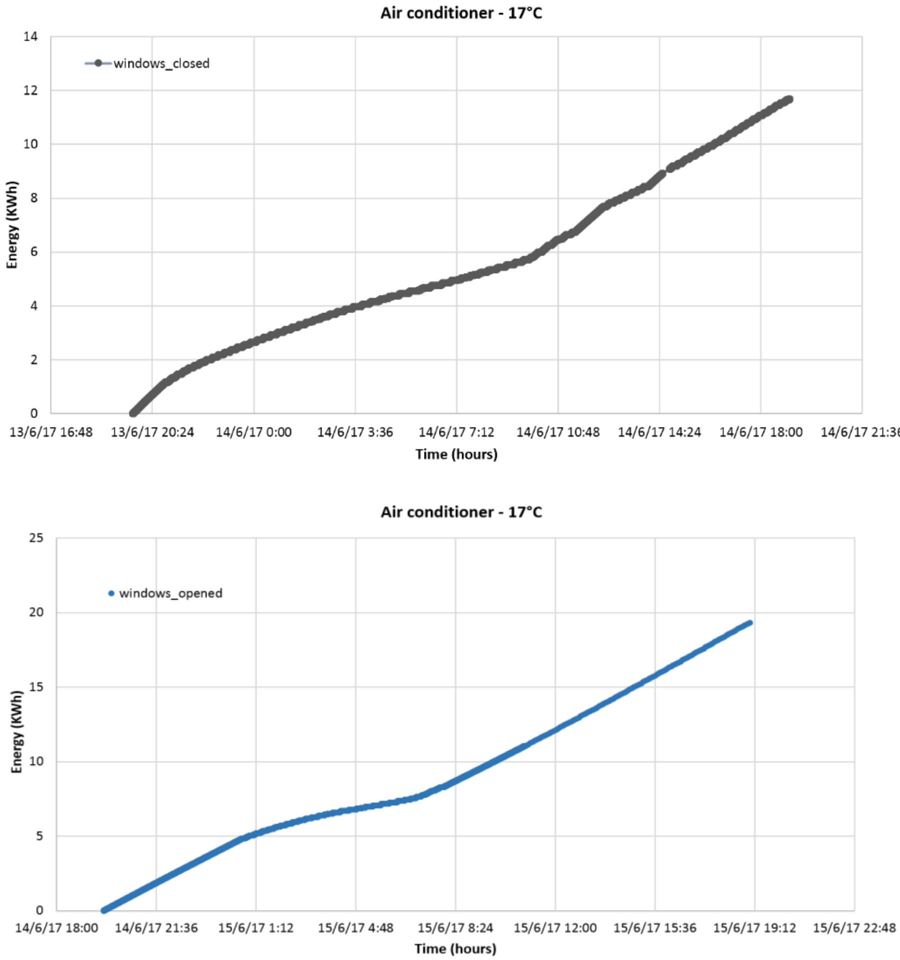

Figure 2.16: Energy consumption for opened and closed windows with time.

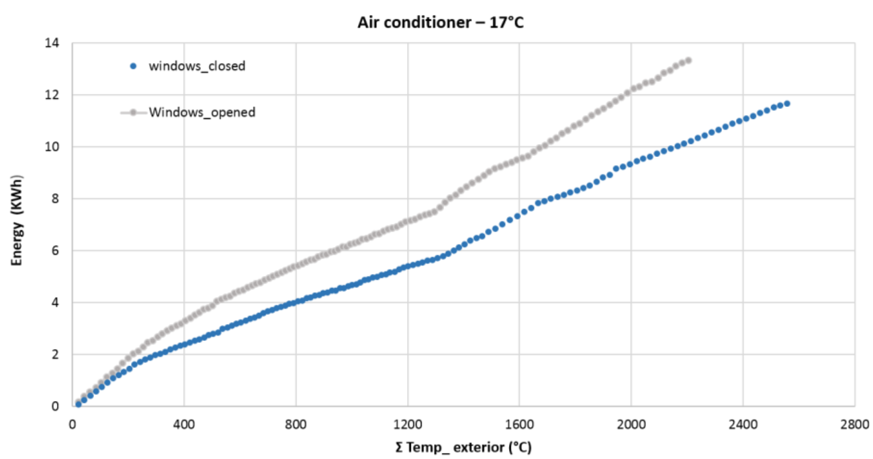

Figure 2.17: Energy consumption in cases of opened and closed windows with exterior temperature.

Afterwards, we closed the curtains for 24h and observed the evolution of the consumption. We noticed an increase by 28% in average when the curtains were closed (figure 2.18).

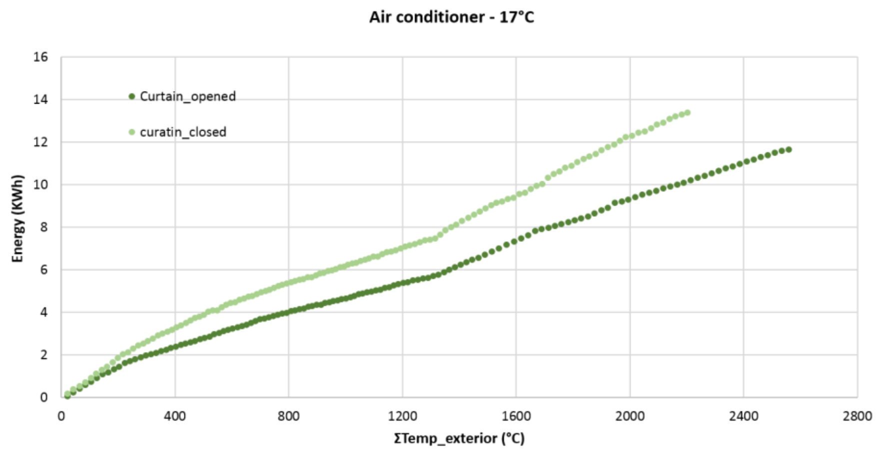

Figure 2.18: Energy consumption in cases of opened and closed curtains with exterior temperature.

We repeated the same experimentations with the air conditioner launched at 20°C. The energy consumed was 5 times less than the one consumed at 17°C. When opening the windows, we noticed that the consumption increased by 50% in average.

Analysis of different usage conditions showed that the energy consumption is largely influenced by the window's opening, the interior operating temperature and the use of stores. This previous study contributes to a better understanding of the building thermal behavior through exploring sources of energy gain and losses.

2.3 Study of the four unoccupied classrooms

2.3.1 Experimental Setup

Four rooms in the same building 'Polytech'Lille' were monitored (figure 2.19). These rooms are unoccupied offices and classroom situated at the fourth floor. The central heating system was off during this period. The first two rooms have a south orientation, the other two have a north one. For the rooms having the same orientation, all windows were closed for the first one and one window was opened for the second one. One-month (June) measurement series were recorded with intensive monitoring of facade temperature and humidity with exterior thermal parameters too. The facade is formed of non-insulated windows. A database was built with a time series measurement having an interval of five minutes. This work was done to complete the analysis of the first study. It reveals the influence of other parameters on the temperature and humidity distribution in order to better understand the thermal behavior of the building.

Figure 2.19: Experimented rooms – fourth floor.

2.3.2 Data analysis

Façade temperature at south and north orientation were compared with the outdoor temperature. Figure 2.20 and 2.21show that the range of the temperature distribution for the façade with south orientation is wider than the north one. It is closer to the outdoor temperature distribution. Thus, south orientation is more influenced by the outdoor conditions. We can notice that the difference of temperature distribution between south and north orientations is larger when windows are closed.

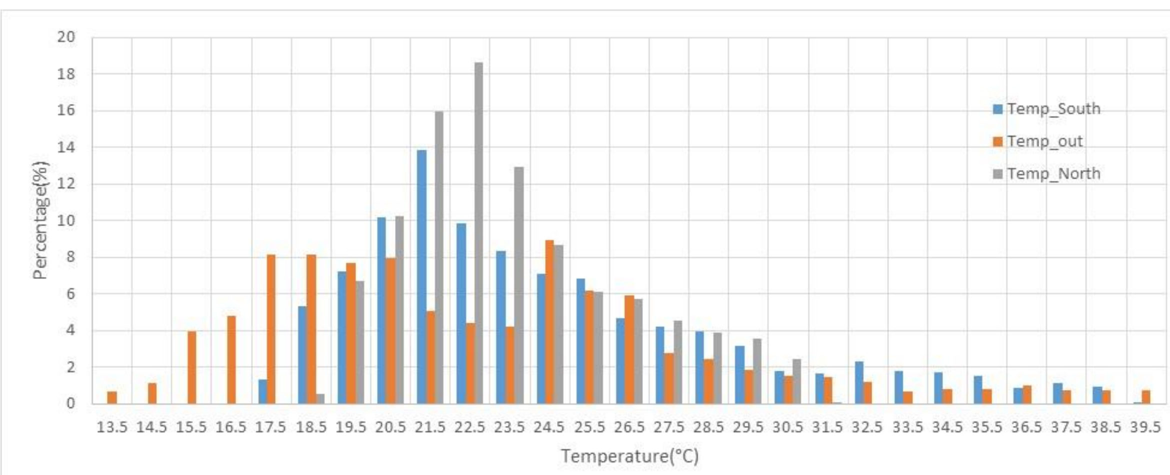

Figure 2.20: Temperature distribution for different orientation - closed windows.

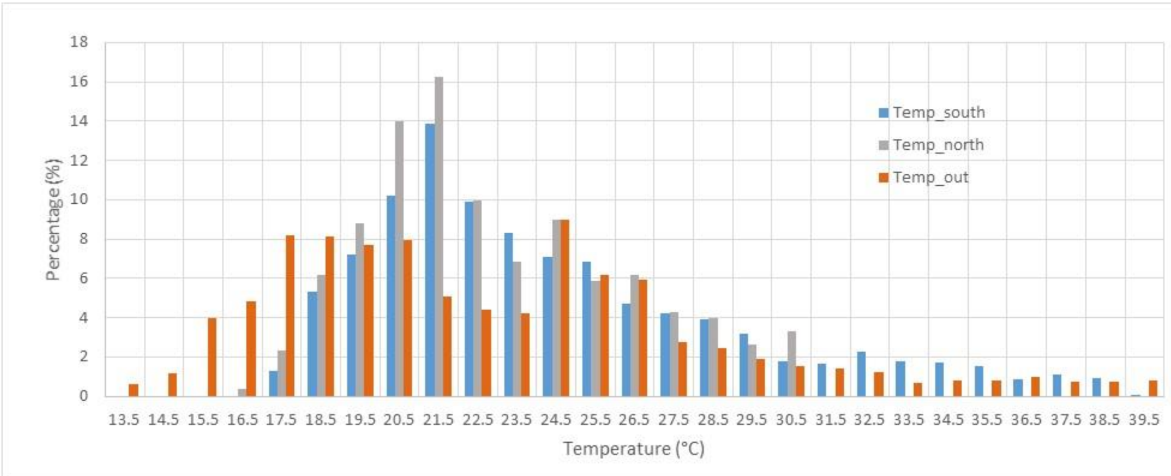

Figure 2.21: Temperature distribution for different orientation - opened windows.

While studying the façade temperature for different orientations, we noticed that the difference between south and north orientations increases up to 10°C during the day and decreases below 2°C at night (figure 2.22). This reveals the influence of the orientation on the indoor temperature variation.

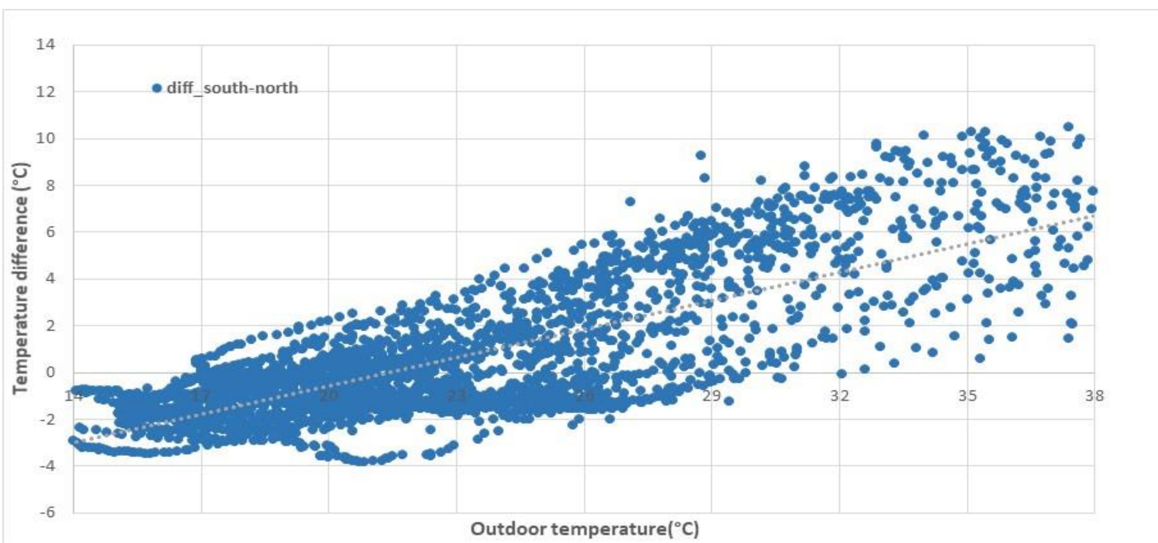

Figure 2.22: Temperature difference for south and north orientation – closed windows.

Same analysis was done to study the influence of windows' state on the façade temperature. Figure 2.23 and 2.24 show that, for both orientations, the highest frequencies are for lower temperatures with opening windows. For elevated temperatures, distribution frequencies are almost similar for opened and closed windows. This can be explained by the lack of insulation for windows.

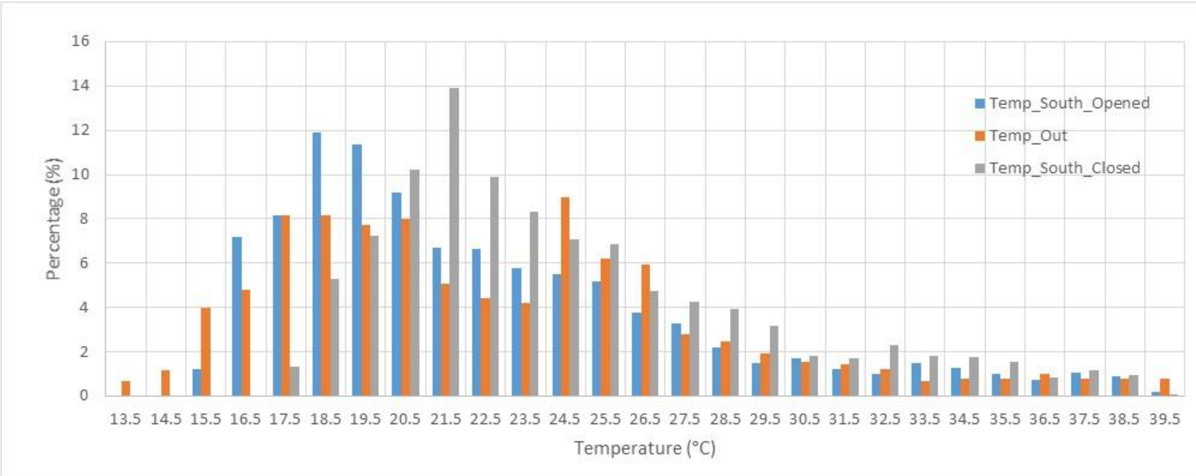

Figure 2.23: Temperature distribution south orientation - closed and opened windows.

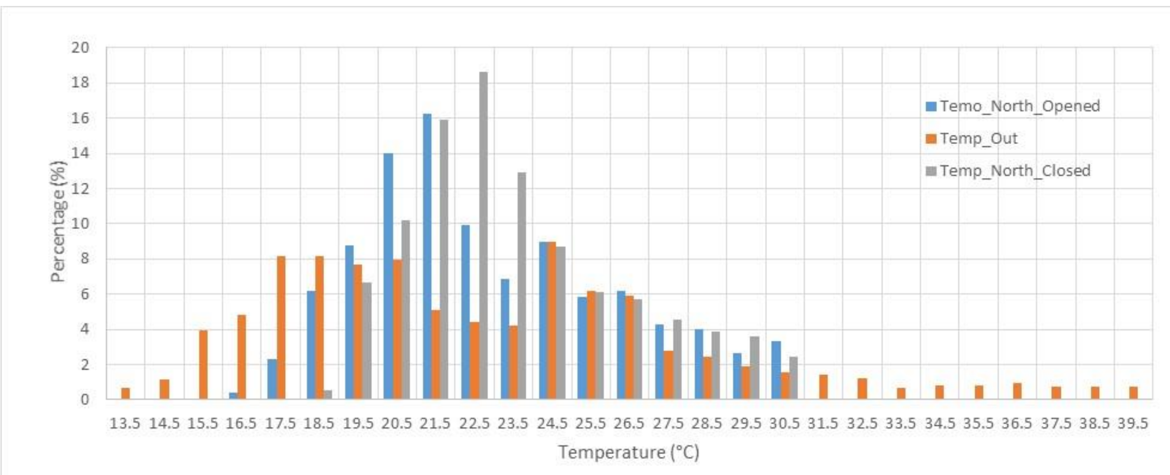

Figure 2.24: Temperature distribution north orientation - closed and opened windows.

Upon studying the façade temperature difference with opened and closed windows for both orientations, we noticed that for low outdoor temperature the difference is almost negligible at the south facade. It increases up to 4°C when the outdoor temperature increases (figure 2.25). While for north orientation, for similar outdoor temperature the difference is higher (2°C) than the south one (figure 2.26).

The analysis of collected data for the four rooms indicates that the façade temperature, thus the indoor conditions, is highly affected by the orientation of the room and the state of windows. These two parameters are considered as major factors for studying building's behavior in the next chapters.

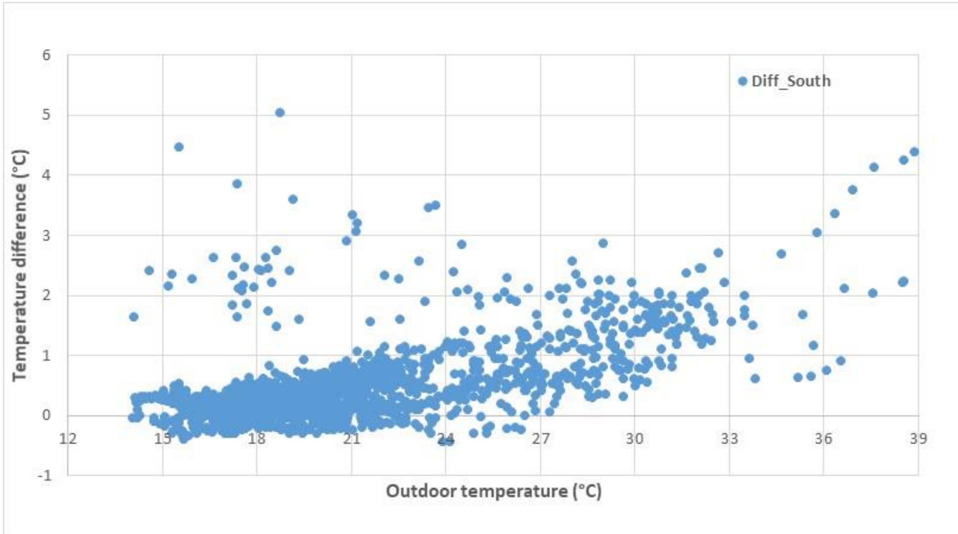

Figure 2.25: Temperature difference opened and closed windows – South orientation.

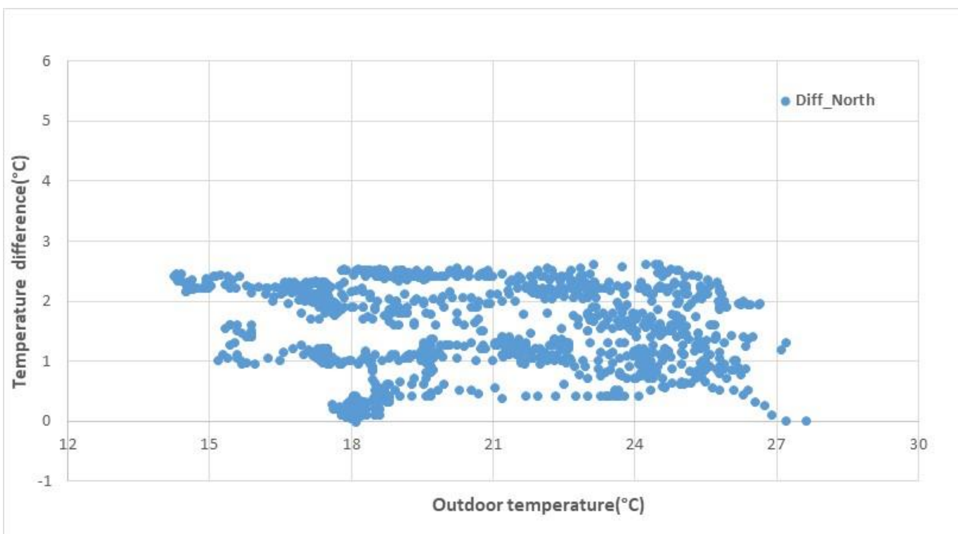

Figure 2.26: Temperature difference opened and closed windows – North orientation.

2.4 Building A4

2.4.1 Experimental Setup

The A4 is a one floor research building formed by many offices and a large open space volume at the center. Offices are equipped by electric radiator as heating system, while the center uses central heating through ventilation openings. More than 100 sensors were installed to measure indoor and outdoor conditions. Façade, walls, windows, indoor air and all central heating openings were monitored. Figure 2.27 illustrates the instrumentation scheme. The study was executed for five months from October 2017 to February 2018.

At first, a general preliminary analysis was executed to understand the thermal behavior of this building. Then, a quantitative and qualitative investigation was performed on the central heating of the open space to study the distribution of the indoor temperature and humidity and to understand and optimize the heating system.

Furthermore, a smart intensive monitoring system was installed in an unoccupied office room in the building. The office is formed of two façades and two internal walls without windows. It is heated by a radiator with two constant power (high level 1500 W and low level 900W) coupled with a control system and a counter. Sensors were installed on all walls (internal and external sides) and at the center of the room to record the temperature at an interval of 5minutes. The instrumentation plan is illustrated in figure 2.28. Data were collected for one month (February 2018), without heating, with low level heating and with high level heating.

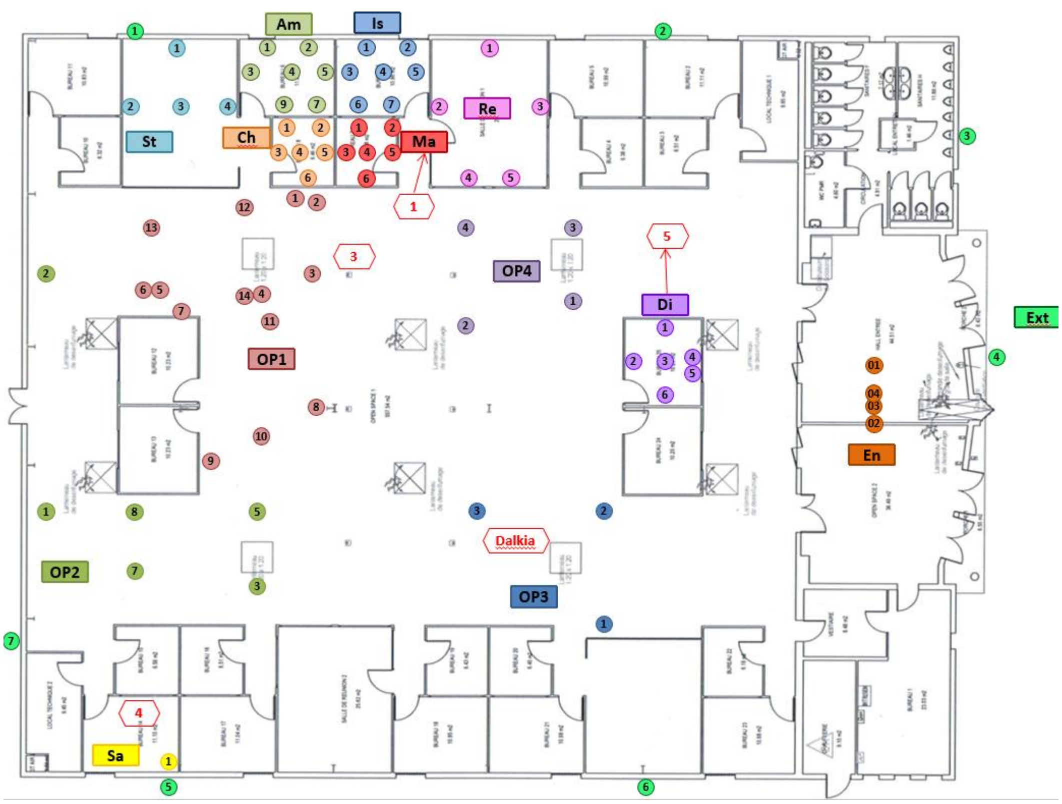

Figure 2.27: Instrumentation scheme for building A4.

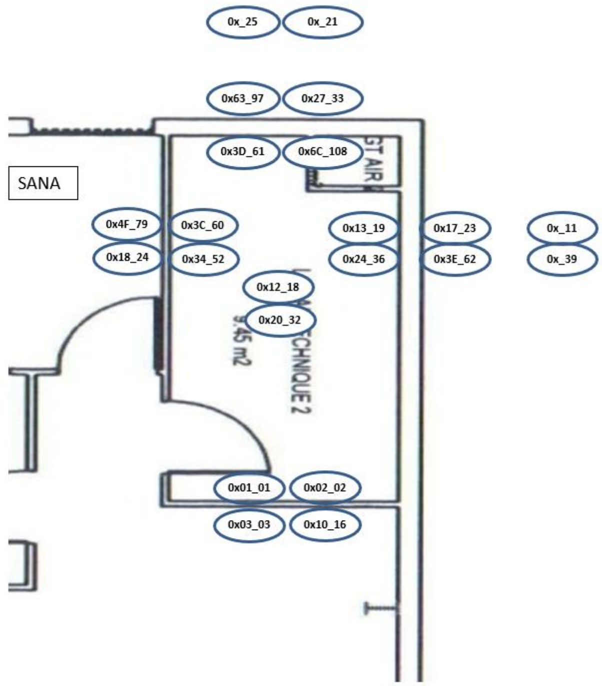

Figure 2.28: Instrumentation plan for the unoccupied room in A4.

2.4.2 Data analysis

2.4.2.1 Generalities

A general investigation was made to understand the building thermal behavior and to determine the range of temperature difference between indoor and outdoor. We started by comparing the temperature of the external and internal sides of the façade. The temperatures follow the same variations (figure 2.29). It is noted that at low outside temperatures, the difference can reach 20°C. This difference decreases with increasing outdoor temperature. The average difference is about 10°C.

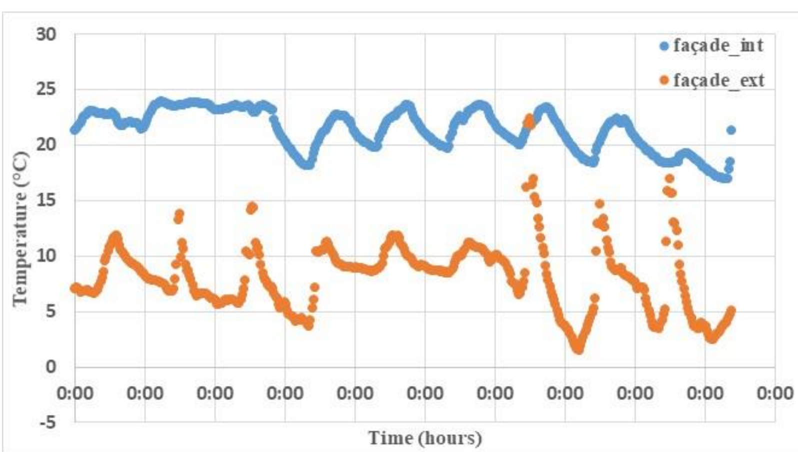

Figure 2.29: Comparison of the temperature at both side of the façade.

It is noted that the window temperature is higher than the external façade temperature. The difference decreases with the increase of the outside temperature to almost zero at a temperature of 20°C (figure 2.30). The average temperature difference varies between 5 and 10°C.

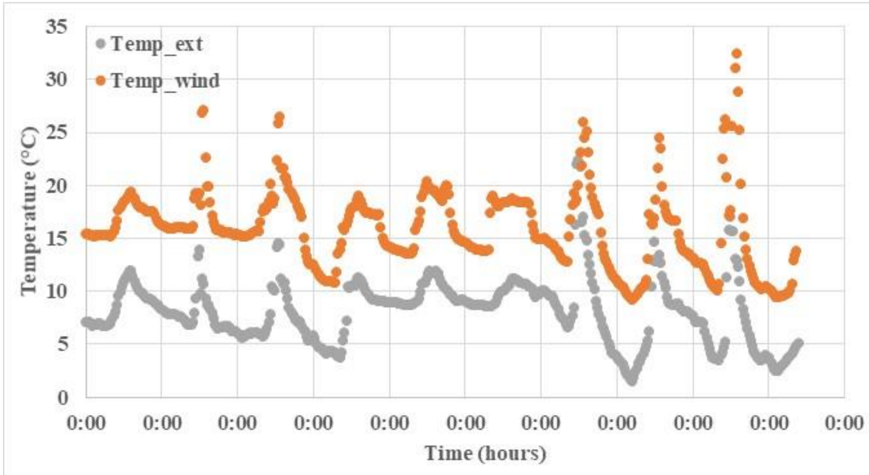

Figure 2.30: Comparison of external façade and window temperatures.

By comparing the internal temperature of the façade with the air temperature, we noted that the air temperature is higher than that of the facade temperature by 1°C in average and can reach a maximum of 2°C around noon (figure 2.31).
Figure 2.32 shows that the internal temperature of the facade is higher than the window's temperature by 5°C in average except for the peaks which vary according to solar radiation.

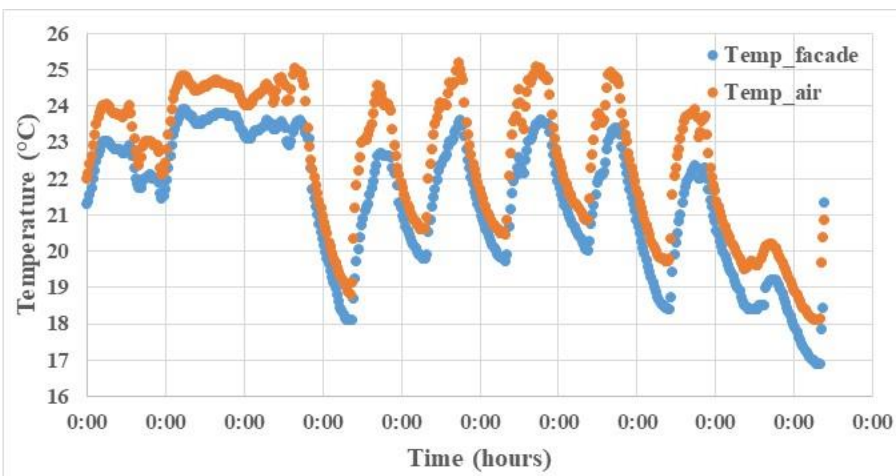

Figure 2.31: Comparison of internal façade and air temperatures.

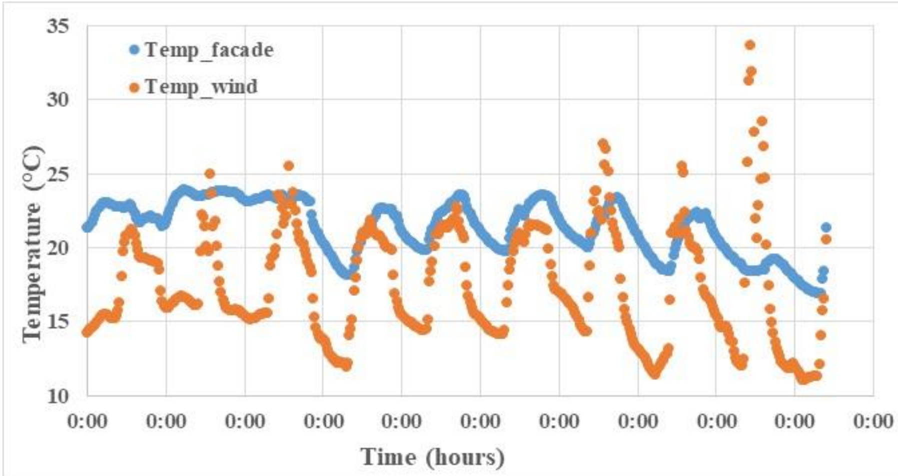

Figure 2.32: Comparison of internal façade and windows temperatures.

This preliminary analysis was performed to get a general idea on the temperature distribution and the isolation level of the building in order to understand its behavior. This study was completed with a detailed investigation of the temperature distribution of the central heating openings located at the ceiling level of the open space.

2.4.2.2 Analysis of the central heating system

The open space of building A4 is heated by a central system through a forced air heating technique. The heated air travels through a system of ducts and is expelled through 15 vents (figure 2.33). A heat pump warms the air that is transported from the entrance (orange color in figure 2.30) to the internal grills. A sensor was placed at each vent's location to measure the expelled air temperature and humidity. Each sensor will be represented by a certain form revealing the zone (1, 2,3 and 4) and the sensor numbers. (for example, O3_1 is the sensors located in zone 3 (blue) and its number is 1, it is located at the intersection of column 1 and line1.)

The analysis started by a quantitative study of the temperature and humidity distributions of the vents system. Then the investigation is followed by a qualitative analysis to visualize these distributions.

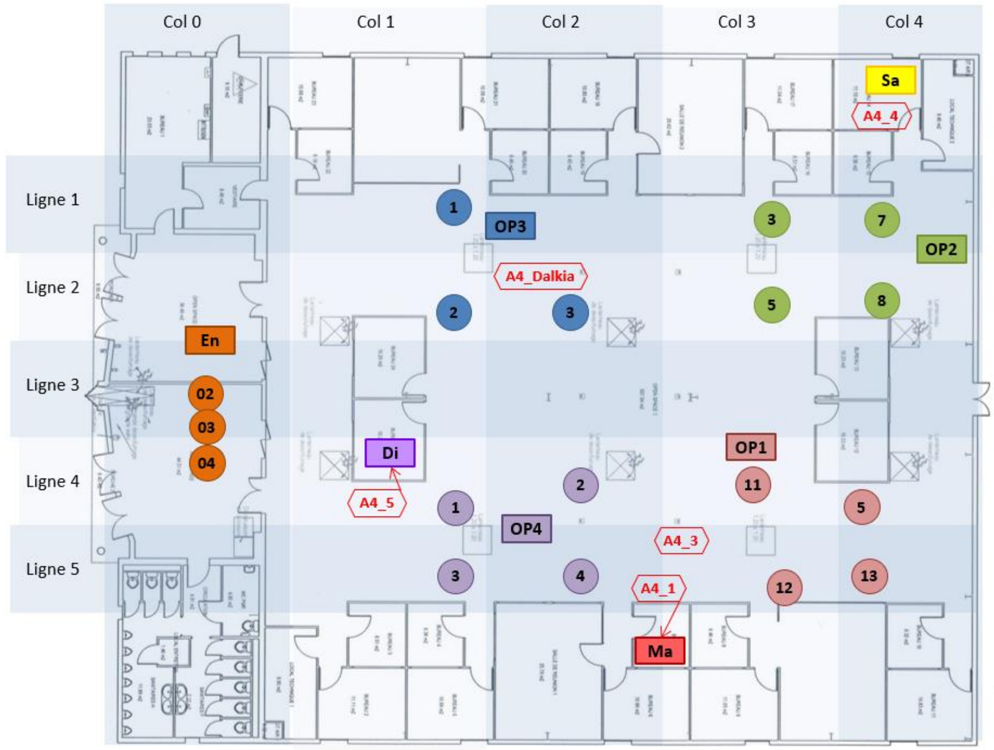

Figure 2.33: Plan of the sensors installed at the position of the vents.

- **Quantitative analysis of the temperature**

The study started by analyzing the daily variation of the temperature. Comparing different sensors' temperature of lines 2 and 5, reveals different variation: during the day and the night, between sensors and between weekday and the weekend.

Figure 2.34 shows that central system is stopped at 21:00 o'clock and launched at 4:00 o'clock in the morning. Temperature of all sensors follows almost the same variation with a difference of 1 to 2°C. Figure 2.35 indicates that during the weekend the open space is heated at a lower temperature than the weekdays.

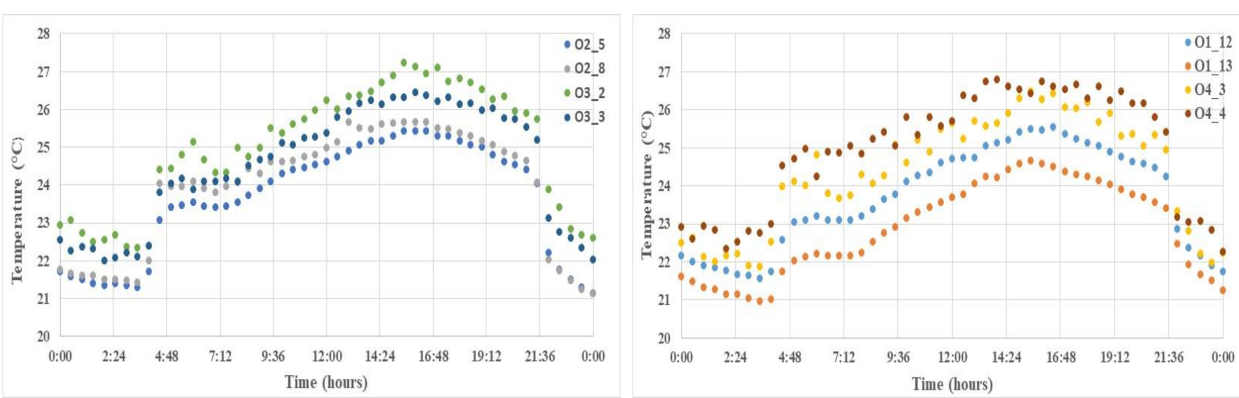

Figure 2.34: Daily week variation of temperature for sensors of lines 2 and 5.

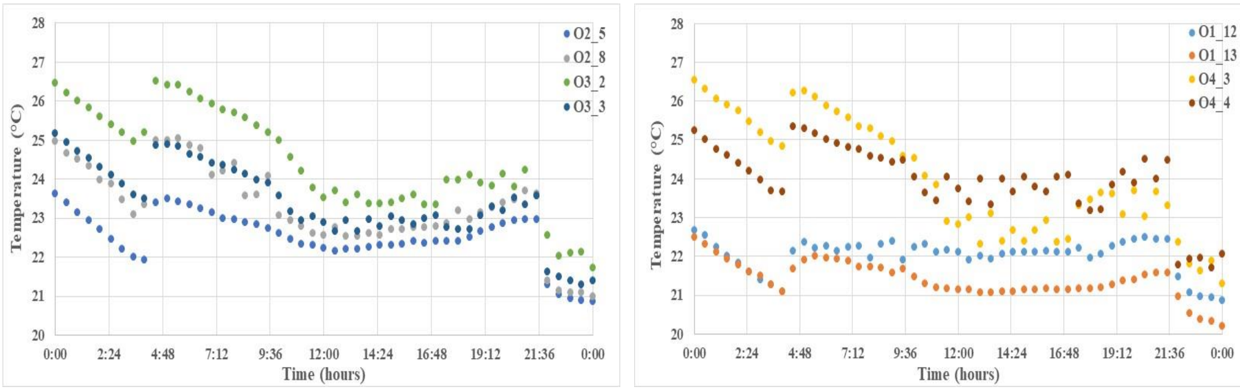

Figure 2.35: Daily variation of temperature during the weekend for sensors of lines 2 and 5.

Referring to this multi-variation of the temperature, for each sensor we have determined some statistical parameters of the temperature distribution for one week. We have calculated the average, the maximum, the minimum and the standard deviation to better understand the distribution and to elaborate some relations with the different vents' locations. Day and night parameters were studied apart.

The variation of these parameters is illustrated in figure 2.36 and 2.37. The distribution of the mean, the maximum and the minimum temperatures are presented for all lines and columns. These graphs show that the average of the temperature decreases for all lines from the entrance to the end of the building for day and night. While for other parameters, almost for all lines, they decrease too. We note that these parameters do not decrease progressively. This investigation was not sufficient to illustrate and understand the variation of the air temperature expelled by the different vents. The study was completed with a spatial visualization of the parameters distribution through the Geographic Information System (GIS) software.

Sensors	Max	Min	Average	Standard deviation
O1_5	29,20	21,27	23,92	1,58
O1_11	27,40	22,87	25,22	1,13
O1_12	25,53	21,30	23,58	1,15
O1_13	24,67	20,53	22,75	1,15
O2_03	26,87	21,73	23,76	1,08
O2_04	30,17	21,60	24,23	1,58
O2_05	27,07	21,70	23,92	1,17
O2_08	29,13	21,90	24,41	1,42
O3_1	27,37	22,13	24,48	1,29
O3_2	30,20	22,87	25,65	1,64
O3_3	28,90	22,33	24,94	1,50
O4_1	29,53	21,70	24,80	1,72
O4_2	29,63	23,10	25,57	1,42
O4_03	30,30	21,90	24,99	1,81
O4_04	29,00	23,13	25,44	1,29
Entrance	50,97	43,63	46,59	1,72

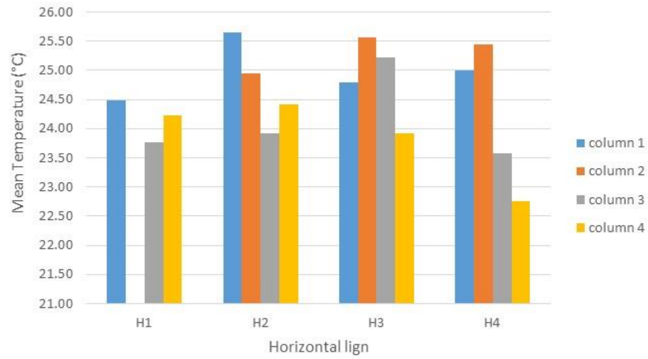

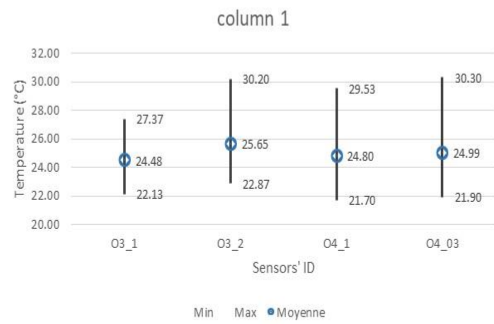

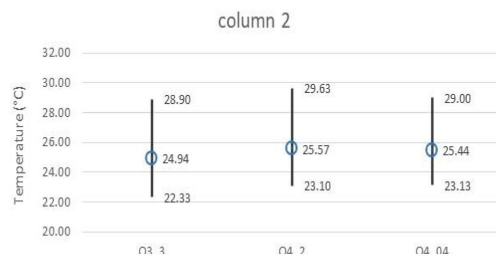

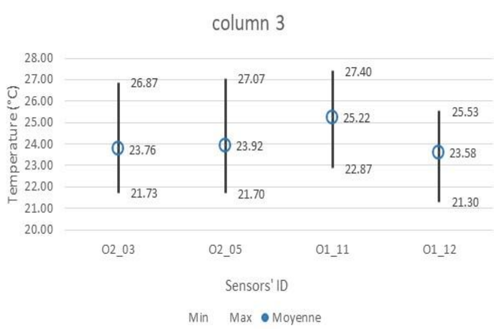

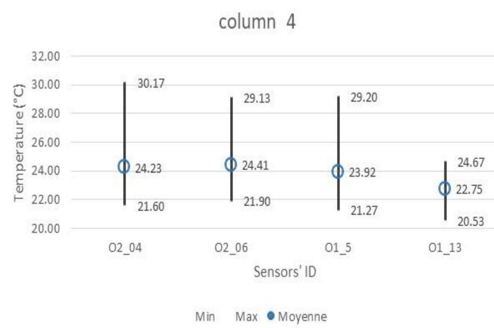

Figure 2.36: Parameters distribution – day.

Sensors	Max	Min	Average	Standard deviation
O1_05	26,03	18,03	20,85	1,67
O1_11	25,10	20,17	22,21	0,95
O1_12	23,97	19,70	21,48	0,88
O1_13	23,80	19,10	21,01	0,95
O2_03	24,87	19,20	21,24	1,09
O2_04	26,47	18,30	20,91	1,72
O2_05	25,03	19,07	21,24	1,14
O2_08	26,40	18,80	21,41	1,53
O3_1	25,93	20,75	22,37	1,13
O3_2	27,73	20,57	22,74	1,56
O3_3	26,67	19,60	22,09	1,41
O4_01	27,40	19,93	22,17	1,63
O4_02	26,87	19,57	22,34	1,40
O4_03	27,97	19,87	22,28	1,76
O4_04	26,63	20,03	22,53	1,26
Entrance	45,60	38,23	41,20	2,11

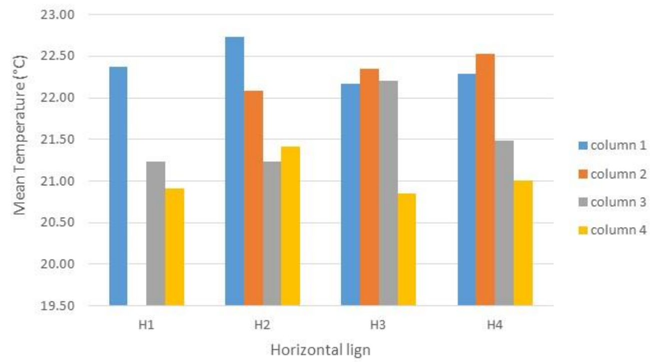

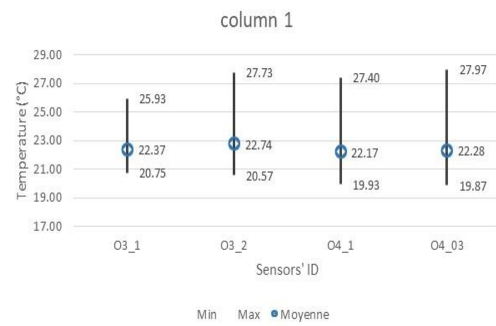

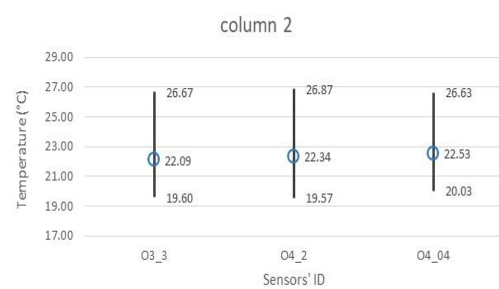

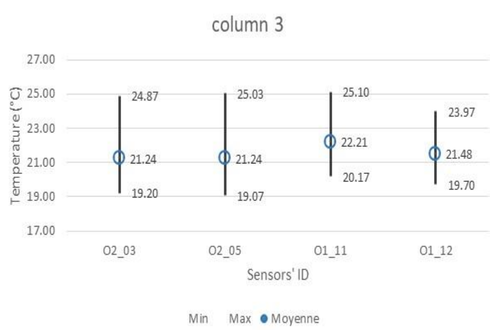

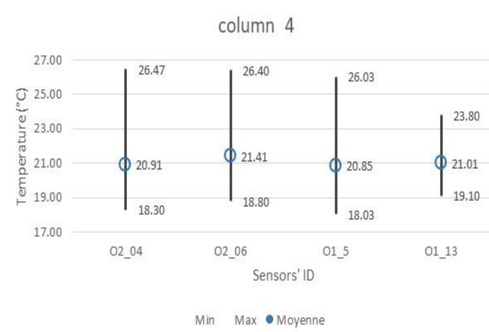

Figure 2.37: Parameters distribution – night.

- **Qualitative analysis of the temperature**

This section presents spatial plans for parameters' distribution of the air temperature expelled by the vents in the open space. These plans were performed on GIS software. Starting by the average temperature distribution, figure 2.38 shows that the mean temperature decreases progressively from the entrance to the end of the building for day and night. This was not clearly observed in the previous analysis according to the parameter's values. While, through presenting the density distribution, the progressive decrease through zones was obviously illustrated. The maximum difference between the start and the end is about 14°C. The plan reveals that the heating system is stopped at night, by showing that temperatures at night are lower than the daily ones.

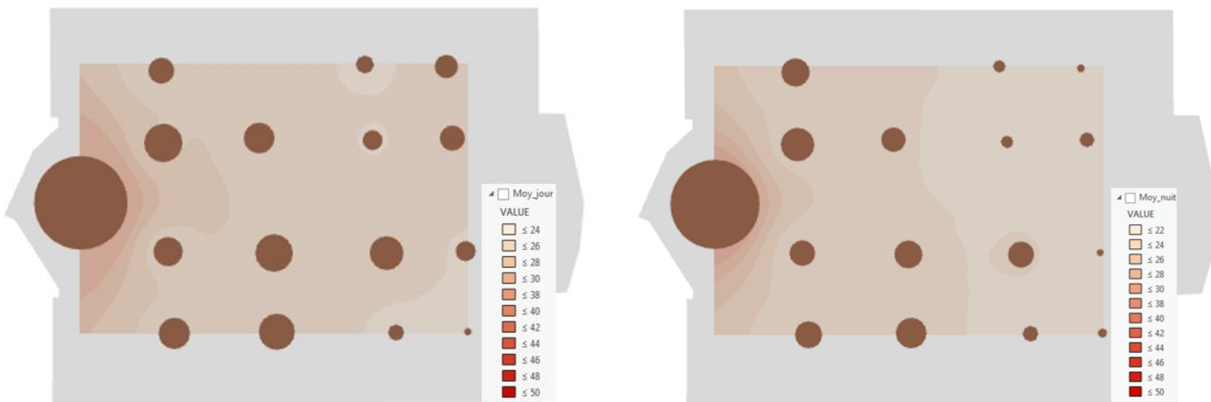

(a) (b)

Figure 2.38: Plan for temperatures' average distribution: (a) day, (b) night.

Furthermore, by comparing the minimum temperature distribution, same analysis was executed as before. Similar distribution variation was observed. The maximum difference between the start and the end is about 8°C (figure 2.39).

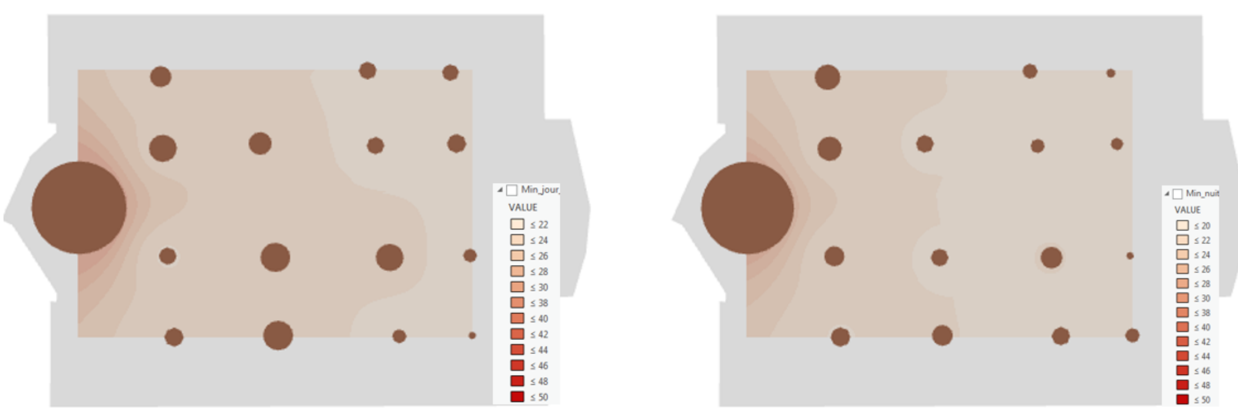

(a) (b)

Figure 2.39: Plan for temperatures' minimum distribution: (a) day, (b) night.

Afterwards, the max temperature distribution is analyzed. A progressive decrease of the temperature is observed from the start until column 3 for day and night. An increase of a maximum of 2°C is noted for the last column. The maximum difference between the start and the end is about 8°C. The plans are illustrated by figure 2.40.

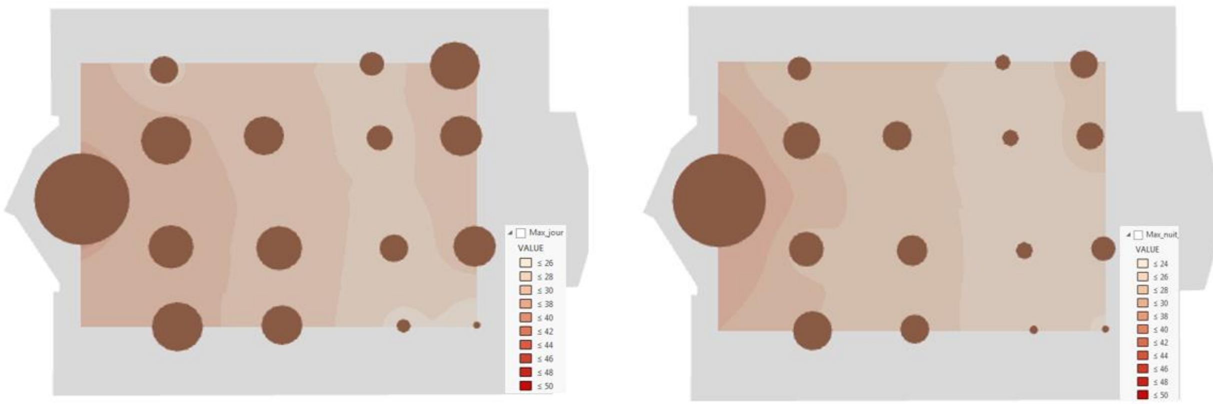

(a) (b)

Figure 2.40: Plan for temperatures' maximum distribution: (a) day, (b) night.

After understanding the temperature distribution of the expelled air, we compared this temperature variation to air and wall temperatures in the open space. Three sensors were installed on three internal walls and another three were installed in the air.

At first, we compare the internal wall and air temperatures in the open space to analyze their daily variation and to determine any differences. Figure 2.41 showed that the two variations are similar, and temperatures are close. Thus, we will not distinguish between air and wall temperature inside the open space.

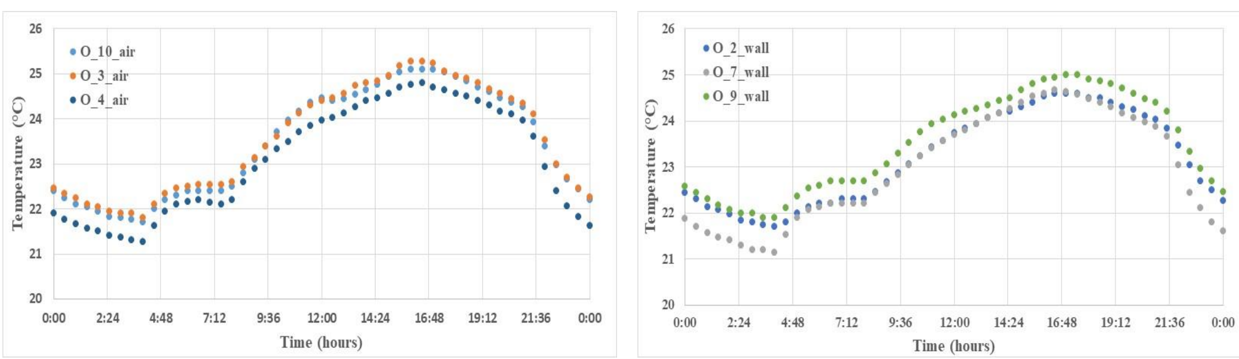

Figure 2.41: Air and wall temperatures variation in the open space.

By comparing the temperature inside the open space to the expelled air temperature, we noticed that at night temperatures are similar, while during the day a difference of 2°C is noted (figure 2.42). Thus, the temperature of the expelled air drops by 2°C while moving from the top ceiling to the human level.

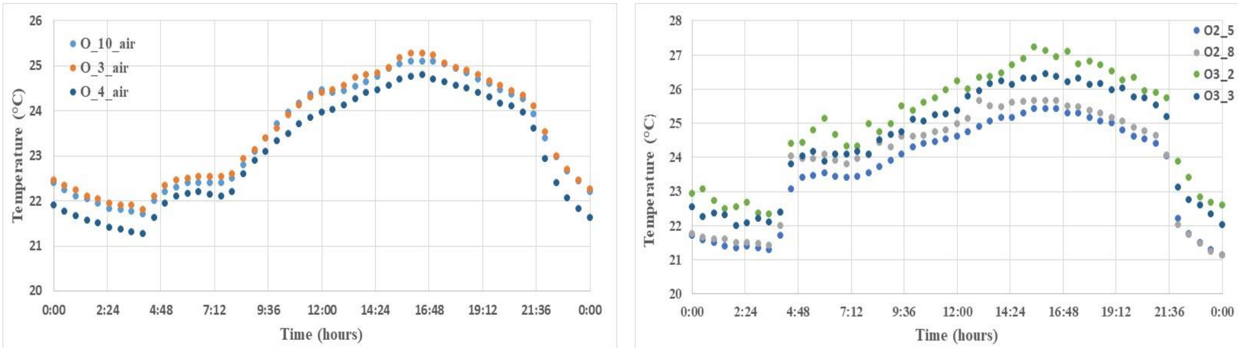

Figure 2.42: Variation of the temperature inside the open space and the expelled air temperature.

Same detailed analysis was performed to study the variation of the relative humidity of the expelled air through the vents. The major observations were a progressive increase from the start to the end for all statistical parameters of the relative humidity. By comparing the relative humidity inside the open space to the relative humidity of the expelled air, we noticed that at night relative humidity are similar, while during the day a difference of 4% is noted. Thus, the relative humidity of the expelled air increases by 4% while moving from the top ceiling to the human level.

The previous study presented the temperature and the relative humidity distribution of the expelled heated air through the vents. The analysis shows that the air temperature inside the open space can reach 25°C during the day. Thus, regulation can be applied to reduce this temperature through reducing the temperature of the expelled air. We have found that significant energy savings can be made through regulation acts.

2.5 Conclusion

This chapter presented an experimental thermal study conducted at three locations at the University of Lille Campus: One office in the first floor, 4 offices at the 4^{th} floor and one open space in 1 level building. Experimentations were conducted using an advanced monitoring system of the temperature and humidity.

The study showed that indoor parameters' distribution is not uniform within the room. We noticed variation of temperature and relative humidity in the room, even along one wall. This analysis allowed the optimization of the monitoring system by focusing on instrumentation of the external wall for the fourth floor. Other parameters were studied to determine their influence on the façade temperature. The study indicates that indoor conditions are largely affected by the orientation of the room and the state of windows. Moreover, two executed sets of scenarios showed the influence of users' behavior on energy consumption.

Furthermore, a detailed analysis of a central heating system for an open space is presented. A detailed investigation of the temperature distribution for the expelled air is executed. It shows that more significant energy savings can be done through regulation.

This chapter constitutes a preliminary study for the modeling approaches that will be presented in the next chapters. It indicates the major factors influencing the indoor temperature for better forecasting and optimization of the heating energy in order to improve buildings performance.

Chapter 3: Artificial neural network model

Introduction

This chapter presents a data-based model for indoor temperature forecasting, which could be used for the optimization of energy device use. The model is based on a black box nonlinear technique: 'artificial neural network (ANN)', which is validated on the recorded data of Polytech'Lille building. Two data set (occupied office and the four unoccupied classroom) will be used to consider different parameters for the prediction of the temperature.

This chapter proposed a methodology for the development of a simplified model for indoor temperature forecasting. This methodology is based on the selection of pertinent input parameters after a relevance analysis of a large set of input parameters, including solar radiation, outdoor temperature history, outdoor humidity, indoor façade temperature, humidity, orientation and state of windows. It shows that an ANN-based model using outdoor and façade temperature sensors provides good forecasting of indoor temperatures.
Flow chart 3.1 presents a summary of different applied ANN models.

3.1 Bibliographic analysis

To achieve an effective energy management strategy in buildings, an accurate indoor temperature prediction model is essential. It can provide a set of future boundary conditions and targets, which can guide a building facility manager to optimize the indoor temperature set-point so that ultimate improvement in building energy consumption and indoor thermal conditions are achieved. It also provides an initial check for facility managers and building automation systems to identify any inconsistency between the expected and actual indoor space temperature. The prediction algorithm can also be integrated with smart sensors and predictive control system and train them for future scenarios [48].
Indoor temperature forecasting could be carried out using physical or data-driven approaches [21]. The data-driven approach is based on the use of collected data for developing relationships (models) between 'input' parameters and 'output' parameters. These relationships could be established by learning from collected data. This application has been widely investigated in heating [49], cooling [50] and electric energy consumption [51] of buildings. Artificial neural networks (ANN) is a subcategory of machine learning which has repeatedly displayed reliable performances in various estimation problems. They can approximate any continuous nonlinear function to arbitrary accuracy leading to increasingly being used in solving complex practical problems [52]. The artificial neural network (ANN) approach was widely used in the literature to build data-driven models [53–55].
Many authors attempted, using ANN to analyze the heat transfer problems [56-58]. Other authors used neural networks to improve performance of built environment [59, 60]. Njau [61, 62] carried out some works on the prediction of surface air temperature and other weather parameters. Neural networks have been used also for the prediction of outdoor air temperature. Gobakis et al. [63] and

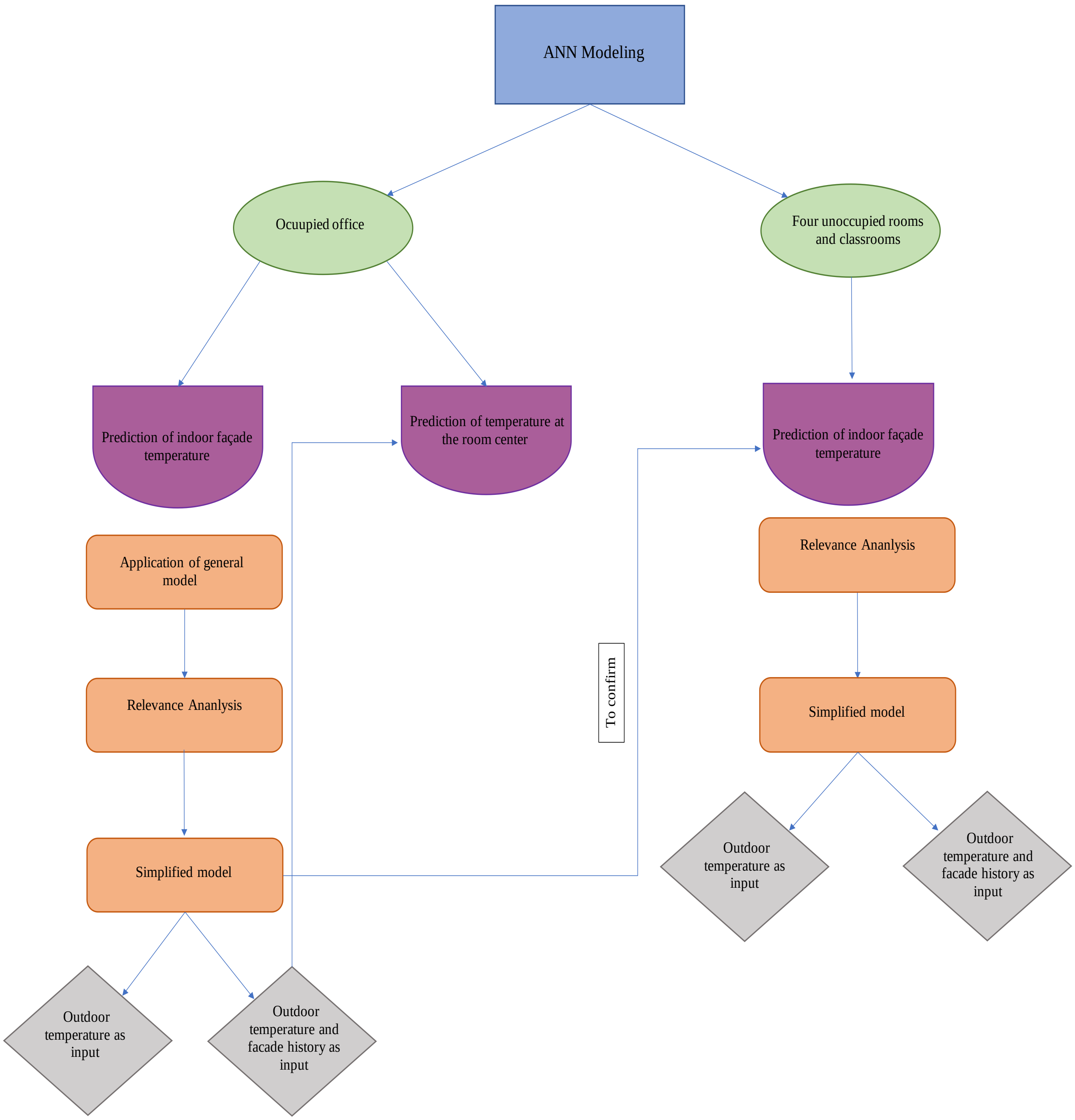

Flow chart 3.1: Different applied ANN models

Mihalakou et al. [64, 65] have predicted outdoor air temperature in Athens, Kolokotroni et al. [66] predicted it for the city of London. Outdoor ambient temperature, relative humidity and air velocity were estimated in India by Parishwad et al. [67]. They developed correlations using monthly mean values of these parameters. Imran et al. [68] used ANN for the prediction of hourly mean values of outdoor ambient temperature 24 h in advance. Soleimani-Mohseni et al. [22] showed that the operative temperature could be well estimated by the ANN approach using the indoor air temperature, electrical power, outdoor temperature, time of day, wall temperature, and ventilation flow rate. Lu and Viljanen [69] used the ANN approach to predict air temperature and relative humidity in a test room using indoor and outdoor temperature and humidity. Recently, Zabada and Shahrour [70] used the ANN approach for the analysis of the heating expenses in social housing. In these works, the ANN model was used as a prediction tool for specific cases.

3.2 Artificial Neural Network approach

The ANN approach is inspired from the ability of the human brain to predict patterns based on learning and recalling processes. It allows the construction of relationships between input parameters and output parameters using artificial neurons, which are arranged in an input layer, an output layer and one or more hidden layers [71]. Result of ANN depends upon number of hidden layer neurons. One way of selecting hidden layer neuron using optimize algorithm technique and other way is hit and trial method. In existing proposed model hit and trial method has been used and they got optimized number of hidden layer neuron very easily. Figure 3.1 represents a schematic diagram of typical multilayer feed-forward neural network architecture.

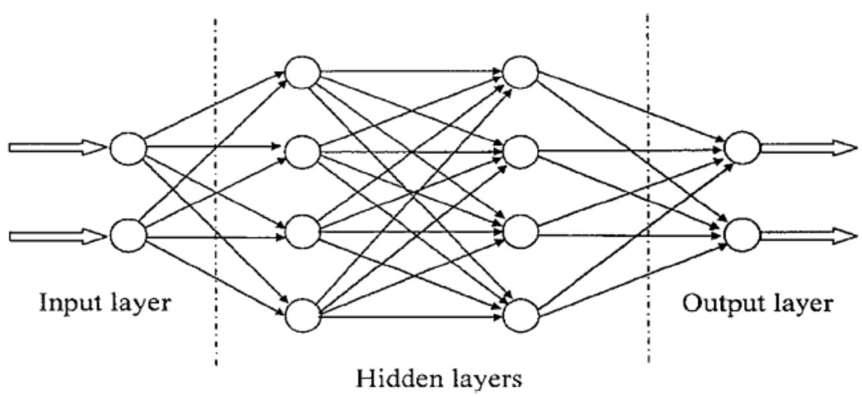

Figure 3.1: Schematic diagram of a fully connected multilayer feed-forward neural network.

In its simple form, each single neuron is connected to all other neurons of a previous layer through adaptable synaptic weights. Starting from an initially randomized weighted network system, input data is propagated through the network to provide an estimate of the output value. When each pattern is read the network uses the input data to produce an output, which is then compared to the training pattern, i.e. the correct or desired output. If there is a difference, the connection weights are altered in such a direction that the error is decreased. After the network has run through all the input patterns, if the error is still greater than the maximum desired tolerance, the ANN runs again through all the input patterns repeatedly until all the errors are within the required tolerance. When the training reaches a satisfactory level, the network holds the weights constant and uses the trained network to make decisions, identify patterns or define associations in new input data sets not used to train it.

The most popular learning algorithms are the backpropagation and its variants [72]. The backpropagation (BP) algorithm is one of the most powerful learning algorithms in neural networks. Back-propagation is a multi-stage dynamic system optimization method of training artificial neural networks to minimize the objective function. It is a supervised learning method and is a generalization of the delta rule. It is most useful for feed-forward networks (networks that have no feedback, or simply, that have no connections that loop). It tries to improve the performance of the neural network by reducing the total error by changing the weights along its gradient.

Analyses in this work were conducted using the multilayer back-propagation neural network on 'Matlab software'. We used a three-layer ANN with n, m, and p as the number of input parameters, hidden and output nodes, respectively, based on the following equation:

$$Y_k = S\left(\sum_{j=1}^{m} W_{jk} \times S\left(\sum_{i=1}^{n} W_{ij} X_i\right)\right), \tag{3.1}$$

where Y_k stands for the output values and $X_i$denotes the input values; W_{ij} gives the weights of connection between the input layer and the hidden layer.

The default method in the Neural Toolbox for improving generalization is called early stopping. In this technique, the available data is divided into three subsets. The first subset is the training dataset (50%). The process of training involves tuning the values of the weights and biases of the network to optimize network performance. The second subset (35%) is the validation dataset. Validation dataset is used to control the overfitting (overfitting occurs when a statistical model describes random error or noise instead of the underlying relationship). The error on the validation dataset is monitored during the training process. The validation error normally decreases during the initial phase of training, as does the training dataset error. However, when the network begins to overfit the data, the error on the validation set typically begins to rise. When the validation error increases for a specified number of iterations, the training is stopped, and the weights and biases at the minimum of the validation error are returned (i.e., minimum MSE). Finally, the testing dataset (15%) is used to evaluate each model.

The ANN performances could be evaluated using the mean square error (MSE) and the coefficient of correlation (R):

$$MSE = \sum_{i=1}^{n} \left(\frac{e_i^2}{N}\right), \tag{3.2}$$

$$R = \pm \sqrt{\frac{\sum_{i=1}^{N}(Y_i - \bar{X})^2}{\sum_{i=1}^{N}(X_i - \bar{X})^2}} = \sqrt{1 - \frac{\sum_{i=1}^{N}(e_i)^2}{\sum_{i=1}^{N}(X_i - \bar{X})^2}} \quad (3.3)$$

where e_i is the error between the ANN output (Yi) and the experimental input (Xi), $\bar{X}$ represents the mean of the input target.

Different ANN architectures exist. The multilayer perceptron (MLP) structure is the most popular [73-78]. Its use with a single hidden layer and a sufficient number of neurons provided good accuracy for the approximated function [68, 79]. This architecture is used in this work.

3.3 Prediction time

Depending on the objective of the prediction model, long-term and short-term load prediction can be used. The long-term load prediction model optimally arranges the operation of the HVAC systems through providing heating or cooling demand in advance. While the short-term load prediction model considers the large load fluctuation that may occur and improves the operational safety of HVAC system [80].

In this work, the short-term prediction is considered. It depends on the building thermal inertia and energy regulation system. Each building is characterized by its time lag and the time of heat transmission delay [81–83]. The determination of the prediction time for ANN models is based on these characteristics. This time should cover the phase of heating exchange through the façade to consider loads' fluctuation to investigate the effectiveness of ANN approach.

To determine the response time of the façade, an air conditioner was launched at a certain temperature (17°C) (detailed experimentations were discussed previously), and the variation of the façade temperature were investigated. Figure 3.2 indicates that the response time of the façade to the temperature variation inside the room is nearly 3 hours.
Thus, the prediction time for ANN models in this work were chosen to range from 0.5 hours to 4 hours (with 30 min interval) to cover the phase of heating exchange through the façade.

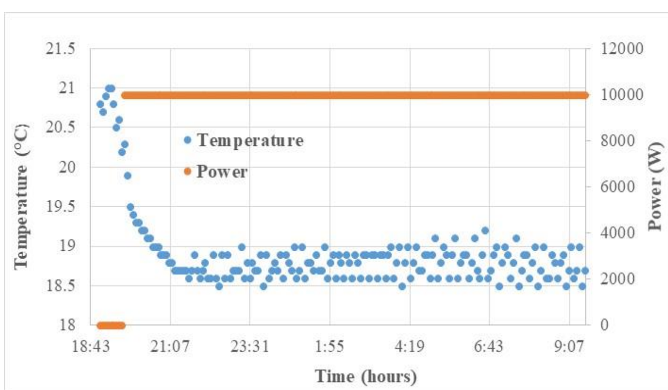

Figure 3.2: Façade temperature variation and the air conditioner power.

3.4 ANN models

3.4.1 Facade Indoor Temperature Forecasting – Occupied office

3.4.1.1 Analysis of the input relevance

The input parameters used in the global analysis are summarized in table 3.1. They concern the outdoor conditions (temperature, humidity and solar radiation), outdoor temperature history (input matrix for the last 3h values having 30min lag between its different columns: if the actual outdoor temperature was recorded at time t, the history matrix corresponds to t-0.5h, t-1h, t-1.5h, t-2h, t-2.5h and t-3h, the indoor facade temperature history (similar matrix history as the outdoor temperature) and time (cumulative minutes of the day).

Table 3.1: Input parameters for the façade temperature forecasting.

Input Parameters
Outdoor temperature
Outdoor Humidity
Solar radiation
Outdoor temperature history
Time
Façade temperature history

The ANN optimal architecture is presented in figure 3.3. It includes 1 hidden layer with 4 neurons. Table 3.2 provides the weight of neurons' connections. We can observe that the weight could be negative or positive providing excitatory or inhibitory influence on each input. It varies for different parameters and neurons revealing complex connections and relations.

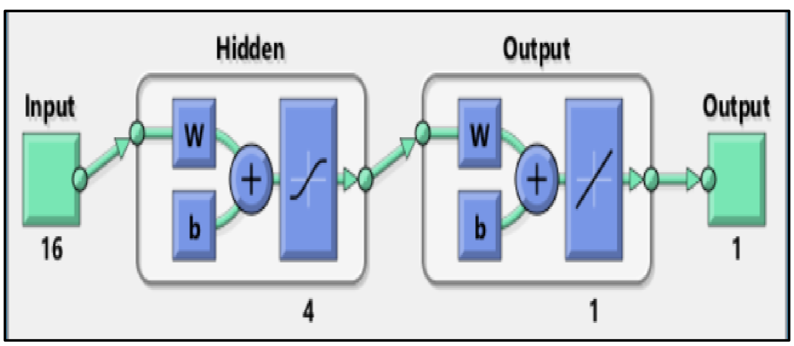

Figure 3.3: ANN optimal architecture.

Figure 3.4 shows a comparison of "predicted" and "recorded" façade temperatures. We observe a good agreement between these values with R=0.9967 and MSE=0.0277. This result shows that the ANN model predicts well the façade indoor temperature. The determination of input parameters requires 2 temperature sensors (outdoor and indoor), an external humidity sensor and a solar radiation sensor.

Table 3.2: Weight of neurons' connections.

Input parameters	Neuron 1	Neuron 2	Neuron 3	Neuron 4
Time	2.59	0.02	1.46	-0.02
Outdoor temperature	1.13	-1.25	-0.05	1.32
History of outdoor temperature	2.55	1.65	-0.93	-1.60
	1.79	-1.05	-1.66	0.93
	2.67	0.62	-2.02	-0.64
	-1.11	-0.95	0.17	0.92
	-1.21	0.21	-0.54	-0.27
	0.86	-0.02	0.23	0.06
History of façade temperature	-2.65	-0.72	-2.76	1.43
	-3.00	0.90	-1.58	-1.12
	-1.04	0.50	-1.20	-0.38
	-0.26	0.61	-1.18	-0.57
	0.50	-0.31	-0.13	0.33
	-0.34	0.07	-1.10	-0.12
Solar radiation	1.27	0.23	3.52	-0.22
Outdoor humidity	0.01	-0.10	-0.43	0.09

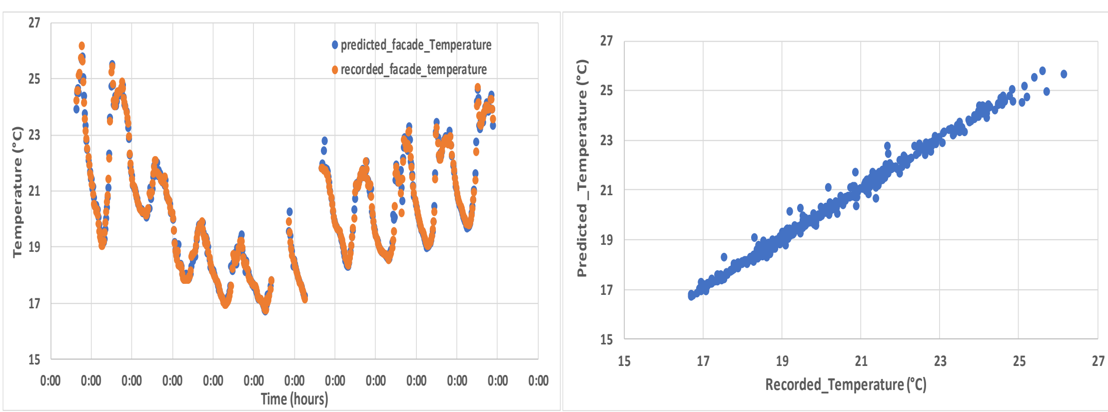

(a) (b)

Figure 3.4: Predicted and recorded façade temperatures: (a) Variation of both temperatures in time domain; (b) Predicted façade temperature with the recorded façade temperature.

In order to determine the most relevant input parameters in the ANN model, IBM SPSS Statistics software was used to analyze the “importance” of these parameters. Table 3.3 summarizes the obtained results. It shows that the solar radiation, time and humidity have a very low role in the model, with an importance factor lower than 5.1%. The outdoor temperature has the highest importance (Importance Factor = 42%), followed by the historical façade temperature (Importance Factor = 31.9%). The historical outdoor temperature has an intermediate influence with an Importance Factor = 12.8%.

Table 3.3: Analysis of the relevance of input parameters.

Parameter	Importance Factor (%)
Solar radiation	3.7
Time	4.5
Humidity	5.1
Historic Outdoor Temperature	12.8
Historic Façade Temperature	31.9
Outdoor Temperature	42.0

Since the role of some input parameters in the ANN model is very weak, analyses were conducted in neglecting these parameters. Table 3.4 summarizes the results of these analyses. It shows clearly that the neglect of solar radiation, humidity and historical outdoor temperature does not deteriorate significantly the quality of the ANN model: The mean square error (MSE) increases from 0.0277 to 0.0365, while the coefficient of correlation (R) decreases from 0.9967 to 0.9959. The additional neglect of the historical data of the façade temperature has a higher influence. MSE increases from 0.0277 to 0.4922, while R decreases from 0.9967 to 0.946. This result shows that the façade temperature could be predicted with a high precision in considering only the outdoor temperature and the historical data of the facade indoor temperature. Figure 3.5 illustrates the results of models 1,5 and 6.

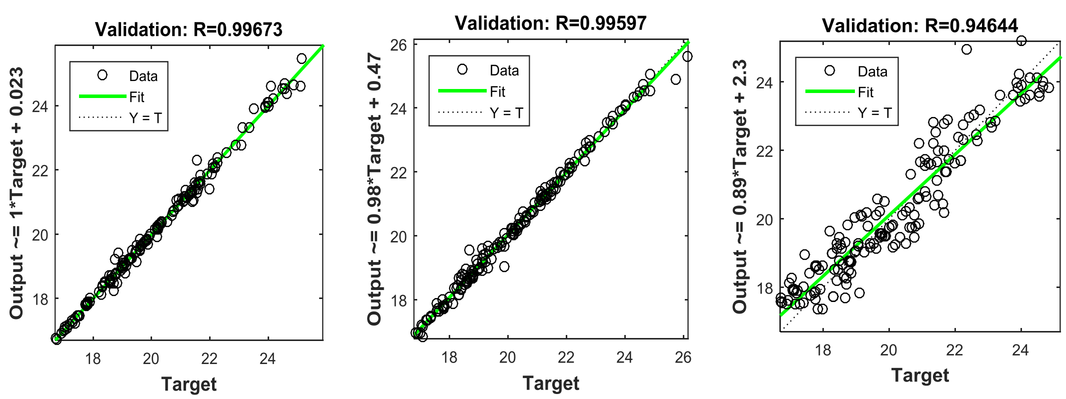

(a) (b) (c)

Figure 3.5: R results for different models: (a) Model 1; (b) Model 5; (c) Model 6.

Table 3.4: Degraded models result.

Model	Input parameter	R	MSE
1	Outdoor Temperature, Historic, Outdoor Humidity, Sun radiation, time, Facade Historic	0.9967	0.0277
2	Outdoor Temperature, Historic, Outdoor Humidity, time, Facade Historic	0.99687	0.0300
3	Outdoor Temperature, Historic, Outdoor Humidity, Facade Historic	0.9969	0.0269
4	Outdoor Temperature, Historic, Facade Historic	0.9975	0.0199
5	Outdoor Temperature, Facade Historic	0.9959	0.0365
6	Outdoor Temperature	0.946	0.4922

3.4.1.2 Façade temperature forecasting model – Use of the outdoor temperature as input parameter

Considering the results of the previous section, the outdoor temperature is first used as input parameter for forecasting the façade indoor temperature. The forecasting model provides the temperature at 0.5, 1, 2 and 4 hours.

Figures 3.6 and 3.7 show the forecasting results at 0.5 and 1.0 hour. We observe that the ANN model reproduces well the recorded temperature. For 0.5-hour forecasting, R is equal to 0.956 and MSE is equal to 0.4369; while for 1-hour forecasting, R = 0.928 and MSE = 0.48454. Figure 3.8 shows the forecasting error distribution for 0.5 and 1 hour. It shows that about 90% of the forecasting error are less than 1° C.

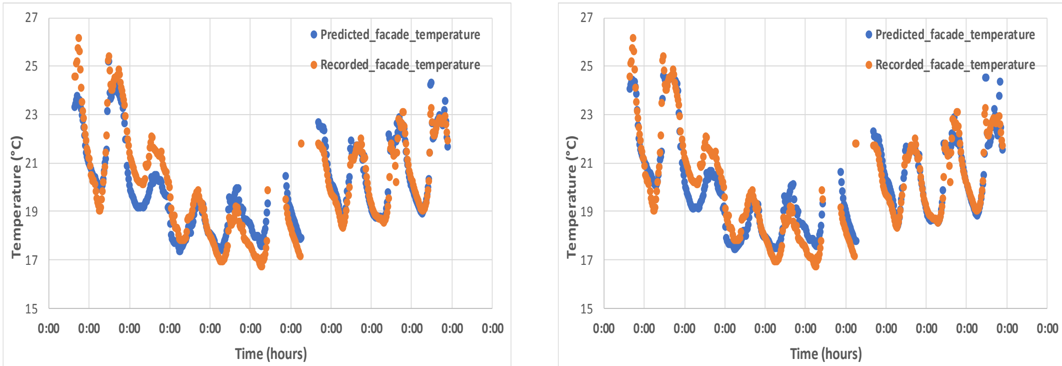

(a) *(b)*

Figures 3.6: Recorded and predicted façade temperature variation in the time domain: prediction for 0.5h; (b) prediction for 1h.

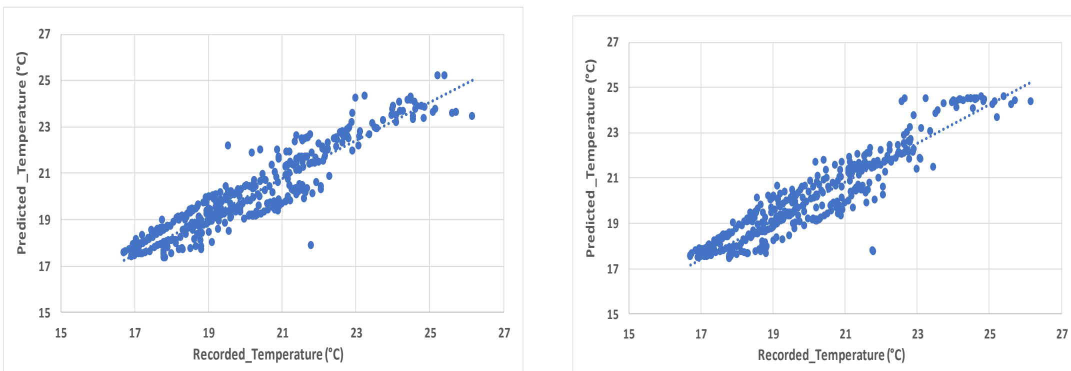

(a) *(b)*

Figures 3.7: Predicted façade temperature with the recorded façade temperature (Input parameter = Outdoor temperature): (a) prediction for 0.5h; (b) prediction for 1h.

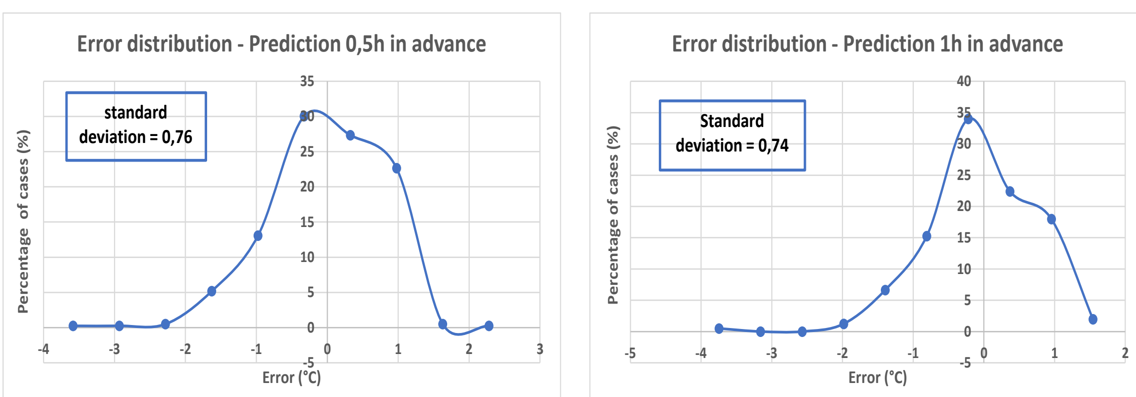

(a) *(b)*

Figures 3.8: Distribution of the error forecasting (Input parameter = Outdoor temperature): (a) prediction for 0.5h; (b) prediction for 1h.

Figures 3.10 and 3.11 shows the forecasting results at 2 and 4 hours. We observe a deterioration in the quality of forecasting regarding to those obtained at 0.5 and 1 hour. For 2 h forecasting, R = 0.9109 and MSE = 0.89078, while for 4-hours forecasting, R = 0.8370 and MSE =1.23783. Figure 3.10 shows the forecasting error distribution for 2 and 4 hours. It shows that for the former, about 70% of the forecasting error are less than 1° C, while for the latter about 64 % of the forecasting error are less than 1° C. Table 3.5 summarizes the forecasting results.

Table 3.5: Performances of the forecasting models (Input parameter = Outdoor temperature).

Model	Time	R	MSE
1	+ 0.5 hour	0.9560	0.436900
2	+ 1 hour	0.9528	0.484594
3	+ 2 hours	0.9109	0.89078
4	+ 4 hours	0.8370	1.23783

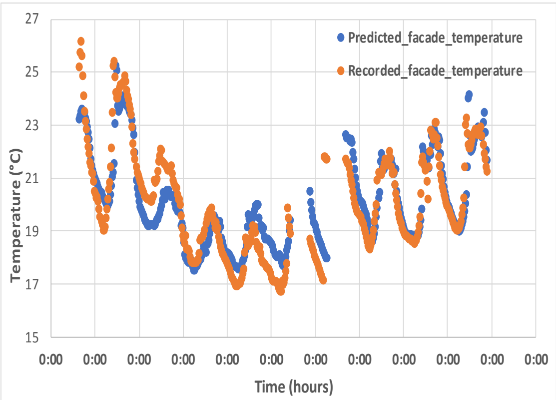

(a)

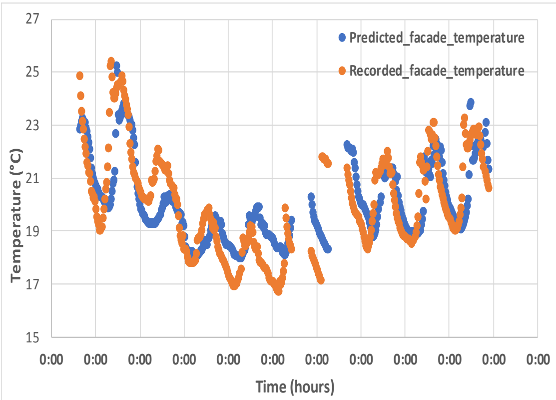

(b)

Figures 3.9: Recorded and predicted façade temperature variation in the time domain: (a) prediction for 2h; (b) prediction for 4h.

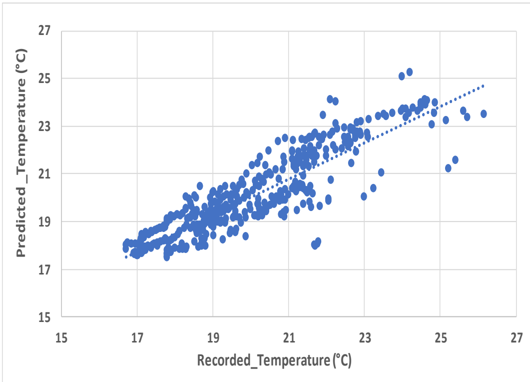

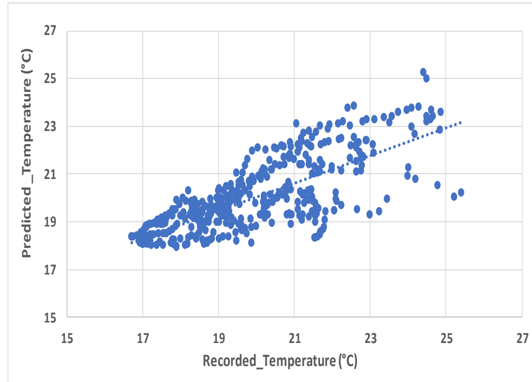

(a) (b)

Figures 3.10: Predicted façade temperature with the recorded façade temperature (Input parameter = Outdoor temperature): (a) prediction for 2h; (b) prediction for 4h.

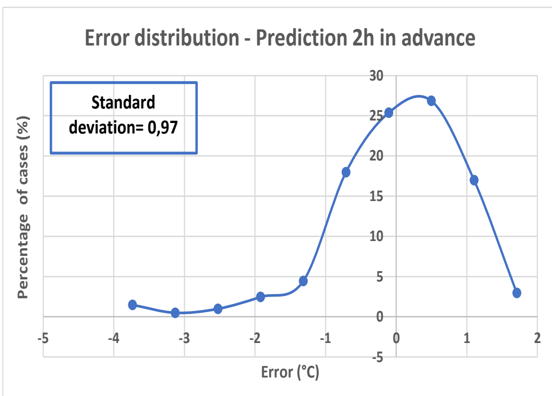

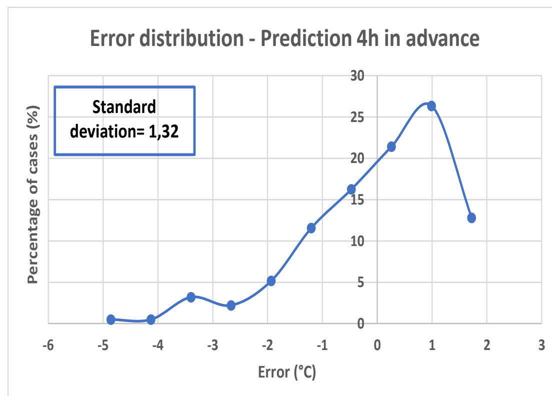

(a) (b)

Figures 3.1: Distribution of error forecasting (Input parameter = Outdoor temperature): (a) prediction for 2h; (b) prediction for 4h.

3.4.1.3 Façade temperature forecasting model – Use of the outdoor temperature and the history of the façade temperature as input parameters

In this section, both outdoor temperature and 3 hours façade temperature history are used as input parameters in the forecasting model. The forecasting model provides the temperature at 0.5, 1, 2 and 4 hours. Table 3.6 summarizes the obtained results. The temperature forecasting is improved regarding the forecasting model using the outdoor temperature as input. This result is particularly interesting for the temperature foresting at 2 hours: R = 0.957 and MSE = 0.3299 to be compared with R = 0.9109 and MSE = 0.89078 obtained with the outdoor temperature as input parameter. Figure 3.12 shows the forecasting error distribution for 2 hours. It shows that about 88% of the forecasting error are less than 1° C to be compared with 70% obtained with the previous model.

The 4-hours forecasting at is still weak with R = 0.852; MSE = 1.0533. About 68% of the forecasting error are less than 1°C (Figure 3.12).

Table 3.6: Performances of the forecasting models (Input parameters = Outdoor temperature and 3 hours façade temperature).

Model	Time	R	MSE
1	+ 0.5 hour	0.992	0.0701
2	+ 1 hour	0.982	0.1515
3	+ 2 hours	0.957	0.3299
4	+ 4 hours	0.852	1.0533

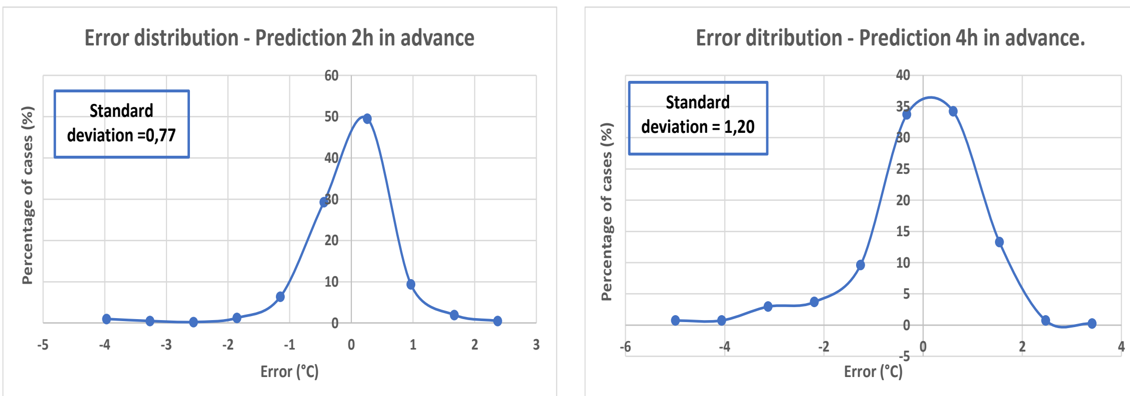

(a) *(b)*

Figures 3.12: Distribution of error forecasting (Input parameter = Outdoor temperature and 3h façade temperature): (a) prediction for 2h; (b) prediction for 4h.

3.4.1.4 Indoor temperature forecasting (room center)

The ANN approach is used for forecasting the temperature at the room center considering only the façade temperature as input parameter. Figure 3.13 shows a comparison of "predicted" and "recorded" indoor temperatures. A good agreement is observed between recorded temperature and ANN prediction: R =0.951; MSE=0.1679. Only 1% of data have a mean absolute error greater than 1° C (Figure 3.14).

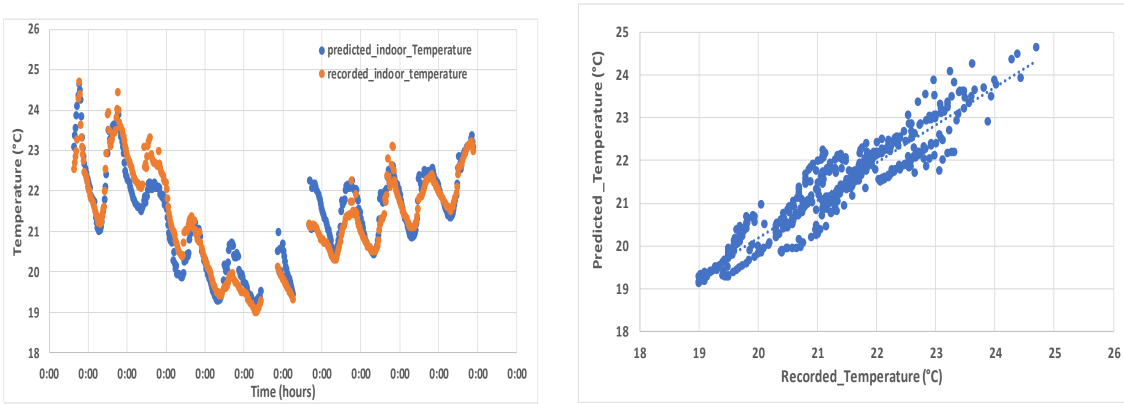

(a) (b)

Figures 3.13: Predicted and recorded indoor temperatures: (a) Variation of both temperatures in time domain; (b) Predicted indoor temperature with the recorded indoor temperature.

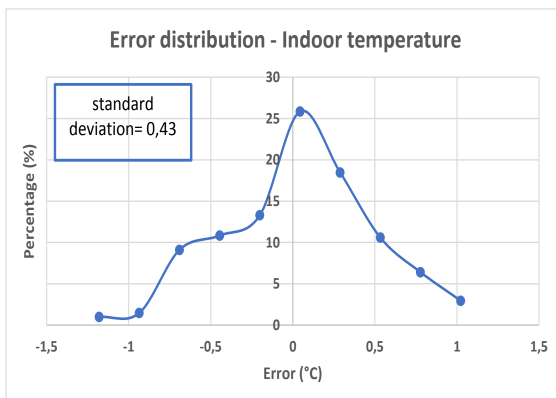

Figure 3.14: Distribution of error forecasting for indoor temperature (input parameters = façade temperature).

The purpose of this section is to forecast the indoor temperature through a simplified ANN-based model to optimize the control of energy building devices. Two ANN models were developed for forecasting the façade indoor temperature and the temperature in the office center, respectively. Analysis shows that the ANN approach can effectively forecast the temperature at the room center considering only the façade temperature as input parameter.

3.4.2 Facade Indoor Temperature Forecasting – Four unoccupied classrooms

3.4.2.1 Analysis of the input relevance

Since the role of some input parameters in the ANN model were shown previously weak, analyses were conducted in neglecting these parameters (solar radiation, humidity and time). Input parameters in this section concern the outdoor temperature, outdoor temperature history (input matrix for the last 3h values having 30min lag between its different columns: if the actual outdoor temperature was recorded at time t, the history matrix corresponds to t-0.5h, t-1h, t-1.5h, t-2h, t-2.5h and t-3h, the indoor facade temperature history (similar matrix history as the outdoor temperature), windows state (open or closed) and orientation of the room (north or south). The input parameters used in the global analysis are summarized in table 3.7.

Table 3.7: Input parameters for the façade temperature forecasting.

Input Parameters
Outdoor temperature
Outdoor temperature history
Windows state
Orientation
Façade temperature history

In order to determine the most relevant input parameters in the ANN model, IBM SPSS Statistics software was used to analyze the "importance" of these parameters. Table 3.8 summarizes the obtained results. It shows that the orientation and state of windows have a very low role in the model, with an importance factor lower than 5%. The outdoor temperature has the highest importance (Importance Factor = 59.7%), followed by the historical façade temperature (Importance Factor = 19.0%) and the historical outdoor temperature (Importance Factor = 17.6%).

Table 3.8: Analysis of the relevance of input parameters.

Parameter classification	Importance %
Orientation	1.3
State of windows	2.5
Historic Outdoor Temperature	17.6
Historic Façade Temperature	19.0
Outdoor Temperature	59.7

Previous analysis showed that the orientation and state of windows have an important influence on the façade temperature distribution. However, table 3.8 reveals their minor role vis a vis the historic of the façade temperature. We should note that these two parameters (orientation and state of windows) were considered implicitly in the historic façade temperature parameter.

To reveal the importance of the orientation and state of windows parameters, many models were executed by increasing the number of input parameters and comparing their performances to be able to study their influence on the façade temperature.

At first, we started by a simple model including the outdoor temperature as input. The façade temperature will be the target (output) in all the models. We noticed that, the model cannot be considered performing with R=0.853 and MSE=4.3328. Then, we added the parameters successively and compared the performance of each model. The results are noted in the table 3.9.

The outdoor temperature is the most important parameter since the simple model results in R=0.853. The second one is the temperature historic of the façade by improving R by 3.4% and MSE by 95%. By adding the orientation parameter, R is improved by 3.1% and MSE by 44.3 %. The state of windows improved R by 5.1%. Comparing models' performance reveals the importance of each parameter. The one contributing in a larger increment of R and decrement of error is more important than the others.

This analysis shows that the façade temperature distribution is influenced by the orientation and the state of windows. Figure 3.15 illustrates the results of the optimal model.

Table 3.9: Performance of different Models for the unoccupied rooms.

Model	input parameters	R	MSE
1	Outdoor Temperature	0.853	4.3890
2	Outdoor Temperature, Historic	0.891	3.3891
3	Outdoor Temperature, Historic, State of windows	0.936	1.9959
4	Outdoor Temperature, Historic, State of windows, Orientation	0.965	1.1534
5	Outdoor Temperature, Historic, State of windows, Orientation, Historic façade temperature	0.998	0.0581

In order to confirm that 'the façade temperature could be predicted with a high precision in considering only the outdoor temperature and the historical data of the facade indoor temperature, similar analysis to the occupied office is executed.

Since the role of some input parameters in the ANN model is weak vis a vis the historic of the façade temperature, analyses were conducted in neglecting these parameters. Table 3.10 summarizes the results of these analyses. It shows clearly that the neglect of the orientation, state of windows and historic of outdoor temperature does not deteriorate significantly the quality of the ANN model: The mean square error (MSE) increases from 0.0595 to 0.1294, while the coefficient of correlation (R) decreases from 0.998 to 0.996. The additional neglect of the historical data of the façade temperature has a higher influence. MSE increases from 0.0595 to 4.2437, while R decreases from 0.998 to 0.852. This result confirms that the façade temperature could be predicted with a high precision in considering only the outdoor temperature and the historical data of the facade indoor temperature. Figure 3.16 illustrates the results of models 4 and 5.

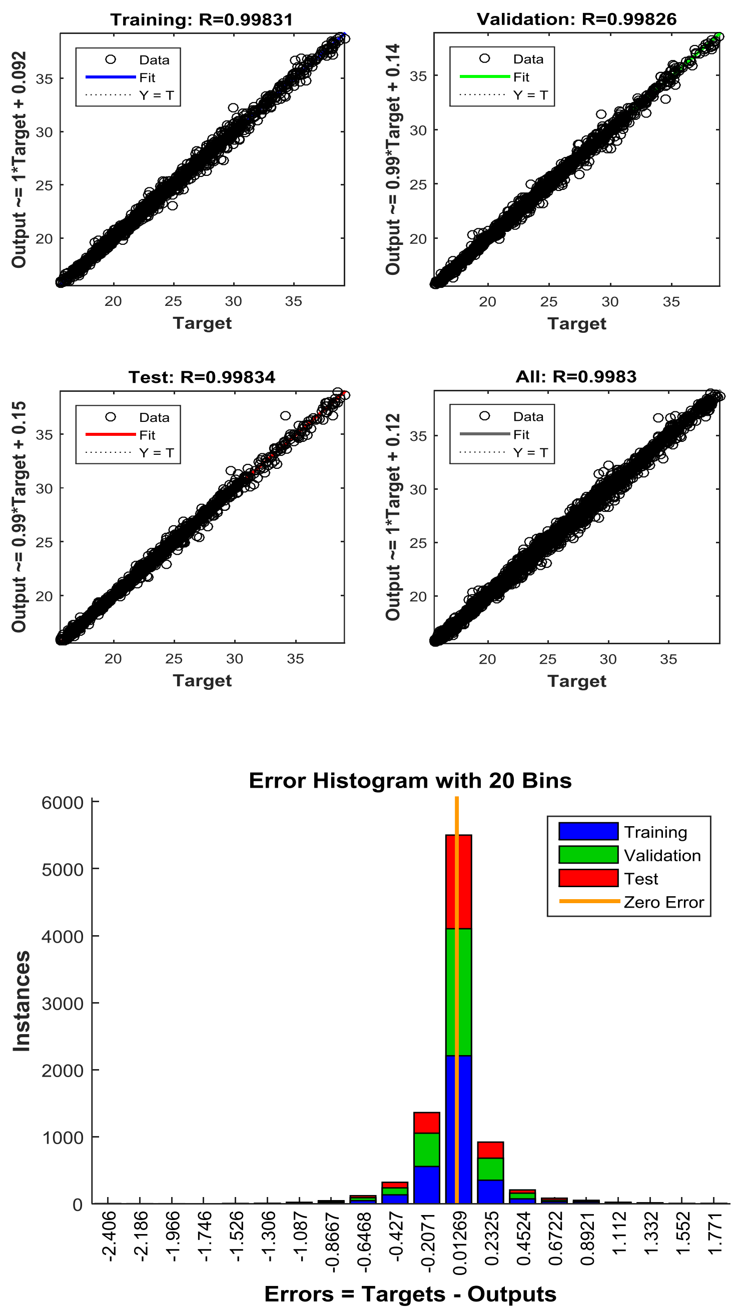

Fig. 3.15: Results of the optimal model for the unoccupied rooms.

Table 3.10: Degraded models result.

Model	input parameters	R	MSE
1	Outdoor Temperature, historic, windows state, Orientation, Façade Historic	0.998	0.0595
2	Outdoor Temperature, historic, windows state, Façade Historic	0.998	0.0716
3	Outdoor Temperature, historic, Façade Historic	0.998	0.0736
4	Outdoor Temperature, Façade Historic	0.996	0.1294
5	Exterior Temperature	0.852	4.2437

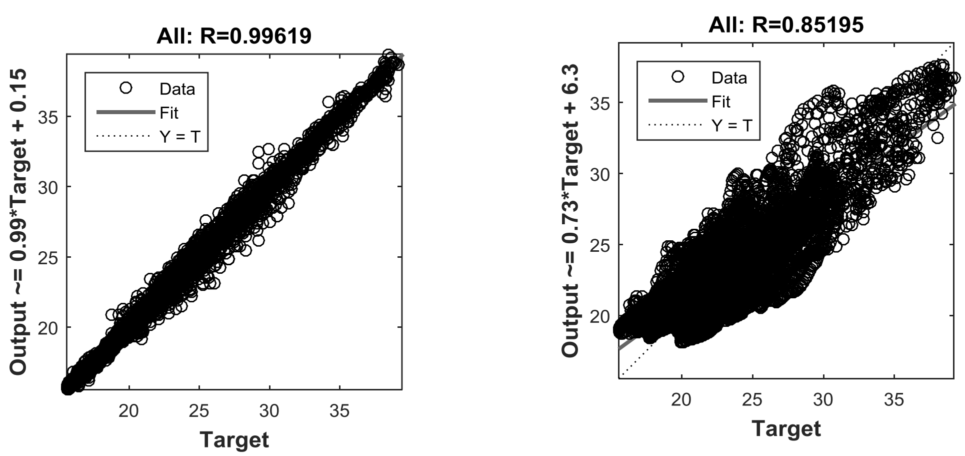

(a) *(b)*

Figure 3.16: R results for different models: (a) Model 4; (b) Model 5.

3.4.2.3 Façade temperature forecasting model – Use of the outdoor temperature and the history of the façade temperature as input parameters

Similar to previous predictions (the occupied office) and relying on prior results, both outdoor temperature and 3 hours façade temperature history are used as input parameters in the forecasting model that provides the temperature at 0.5, 1, 2 and 4 hours.

Table 3.11 summarizes the obtained results. We observe that the ANN model reproduces well the recorded temperature. For 0.5-hour forecasting, R is equal to 0.991 and MSE is equal to 0.2727; while for 1-hour forecasting, R = 0.981 and MSE = 0.6753. Figure 3.17 shows the forecasting error distribution for 0.5 and 1 hour. It shows that about more than 80% of the forecasting error are less than 1° C (respectively 88% and 81%).

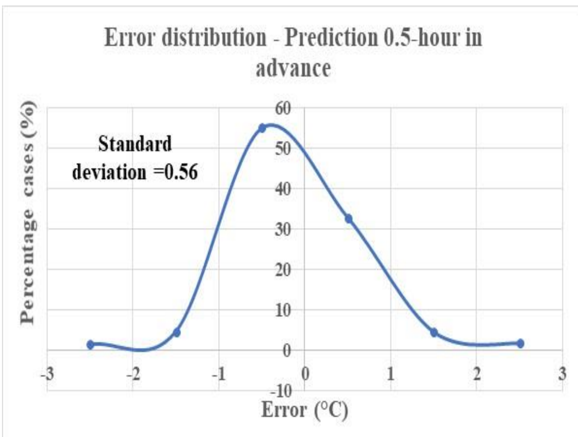

(a)

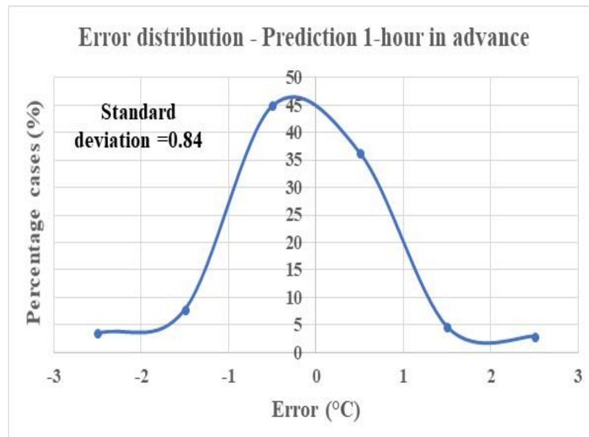

(b)

Figures 3.17: Distribution of error forecasting (Input parameter = Outdoor temperature and 3h façade temperature): (a) prediction for 0.5h; (b) prediction for 1h.

For 2-hour forecasting, R=0.951 and MSE=1.5473. Figure 3.18 shows the forecasting error distribution for 2 hours. It shows that about 60% of the forecasting error are less than 1° C (it can be considered relatively acceptable).

For 4-hour prediction, we observe a deterioration in the quality of forecasting regarding to those obtained at 0.5, 1 and 2-hour. The 4-hours forecasting is weak with R=0.890 and MSE=3.6500. About 45% of the forecasting error are less than 1°C (Figure 3.18).

This section confirms the prediction results obtained previously for the forecasting of the façade temperature for the occupied office.

Table 3.11: Performances of the forecasting models (Input parameters = Outdoor temperature and 3 hours façade temperature).

Model	Time	R	MSE
1	+ 0.5 hour	0.991	0.2727
2	+ 1 hour	0.981	0.6753
3	+ 2 hours	0.951	1.5473
4	+ 4 hours	0.890	3.6500

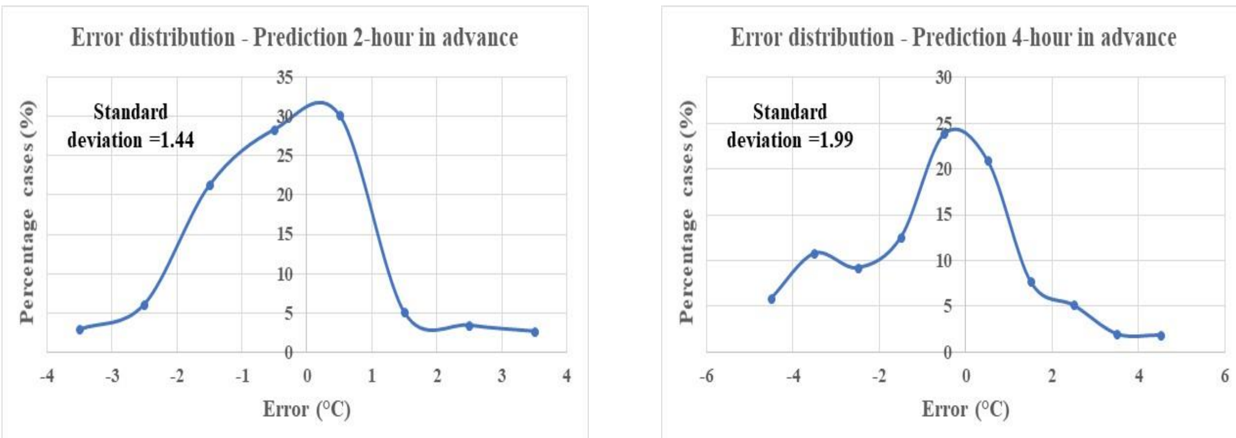

(a) *(b)*

Figures 3.18: Distribution of error forecasting (Input parameter = Outdoor temperature and 3h façade temperature): (a) prediction for 2h; (b) prediction for 4h.

3.5 Conclusion

This chapter presented ANN prediction models for forecasting façade and indoor temperature for the 'polytech'Lille' building. This study proposed a methodology for the development of a simplified ANN-based model for forecasting indoor temperature. The methodology includes two steps. The first step concerns the forecasting of the indoor façade temperature considering outdoor and indoor conditions, while the second step concerns the prediction of the temperature at the room center considering only the indoor façade temperature.

This chapter showed that both relevance analysis and the use of different sets of input parameters could lead to a simplified forecasting model with restricted input parameters. This methodology was illustrated through its application to data collected in an old building. Data included outdoor and indoor temperature and humidity, as well as solar radiation, orientation and state of windows. Analyses showed that two-hour façade temperature forecasting could be conducted with good precision using only the outdoor temperature and three-hour façade temperature history. This result could not be generalized. However, the proposed methodology could be used for other situations by using at first only temperature sensors for measuring the outdoor and the indoor façade temperatures. Concerning the second step, the ANN model gave good forecasting of the temperature at the room center in considering only the façade temperature.

Chapter 4: Grey box model

Introduction

This chapter presents a preliminary study for the generation of an automated process for model's training and identification to determine short term indoor temperature prediction and buildings characteristics based on grey-box modeling.
The study is based on a methodology capable of finding the most reliable set of data that describes the best the building's dynamics. It shows that the data set used for identification and the estimation period has an important influence on the robustness of the identified models.
In this investigation, three distinct set of collected data from building A4 were used and applied on four different grey-box structures. The analysis of results indicates that the quality of the obtained model is governed by the dynamic information of collected data.
Flow chart 4.1 presents a summary for the applied grey box model.

4.1 Bibliographic analysis

Reduced order grey-box models constitute a suitable approach in predictive control as they combine building physics and model structure knowledge (typical of the white-box approach) with parameters' estimation through measured data (black-box approach).
Grey-box models have been formulated for separate building components i.e. walls [84,85] as well as for whole buildings [86–88]. Most authors focus on determining the required order of the model and the building elements that should be lumped into separate capacities [90]. Hedgaard and Peterson [91] investigated grey-box model structures to identify the building dynamics and to determine buildings' characteristics. The results indicated that both second and third order models produce good estimation for the short time constant, the effective thermal mass and the total heat loss coefficient. Bacher and Madson [92] evaluated different models for predicting the indoor temperature using data from unoccupied building as reference. They showed that results were not improved by increasing the model order beyond 3. Moreover, Fux et al. [93] compared reduced-order grey box models and concluded that a one-capacity model is sufficient to forecast the indoor temperature of a residential building.
Since simulated data are often used in the literature for modeling, Harb et al. [94] used parameters estimation models entirely based on historical data without any pre-knowledge requirements about the occupied building. This study presented an optimization algorithm to find a model parameters' set which gives the best approximation of the simulated indoor air temperature to the respective measured values. Furthermore, Fonti et al. [95] used measured data and analyzed an identification procedure to investigate the accuracy of different grey-box model order for short-term thermal behavior prediction in a real building, part of a living smart district. Grey-box building models presented in the previous studies tend to be too specific in their application. In the following, we

present the Grey Box approach and then its use for predicting the indoor temperature of an instrumented building of Lille University "A4".

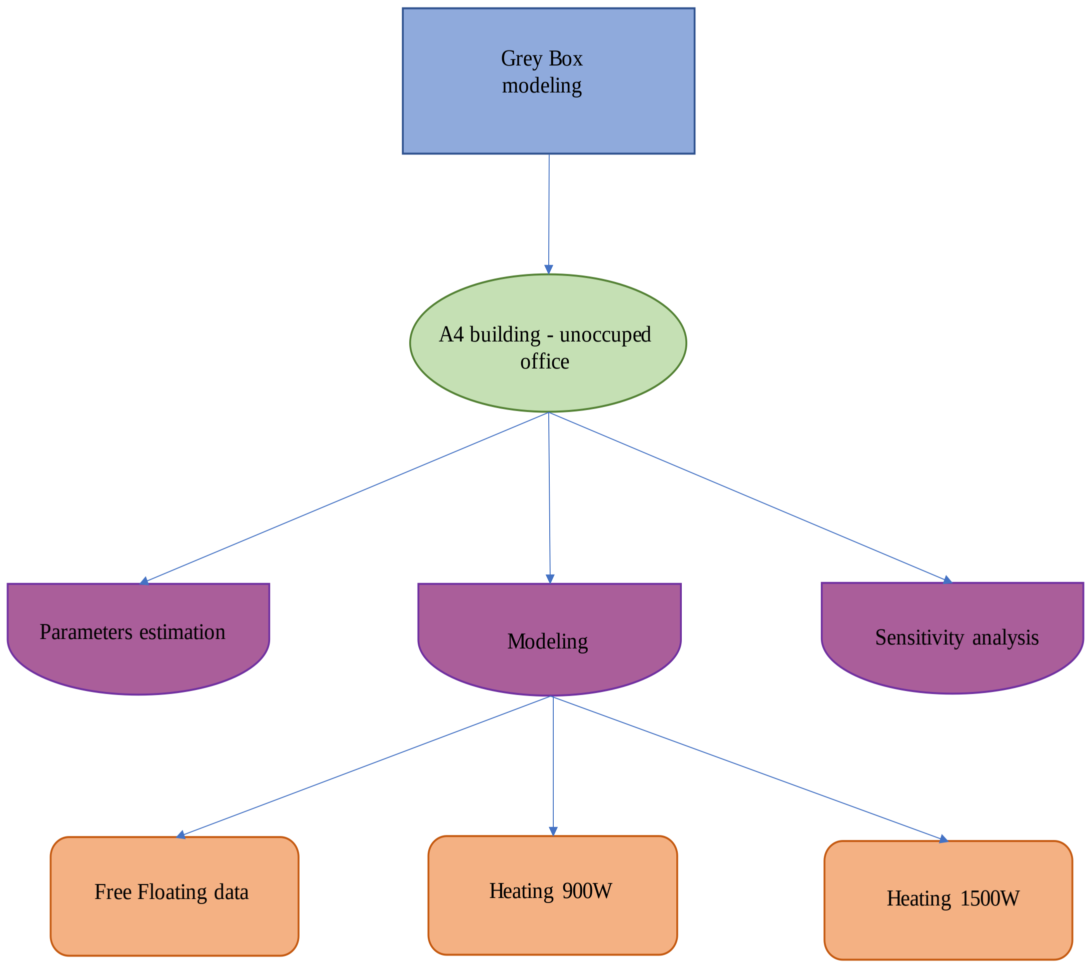

Flow chart 4.1: Grey box modeling summary.

4.2 Grey Box approach

The thermodynamic behavior of a building can be described by a so called "lumped parameter" model [96] in the form of an RC equivalent circuit. The concept of a "thermal network" describes how heat energy can flow between elements of the building and its surroundings, modeled as nodes in a Resistor-Capacitor (RC) circuit.

In Figure 4.1 a building with a simple RC model is presented, showing how a resistor can be used as a model of the walls' resistance to heat flow, while a capacitor represents the buildings capacity to store thermal energy. The node market represents the interior of the building.

Thermal behavior of a building is described by the flow of heat Q and the temperature T at specific points [97]. Heat flow, in the unit of Watt (W), can be induced by a heater, solar irradiation or building occupants and it can be driven by a temperature differential, in the unit of Kelvin (K) or Celsius (C). For a differential between two absolute temperatures the units K and C are interchangeable.

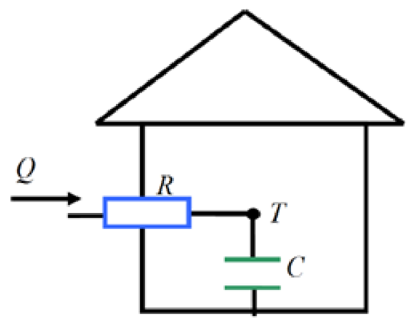

Figure 4.1: Thermal model of a building.

Relationship between temperature differential and heat flow, is determined by the thermal resistance that the temperature differential acts across [97], in the unit of Kelvin per Watt. Thermal energy can be stored in objects, such as furniture, walls and roof, as determined by the object's thermal capacity, in the unit of Joules per Kelvin [97]. The amount of energy required to raise the temperature in an object depends on the thermal capacitance. All these thermal parameters can be described by electrical equivalents, and the building can then be modeled as a simple Resistor-Capacitor (RC) circuit [97], and analyzed using conventional circuit theory, e.g. Kirchhof's Laws, potential dividers, Ohms Law and Laplace transformation for impedance computations [98].

Flow of heat is modeled as current in an electric circuit, where the driving potential is the temperature, modeled as voltage. Using this analogy, a resistor becomes thermal resistance, while thermal capacitance is modeled as electrical capacitance [97]. Modeling thermal flow in a building using the electrical circuit analogy has the advantage of being simple. The intuitive understanding gained from these simple model structures is important when working with grey-box models. Since no accurate physical model, i.e. white box, is needed, the intuitive, or cognitive [96], derivation of an RC network allows models to be derived based on knowledge about the building's thermal behavior, without use of complicated thermodynamic laws and equations.

Grey box models are established using the combination of building's physics and statistics. Physical knowledge derived from building's dynamics is formulated by a set of continuous stochastic differential equations formulated in a state space form [99]. Statistical measurements present information embedded in the collected data.

$$dX(t) = A(\theta)X(t) + B(\theta)U(t) + \sigma(\theta)dw \qquad (4.1)$$

$$Y(t) = C(\theta)X(t) + D(\theta)U(t) + \varepsilon$$

In these equation X(t) represents the vector state of the dynamic system, in this research, the states correspond to the temperature of different building components. U(t) is a vector of the measured input parameters (outdoor temperature, sun radiation and heating power). W is a random function of time (Wiener process). Y(t) consists of the measured output. ε is the measurement error. Parameters θ were estimated using Matlab software. The model structures are derived from (RC) networks analogue to electric circuit. In this work, first, second, third and fourth order-models presented in figure 4.2 were investigated.

The full model includes four state variables:

- T_i: indoor air temperature,
- T_f: Temperature of building envelope, consists of T_{fe} the temperature of the external building façade, and T_{fi} the temperature of the internal building façade,
- T_m: The temperature of internal wall.

The parameters of the model represent different thermal properties of the building. This includes thermal resistances:

- R: between indoor and outdoor medium,
- R_e: convection resistance of outdoor air,
- R_i, R_m: convection resistance of indoor air,
- R_f: conduction resistance of the façade.
- The heat capacities of distinct parts of the building are represented by:
- C: equivalent mass capacity for building,
- C_i: air mass capacity,
- C_f: envelope mass capacity consists of C_{fe} and C_{fi} for internal and external capacity of the façade,
- Cm: mass capacity of internal walls.

Finally, the input vector consists T_e the outdoor temperature, and the internal energy sources which are presented by Q_s: solar energy gain and Q_h: heating energy gain.

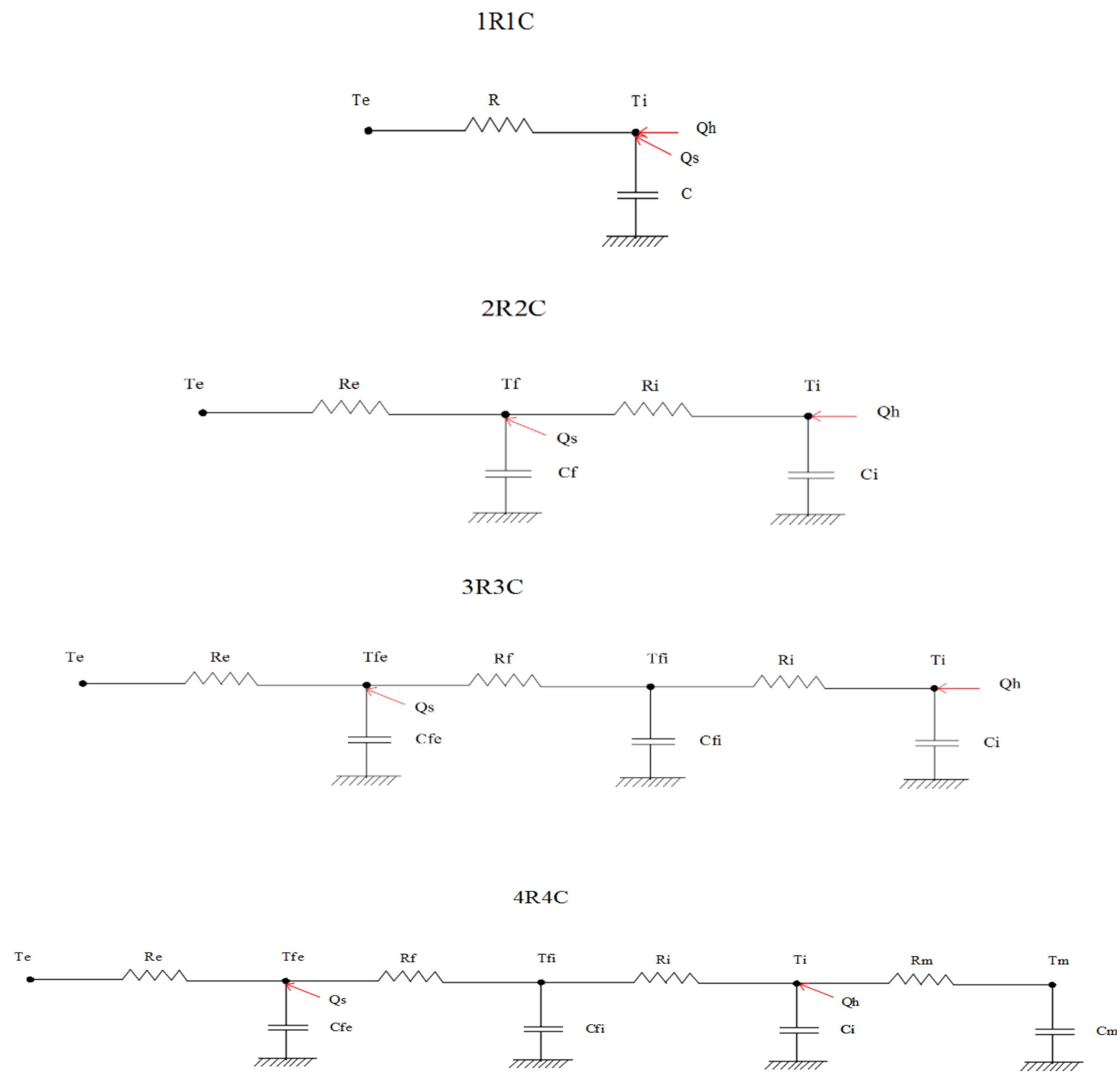

Figure 4.2: RC networks for the four models.

An example of a simple model (1R1C) is given here. By applying the dynamic heating balance equation, we get:

$$C\frac{dTi}{dt} = \frac{1}{R}(Te - Ti) + heating\ source$$

$$C\frac{dTi}{dt} = \frac{1}{R}(Te - Ti) + Qs + Qh \tag{4.2}$$

Same methodology was applied for the other orders.

Since the RC equivalent thermal network circuit models are a type of "lumped parameter" model, [93] it follows that their parameters do not correspond directly to a single physical part of the building. Each element may model several structural parts of a building. As an example, all outer walls are typically modeled as a single resistance, while any heat loss directly from indoor to outdoor temperature, such as through windows and doors, is modeled by a separate resistor. Similarly, the energy storage capacity of all walls is modeled as a single capacitance. This example illustrates how the thermal behavior of the building, by a cognitive, i.e. not based on physics equations, analysis determines the structure of the RC thermal network. The physical structure of the building itself could conceivably be used to model each wall separately, including any windows and doors, but from a thermal behavior viewpoint the above approach is more meaningful [93].

4.3 Parameters' estimation

The goal of the model identification process is to determine the set of parameters which reproduces the building thermal behavior most accurately given the measured input variables. For this purpose, a procedure has been conducted using the 'greyest' function in Matlab. This function contributes to the maximum likelihood estimates by using three different algorithms as search method for the iterative parameter estimation: The Gauss-Newton direction, the Levenberg-Marquardt and the steepest descent gradient search method. This function chooses the search method contributing to the minimum error [95-98], [89,99]. Initialization of parameters was calculated by applying the French thermal code (RT 2005 - 2012) [100-102]. Table 4.1 presents the initial values of parameters defining buildings' characteristics.

Table 4.1: Initial values for the estimated parameters.

C_i (J/K)	1.47×10^5
C_{fe} (J/K)	1.77×10^8
C_{fi} (J/K)	9.36×10^6
C_m (J/K)	4.54×10^6
R_i, R_m (K/W)	1.82×10^{-2}
R_e (K/W)	3×10^{-3}
R_f (K/W)	1.1×10^{-1}

The performance of the model is evaluated using: the root-mean-square error (RMSE-values); the final prediction errors (FPE); the level of fit (FIT) or normalized root mean square error (NRMSE) and the auto-correlation of the residuals [103]. RMSE corresponds to the residuals obtained by the estimation method indicating the goodness of fit. The FPE-values describes the model quality, the most accurate model has the smallest FPE [104]. FIT-values summarize in percentage the model goodness of fit (similarly to RMSE). Finally, the level of the autocorrelation in the residuals indicates if the model explains well the dynamics contained in the dataset.

4.3.1 Initialization of parameters

Many methods exist to initialize the parameters. Here we propose to use standard values of the RT2012, the bylaw of 9 November 2006 on DPE calculation methods (Standard, 2006) and on-site observations.

Necessary information obtained by "on-site observation":

- Year of construction or renovation
- Type of use (offices, shops, ...)
- Heated surface (Sh)
- Surface of vertical walls (Sm)
- External exchange surface (Sext)
- Internal exchange surface (Sint)
- Indoor air volume (Vint)
- Coefficients of internal convection (hint) and external (hext), supposed constant.

Information to look for in RT 2012:

- Daily capacity (Cq in kJ / K.m²) according to the inertia class (tables 4.2 and 4.3).
- The impact of the furniture on the air capacity (Mob = 20 kJ / K.m² for non-empty buildings and zero otherwise).

Information to be found in the decree of 9 November 2006 on DPE calculation methods:

- Conductivity of the outer walls: "U_{wall}", "U_{slab}" and "U_{roof}", depending on the year of construction (table 4.4).

Here are the formulas to initialize each parameter: (tables 4.4, 4.5, and 4.6) [101-102]

$$C_i = \rho_{air}\ x\ C_{air}\ x\ V_{int} + Mob\ x\ S_h$$
$$C_f = C_q\ x\ S_h \qquad (4.3)$$

$$R_i = \frac{1}{h_{int}\ x\ S_{int}}$$
$$R_e = \frac{1}{h_{ext}\ x\ S_{ext}} \qquad (4.4)$$
$$R_m = \frac{1}{U_{wall}\ x\ S_m}$$

Table 4.2: Inertia classes for building.

Plancher Bas	Plancher haut	Paroi verticale	Classe d'inertie
lourd	lourd	lourde	très lourde
-	lourd	lourde	lourde
lourd	-	lourde	lourde
lourd	lourd	-	lourde
-	-	lourde	moyenne
-	lourd	-	moyenne

Table 4.3: Daily capacity.

Classe d'inertie quotidienne	Capacité quotidienne C_m (KJ/K)	Surface d'échange $A_m(m^2)$
très légère	80 x Abât	2.5 x Abât
légère	110 x Abât	2.5 x Abât
moyenne	165 x Abât	2.5 x Abât
lourde	260 x Abât	3 x Abât
très lourde	370 x Abât	3 x Abât

Tableau 4.4: Conductivity values.

Année de construction	H1		H2		H3	
	Effet joule	Autres	Effet joule	Autres	Effet joule	Autres
de 1948 à 1974	2.5		2.5		2.5	
de 1975 à 1977	1		1.05		1.11	
de 1978 à 1982	0.8	1	0.84	1.05	0.89	1.11
de 1983 à 1988	0.7	0.8	0.74	0.84	0.78	0.89
de 1989 à 2000	0.45	0.5	0.47	0.53	0.5	0.56
de 2001 à 2005	0.4		0.4		0.47	
à partir de 2006	0.36		0.36		0.4	

Tableau 4.5: Coefficient of internal and external convection.

Position de la paroi	Émissivité	h_{int}	h_{ext}		
			Normale	Abriée	Sévère
Verticale	0.9	8.13	18.2	12.5	33.3
Verticale	0	3.29	14.9	9.1	33.3
Plafond externe	0.9	9.43	22.2	14.3	50
Plafond externe	0	4.59	18.9	11.1	50
Plancher externe	0.9	6.67	20	20	20
Plancher externe	0	1.78	20	20	20
Horizontale interne	0.9	8	-	-	-
Horizontale interne	0	3	-	-	-

4.4 Prediction time

A smart monitoring system was installed in an unoccupied room in the research building ‘A4’ as mentioned previously. It is heated by a radiator with two constant powers (high level 1500 W and low level 900W) coupled with a control system and a counter. Data were collected for one month, without heating, with low level heating and with high level heating. Analysis of indoor temperature variation of the room was executed to determine the time of heat transmission delay in order to define the prediction time needed to cover the phase of heating exchange. Figure 4.3 shows the variation of indoor temperature and its difference with the outdoor temperature while heating at low and high levels. For the indoor temperature variation, the graph indicates that for 4 hours high heating, 18 min is needed for a variation of 1°C, while 30min is needed for low heating. By decreasing the heating time by 2 hours, 12min is needed for a variation of 1°C at 1500W heating. For the variation of the indoor and outdoor temperature difference, the analysis shows that for 4 hours high heating, 25 min is needed for a variation of 1°C, while 40min is needed for low heating. By decreasing the heating time by 2 hours, 15min is needed for a variation of 1°C at 1500W heating.
Hence, prediction models will be executed for 15min, 30min, and 60min.

After the selection of the prediction time needed, we propose to compare four grey box models concerning their ability to predict the indoor temperature while using three data set generation: free floating (without heating), dynamic heating at low and high levels (random sequence for the on/off control of the heating system) [105]. Data were obtained through real measurements. Each set of data is applied on four grey-box models of reduced structures for three prediction times 15, 30 and 60min. Comparison of the models’ performance for the different order and different prediction time was executed for each set of input parameters.

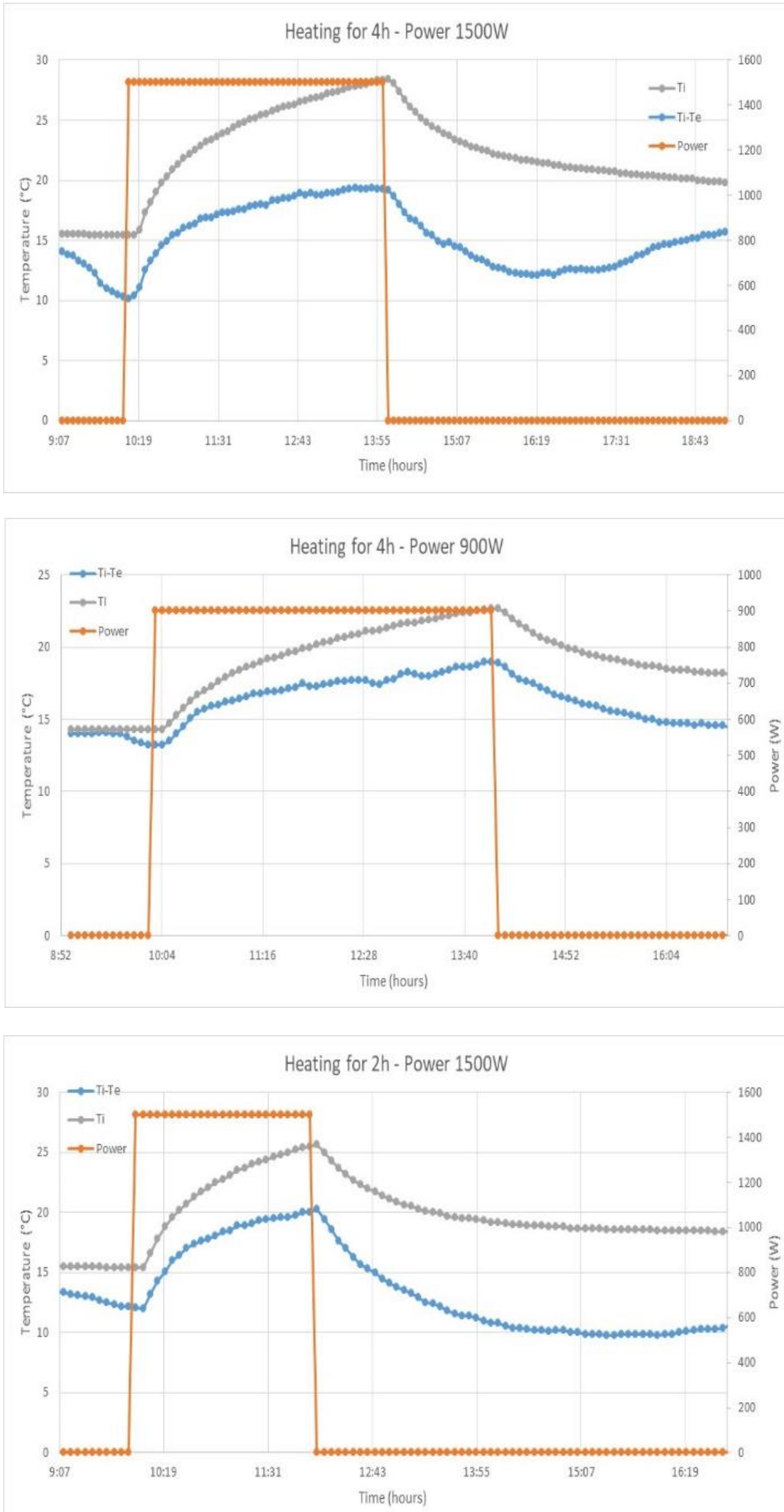

Figure 4.3: Variation of indoor and outdoor temperature while heating.

4.5 Grey box models

In order to evaluate the influence of the data dynamics on the predictions' performance, three data set were used as mentioned before. For each set, the prediction is executed for 15, 30 and 60 min for the first, second, third and fourth order. Comparison and interpretation of all models were made to generate a general automated process for model's identification to get the best thermal prediction of indoor temperature. To simplify the comparison, results will be presented in terms of RMSE and fit percent to determine the best performant model.

4.5.1 Free Floating data set

We will start by the free-floating data. This simple experiment does not present any excitation frequencies [105]. This explains the results (no convergence) for all the prediction of the fourth order which is considered a complex order for this set of data. We should note that the order 2 is the most performant for all predictions with a slight difference with other orders (1 and 3). Since by increasing the model order above 1, the improvement is considered negligible, order 1 can be retained for this data set as the simplest structure. Predictions for 15, 30 and 60 min were performant for order 1, 2 and 3 having RMSE < 1 and the fit % > 80%. Tables 4.6, 4.7 and 4.8 illustrate the results.

Comparison of the error distribution corresponding to the first order is made. About 99% of the data have an error less than 0.5°C for 15, 30 and 60 min predictions (figure 4.4). We can notice that reduced first-order grey box model is effective for short term prediction for the free-floating data.

Table 4.6: 15 min prediction results for the free-floating data.

	1R1C	2R2C	3R3C	4R4C
Fit percent	95.11	95.35	95.12	10.09
RMSE	0.0656	0.0616	0.0648	1.2004

Table 4.7: 30 min prediction results for the free-floating data.

	1R1C	2R2C	3R3C	4R4C
Fit percent	91.86	92.91	91.97	-
RMSE	0.1086	0.0949	0.1072	-

Table 4.8: 60 min prediction results for the free-floating data.

	1R1C	2R2C	3R3C	4R4C
Fit percent	87.83	90.24	88.05	-
RMSE	0.1625	0.1304	0.1594	-

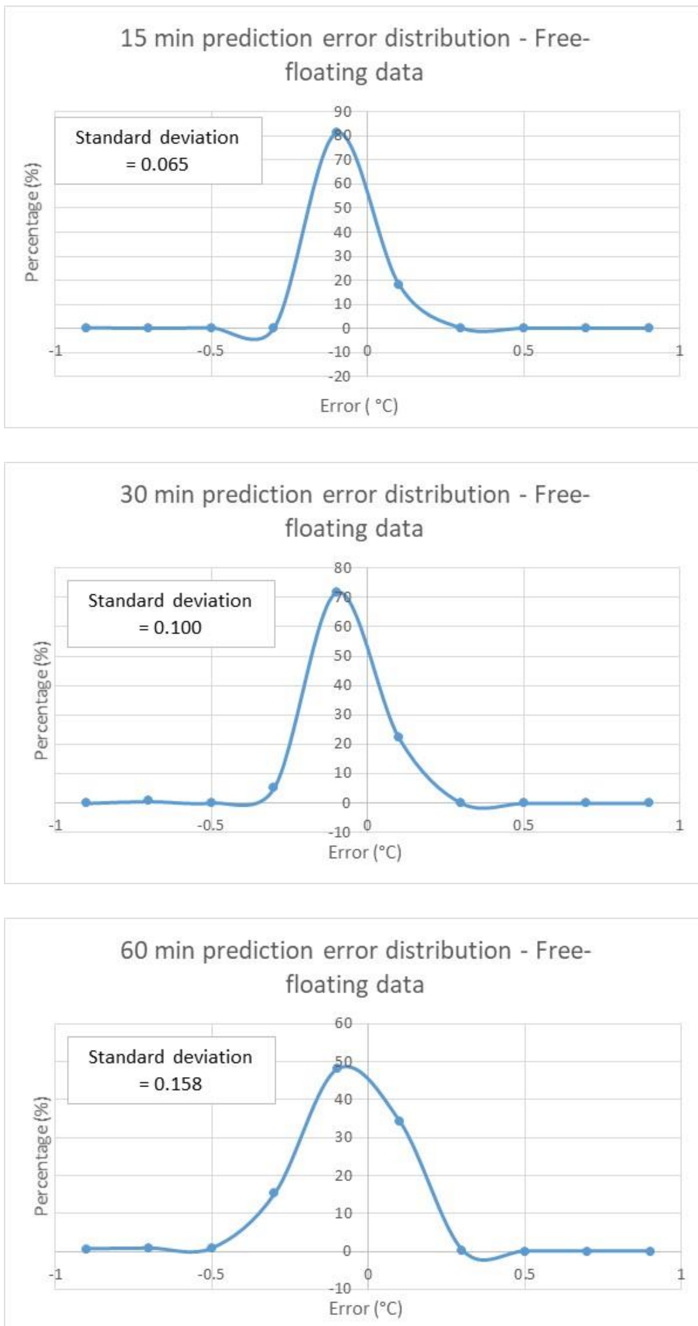

Figures 4.4: Error distribution for 15,30 and 60min prediction - Free floating data – order 1.

4.5.2 Dynamic data

Two data sets are used in this section corresponding to random heating at 900 W and 1500W. This experiment reveals the dynamic of the building.

By starting the heating at 900W, results indicate that the model of order one is not sufficient to explain the data dynamics. This explains the non-convergence of the forecasting models for this order. By increasing the order of the model, the forecasting results are improved. We noticed that for order 4, models become more sensible and complex for this set of data. Tables 4.9, 4.10 and 4.11 illustrate the results. They show that model of order 3 is the most performant for all forecasting models. Predictions for 15, 30 and 60 min were performant for order 2 and 3 having RMSE < 1 and the fit % > 80%.

Figure 4.5 presents the error distribution for the order 3. We can notice that reduced third-order grey box model is effective for short term About 99% of the data have an error less than 0.5°C for 15 and 30 min predictions. 97% of the data have an error less than 0.5°C for 60 min prediction. prediction for this data set.

Table 4.9: 15 min prediction results - heating at 900W.

	1R1C	2R2C	3R3C	4R4C
Fit percent	-	93.97	95.43	44.15
RMSE	-	0.1204	0.0917	1.1170

Table 4.10: 30 min prediction results - heating at 900W.

	1R1C	2R2C	3R3C	4R4C
Fit percent	-	87.6	92.98	36.52
RMSE	-	0.2480	0.1404	1.2697

Table 4.11: 60 min prediction results - heating at 900W.

	1R1C	2R2C	3R3C	4R4C
Fit percent	-	80.65	90.71	31.25
RMSE	-	0.3869	0.1857	1.3751

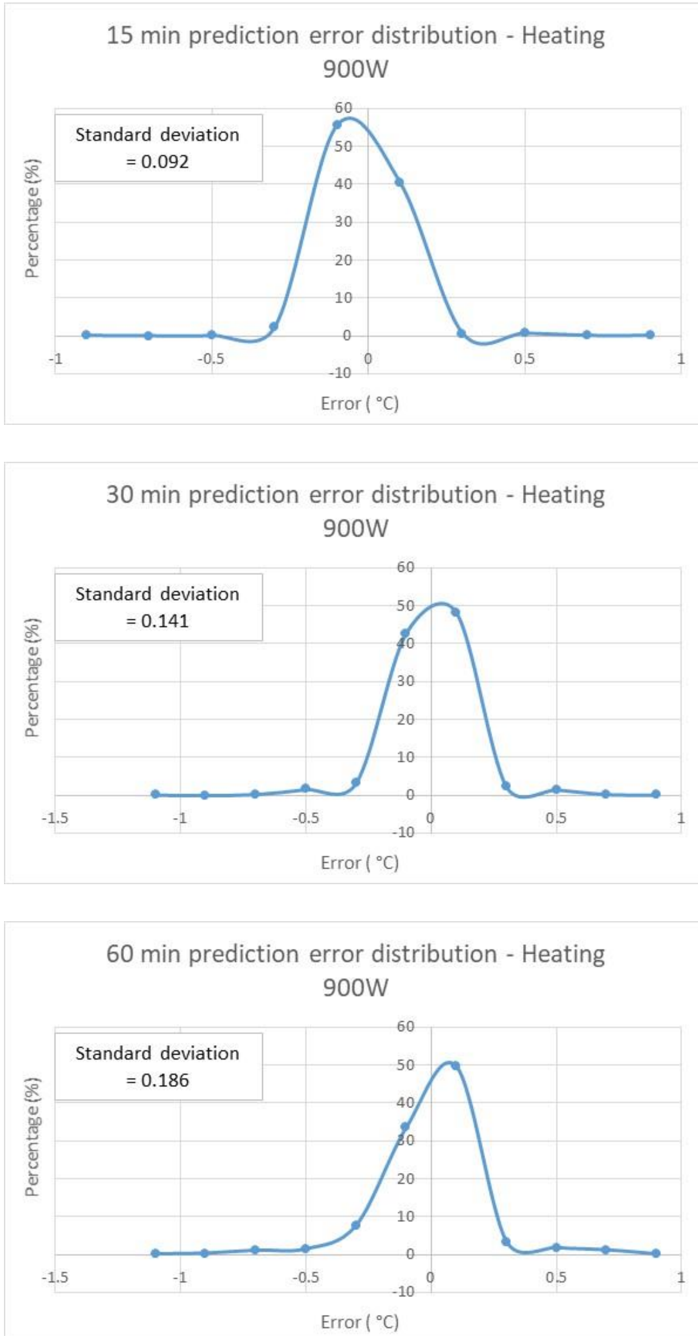

Figures 4.5: Error distribution for 15,30 and 60min prediction – Heating 900W- order.

Figure 4.6 shows the autocorrelation of residuals for order 3 calculated with a lag of 25. Yellow interval indicates a 99% limit of confidence. The autocorrelation levels for the third order model are within the confidence limit, meaning that this model describes well the building dynamics in the dataset. We can also note that some behaviors and approximations are not considered by the model.

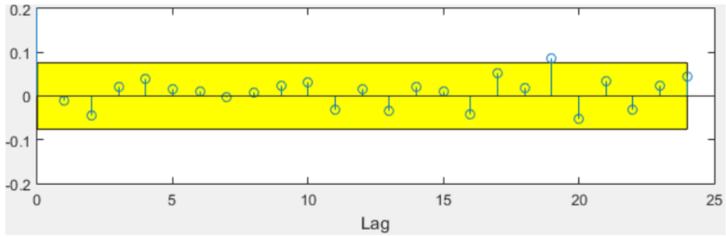

Figure 4.6: Residual autocorrelation – heating 900W – order 3.

Afterwards, the second experiment with random heating at 1500W is executed. This dataset explains the best the building's dynamics, since all models' orders present satisfactory performances with the greatest fit percentage and the lowest RMSE. Model of order 2 is the most performant for all the predictions. Models of order 3 and 4 present reliable results illustrated in tables 12, 13 and 14.

Figure 7 presents the error distribution for the order 2. About 99% of the data have an error less than 0.5°C for 15 and 30 min predictions. 97% of the data have an error less than 0.5°C for 60 min prediction. Grey box models of order 2 presents the most reliable results for this set of data.

Table 4.12: 15 min prediction results - heating at 1500W.

	1R1C	2R2C	3R3C	4R4C
Fit percent	93.36	97.2	95.7	96.18
RMSE	0.2349	0.0990	0.1523	0.1353

Table 4.13: 30min prediction results - heating at 1500W.

	1R1C	2R2C	3R3C	4R4C
Fit percent	83.34	95.56	90.7	92.17
RMSE	0.5895	0.1572	0.3291	0.2769

Table 4.14: 60 min prediction results - heating at 1500W.

	1R1C	2R2C	3R3C	4R4C
Fit percent	71.49	93.54	84.71	87.59
RMSE	1.0090	0.2285	0.5410	0.4392

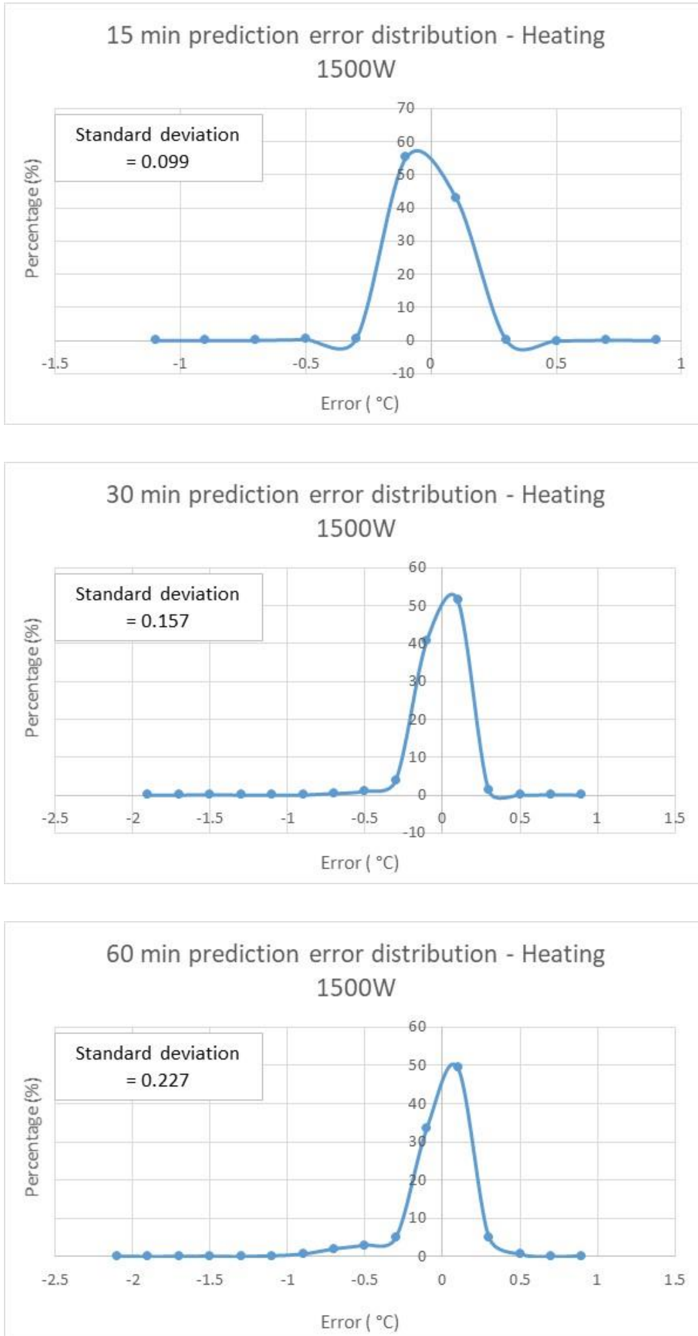

Figures 4.7: Error distribution for 15,30 and 60min prediction – Heating 1500W- order 2.

Figure 4.8 shows the autocorrelation of residuals for order 2 calculated with a lag of 25. Yellow interval indicates a 99% limit of confidence. The autocorrelation levels of the second order model are within the confidence limit, meaning that this model describes well the building dynamics in the dataset. We can also note that some behaviors and approximations are not considered by the model.

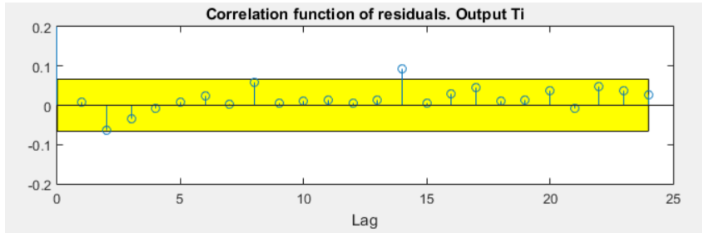

Figure 4.8: Residual autocorrelation – heating 1500W – order 2.

By analyzing the previous results, we noticed that the choice of the model's order depends on the data dynamics. The prediction for the most reliable order for all the data sets present performant results for short term forecasting. Dynamic data with heating at 1500 W reveals the most buildings' dynamics. We can notice the need of an automated process combining many data set and grey-box models to be able to determine the most performant order for the best data set revealing the real dynamics of the building.

4.6 Sensibility analysis

To verify that all models' parameters are necessary for the predictions, we perform a sensitivity study by calculating the Sobol index. This method allows measuring the overall impact of a parameter on the (scalar) output of the model. The total Sobol index (St) is dimensionless, measures not only the direct impact (i.e. first order impact) of parameter variation but also all the possible nonlinear interactions between parameters (i.e. higher order effects). When the total Sobol index is high (close to 1) the parameter has a strong impact on the model output and when it is close to 0, the parameter has a small impact on the model output.
Eq. (4.5) presents the total Sobol index formula.

$$ST_i = \frac{E_{X\neq i}\left(V_{Xi}(Y/X_{\neq i})\right)}{V(Y)} \qquad (4.5)$$

where i is the studied parameters, V(Y) is the model output variance when all parameters vary, $V_{Xi}(Y/X_{\neq i})$ is the model output variance when all parameters vary except the i^{th}, $E_{X\neq i}$ is the expectation value.

Saltelli [106] and Jansen [107] proposed another equation for the total Sobol index determination allowing a fast convergence and reducing computing time. They propose the following equation:

$$ST_i = \frac{\frac{1}{2N}\sum_{w=1}^{N}(Y_b - Y_{ci})^2}{Var(Y_a\,,\ Y_b)} \qquad (4.6)$$

Where N is the number of samples, Y_b and Y_a are two vectors of output data in which all parameters vary, each vector corresponding to a different input sample; Y_{ci} is an output vector in which all parameters vary except the i^{th}. The model comparative criterion (Y) is the Root Mean Squared Error (RMSE, Eq. (4.7)) between the predicted data and the reference data. The quasi-random LHS (Latin hypercube sampling) type method is used to accelerate convergence. All parameters vary by plus or minus 30% of their adjusted value (values after learning).

$$RMSE = \sqrt{\frac{\sum_{i=1}^{n}(y_i - \hat{y}_i)^2}{n}} \tag{4.7}$$

Figure 4.9 presents the results of this analysis. For each dataset, the most performant order is investigated. If the variation of a parameter has no impact on the output of the model, then it cannot be identified correctly. It is therefore necessary that the total Sobol index is sufficiently high for all parameters for the model architecture to be validated. According to table 4.15, all parameters have a significant impact on forecasts having similar magnitude order [103].

For the dynamic data study (900W and 1500W heating), the "R_i" parameter is among the two highest indices. It represents the thermal resistance of indoor air in the building. It shows that this phenomenon has a preponderant impact on the thermal behavior of the building.
For the 900W heating study, C_i and C_{fe} have low total sobol indices comparing to other parameters (0.07 and 0.09), but their values are not negligible. This can be referred to the subjection of these parameter to a small amplitude of variation (± 30%) compared to the dispersion observed in a real building.

This study of sensitivity has shown that all identified parameters play a significant role in predicting the thermal behavior of the building. They are well identified and are essential for the forecast.

Table 4.15: Calculated total Sobol index.

	Free-Floating		Heating - 900w						Heating - 1500W			
Paramete r	C	R	C_i	C_{fe}	C_{fi}	R_i	R_e	R_f	C_i	C_f	R_i	R_e
ST_i	0.98	0.99	0.07	0.09	0.24	0.60	0.12	0.18	0.62	0.85	0.72	0.59

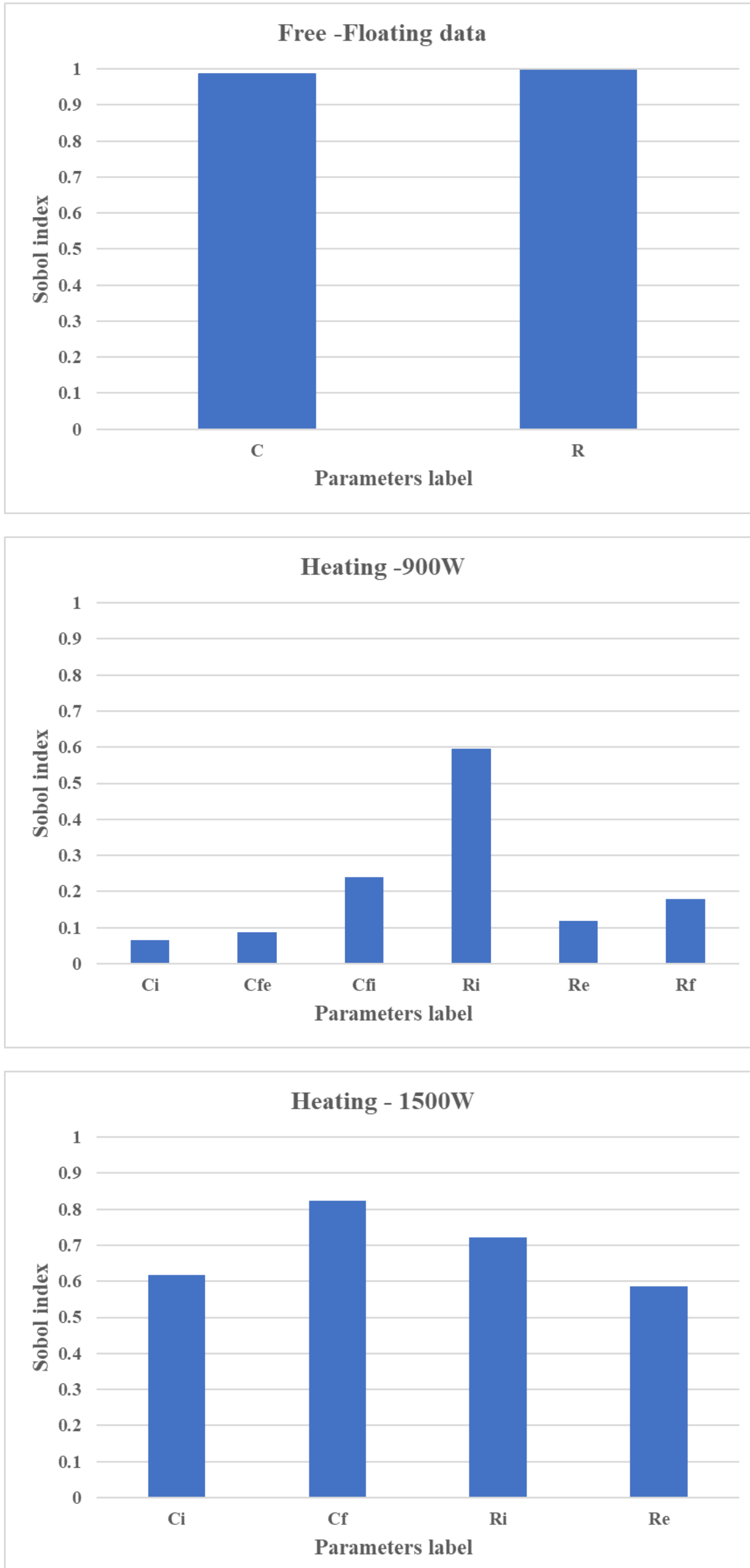

Figure 4.9: Results of sensibility analysis.

4.7 Conclusion

This chapter presented the use of Grey Box models to predict indoor temperature of A4 building. It included also analysis of the influence of the data dynamics on the prediction of the indoor temperature.
The research was conducted according to the following methodology. At first, analysis of the indoor temperature variation while heating permits the determination of the time needed to cover the phase of heat exchange and therefore the prediction time for the modeling process. Three data sets were used (free-floating and dynamic heating 900 W and 1500 W) and four reduced-order models' structures to predict the indoor temperature at 15, 30 and 60min.
Results showed that the most performant order for forecasting is not unique. It varies with the data dynamics. Reduced model of order 1 is sufficient to predict the indoor temperature without heating. For dynamic data, model of order 3 was the most performant for heating at 900W. Whereas, model of order 2 was the most performant for heating at 1500W. We should note that, prediction models become more sensible for higher orders (order 4) for the first two experiments. It indicates that complexity and higher orders are always required for modelling buildings' characteristics and dynamics.

A sensitivity study showed that all the parameters of the three most performant models have a significant impact on model outputs (temperature). This validates the model architecture and ensure that all parameters are identifiable.

Chapter 5: Control model

Introduction

This chapter presents a control approach based on the application of an empirical on/off method by exploiting the following three elements: the building inertia, the occupation profile and the dynamic pricing. It completes the previous grey box investigation.
The study is based on a methodology capable of finding the most convenient heating power after the application of a simple on/off control heating.
In this investigation, the two most performant model's orders are studied (2 and 3). The analysis of results indicates that the applied control method reduces largely the energy consumption and maintain the thermal comfort.

5.1 Bibliographic study

The main objective of heating system control is to maintain a certain level of comfort and satisfy occupants needs. While on the other hand, an optimized control is not only dedicated to maintaining the comfort, but also to reduce the consumption and the costs.

The interior temperature is considered the main indicator of the thermal comfort in most practical applications because it highly affects the energy consumption and it depends on several factors:

- Building usage;
- Outdoor temperature;
- Occupation;
- Internal heat gains.

Many investigations have working on the determination of optimal environment in buildings considering energy consumption and human comfort [108] or in a certain type of buildings as the office buildings optimal working environment in [109] [110] and residential buildings in [111].
A study of the American Society of Heating, Refrigerating, and Air- Conditioning Engineers (ASHRAE) has proposed a simplified method to define a 90% and 80% acceptability range where people feel comfortable as a function of the outdoor temperature [112] [113] [114].

$$\text{The 90\% acceptability level} \begin{Bmatrix} T90\,(min) = 0.31xTout + 15.3 \\ T90(max) = 0.31x\,Tout + 20.3 \end{Bmatrix} \tag{5.1}$$

$$\text{The 80\% acceptability level} \begin{Bmatrix} T80\,(min) = 0.31xTout + 14.3 \\ T80(max) = 0.31x\,Tout + 21.3 \end{Bmatrix} \tag{5.2}$$

The temperature normally used as set temperature for control systems is:

$$T_{comfort} = 0.31\text{x Tout} + 17.3 \tag{5.3}$$

The second objective is to minimize the energy consumption and cost. By integrating the power supplied over time, energy consumption can be determined. In France, the electricity subscription is priced depending on the supplied power P(W) and the consumed energy Q(KWh). A day time is also priced into two types: peak hours and normal hours. Table 5.1 shows an example of a dynamic pricing plan of the electricity in 2018 in France (euro/KWh).

Table 5.1: Hours classification according to the price of KWh in France 2018.

	Normal hours	Peak hours
Hour	22h00- 6h00	6h00-22h00
Price (euros/KWh)	0.1244	0.1593

Thus, the timing of consumption must be well planned in order not to exceed the maximum power supplied on one hand and to minimize the consumption cost on the other hand.

5.2 Proposed control methodology

This study uses the on/off control method. Heating system is controlled according to the room temperature error (equations 5.4 and 5.5).

$$e = T_{comfort} - T_{room} \tag{5.4}$$

$$S = f_{on\text{-}off}(e) \tag{5.5}$$

Where e is the temperature error and S is the heating device state.

This analysis completes the previous modeling study. Same room was investigated after the identification of buildings' parameters. As deduced previously, models of order 2 and 3 were the most performant models in case of dynamic data, thereby they will be used in this study.

The methodology of this control approach is based on, firstly, comparing the indoor predicted temperature to the comfort one determined from equation 5.3. The study will consider the occupation as well to adjust the heating device state (on or off). Initially, heating will be launched at 1500W (high level heating) for a certain time (should be defined later), before the occupation period of the room, to minimize e (equation 5.4) and then heating at lower power will be applied for the rest of the day. The main objective of this work is to find the most convenient power to be used in order to achieve the main two keys of applying the control on the heating system: maintaining thermal comfort and performing energy saving. 'Matlab' software was used to code this control approach.

5.3 Response time determination

After the parameters' identification and the indoor temperature prediction, a simple on/off control was applied with 1500W heating in the studied room. This process provides the period of high-level heating required before reducing the power of the radiator. Figures 5.1 and 5.2 enable the determination of the response time of the room needed to reach the comfort temperature while heating at 1500W.

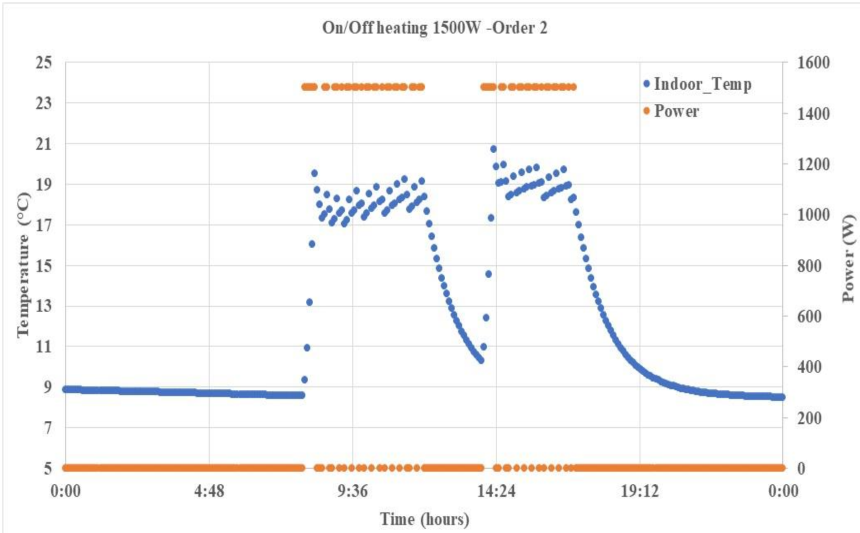

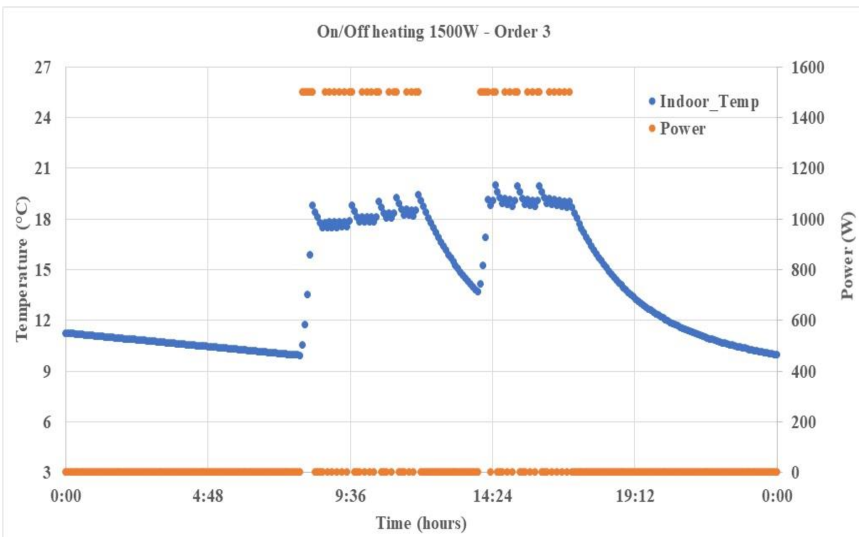

Figures 5.1: Indoor temperature variation with on/off 1500W heating for order 2 and 3 respectively.

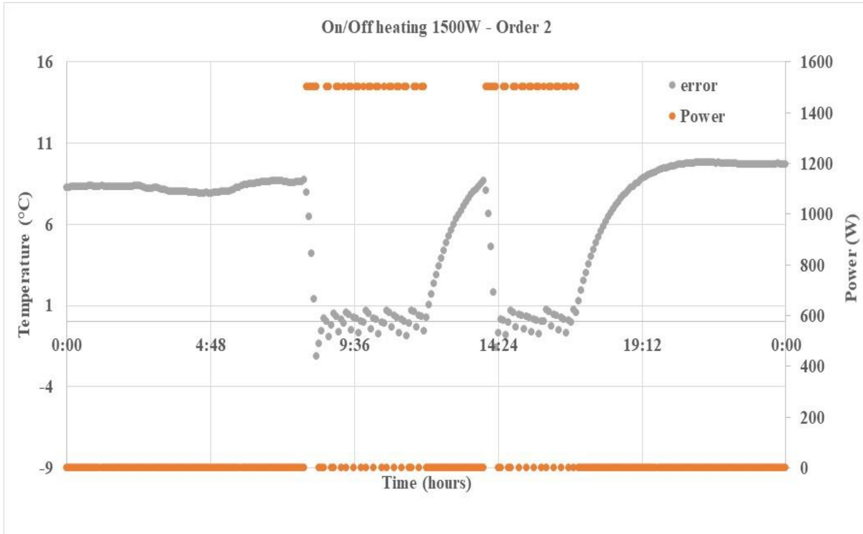

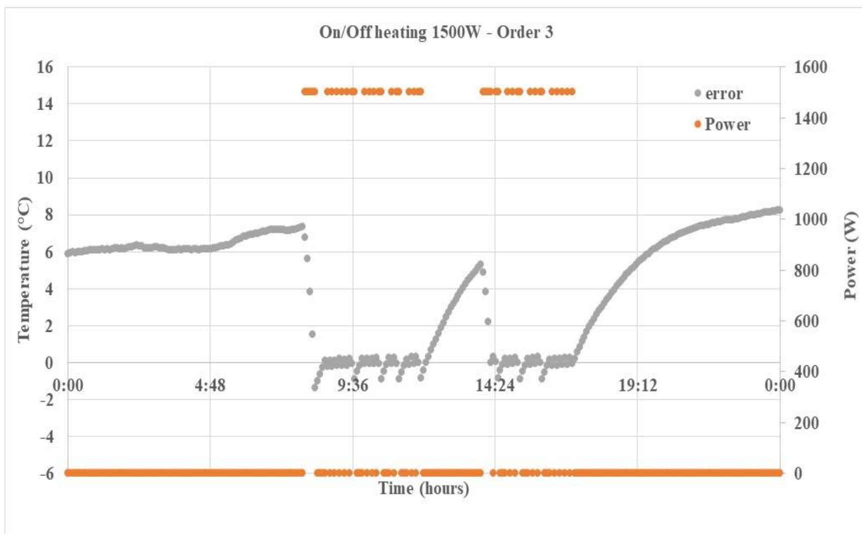

Figures 5.2: Error temperature variation with on/off 1500W heating for order 2 and 3 respectively.

From previous graphs, we can notice that 20min of 1500W heating were required for the indoor temperature to reach the comfort level. Thereby, the initial period of high-level heating needed for this control approach is 20min. Thus, the heating will be launched at 1500W for 20min before the occupation period.

5.4 Results of the applied control

The objective of this control method is to minimize the 1500W power used for on/off heating. The application of this technique considers the thermal comfort level and the occupation period. Thus, the occupation period for one week of February 2018 (figure 5.3) was known and the comfort temperature was determined for the same period (figure 5.4).

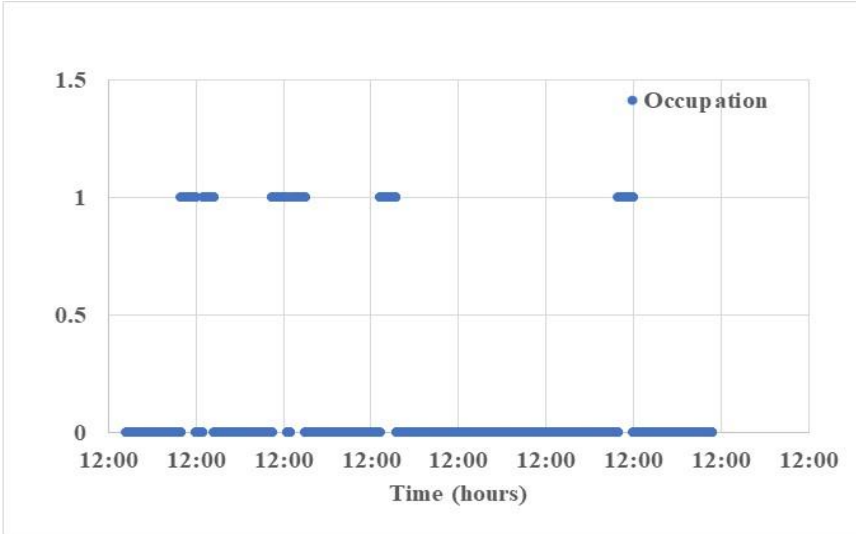

Figure 5.3: Occupation schedule for the studied room for one week of February 2018.

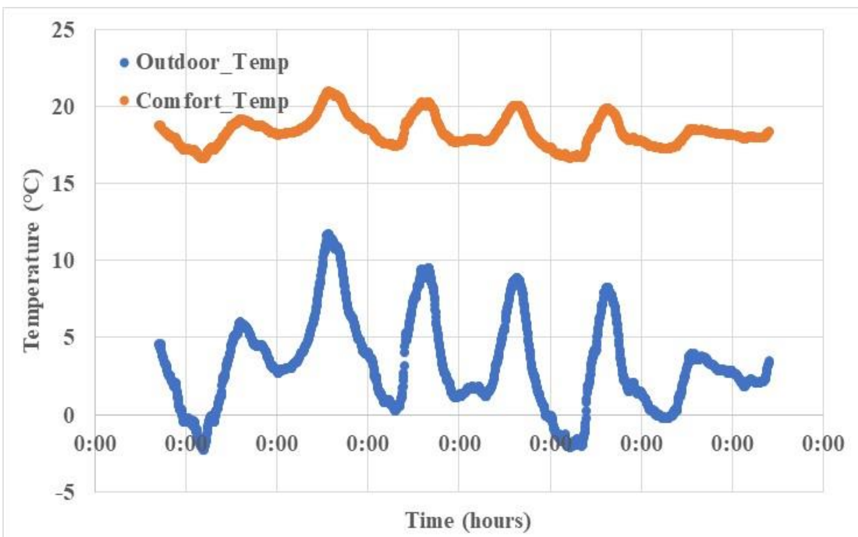

Figure 5.4: Outdoor and comfort temperatures.

Following the grey box models' application, the indoor temperature is determined considering different heating powers in order to optimize the energy consumption. After several attempts to find the most convenient heating power, it was noticed that 150W heating during occupation period was enough to provide the thermal comfort for models of order 2 and 3. The error between the indoor temperature and the comfort one is less than 0.5℃. Figures 5.5 and 5.6 illustrates the results.

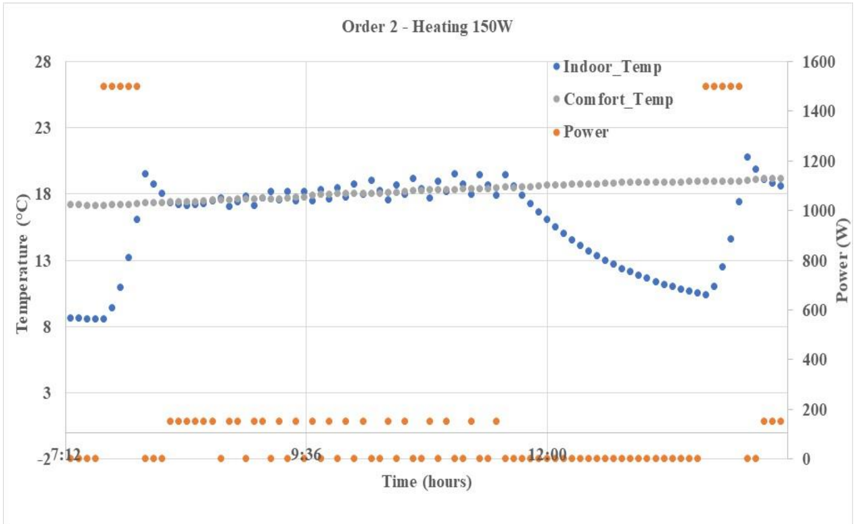

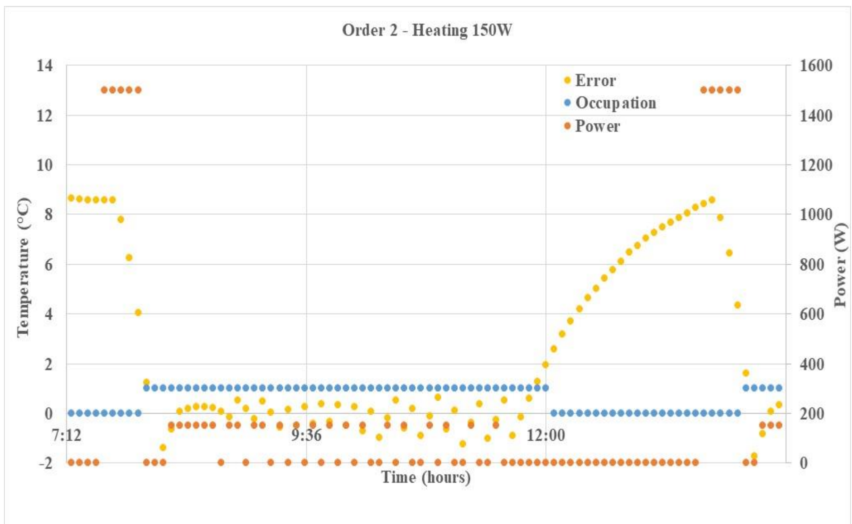

Figures 5.5: Empirical on/off control heating 150W – Model of order2.

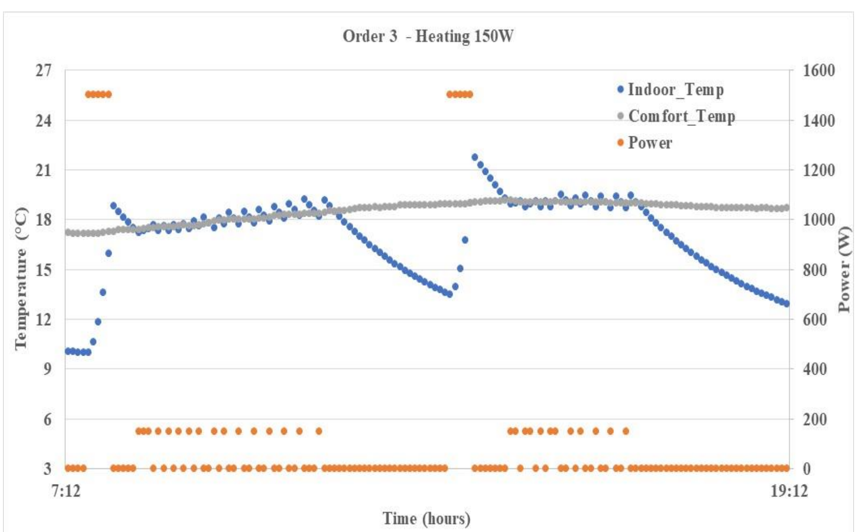

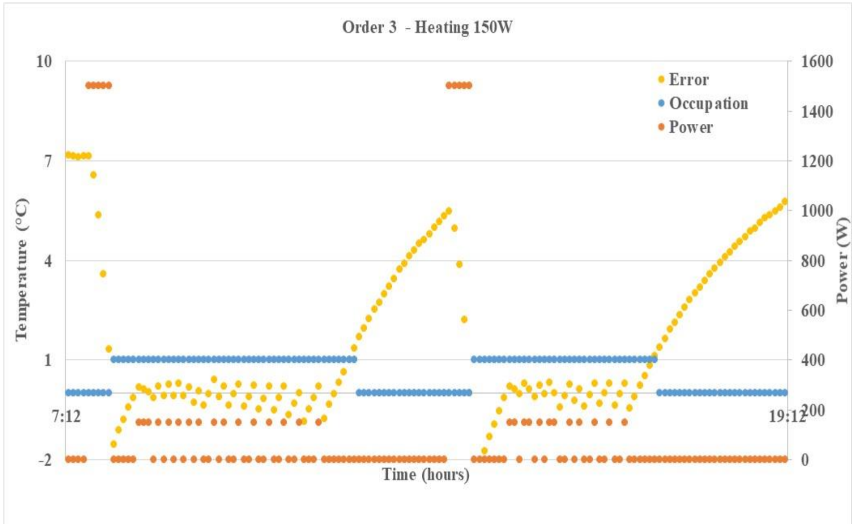

Figures 5.6: Empirical on/off control heating 150W – Model of order3.

The energy consumed by applying the empirical on/off control is four times less than the energy consumed while applying a simple on/off control. Figures 5.7 and 5.8 illustrate a comparison of energy consumption and cost for 24h for different control methods. It indicates that for the two model's orders, the used control method is efficient and provides 3 to 4 times less energy consumption from a simple on/off control. We should note that a simple on/off control can also contribute to an important energy saving.

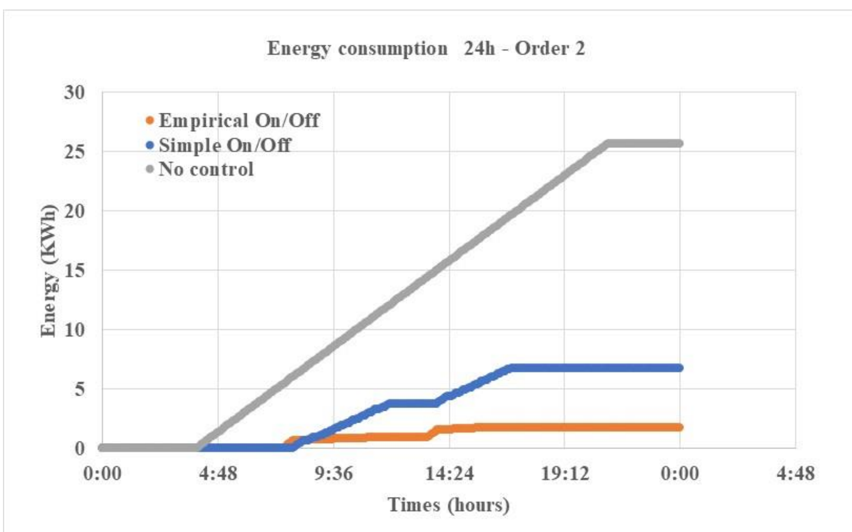

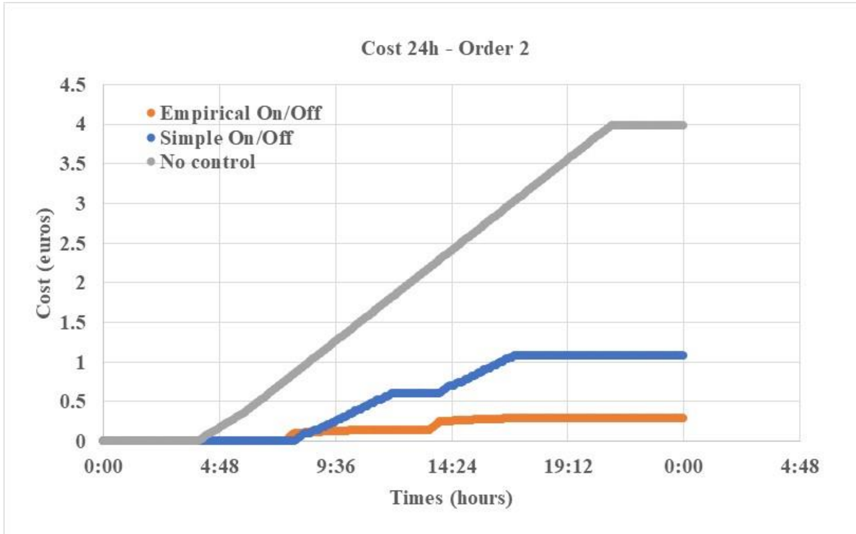

Figures 5.7: Comparison of energy consumption and cost for 24h for different control methods – Model of order 2.

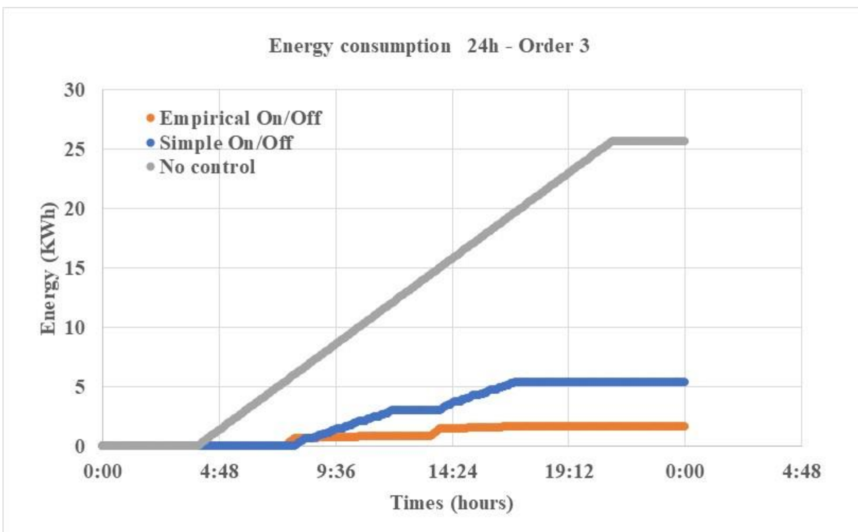

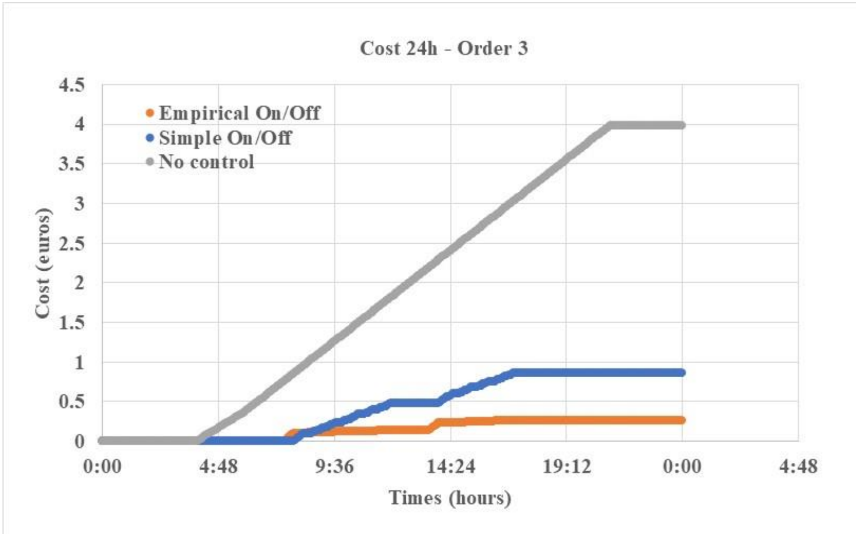

Figures 5.8: Comparison of energy consumption and cost for 24h for different control methods – Model of order 3.

Previous analysis indicates that this empirical on/off control method is effective. It maintains the thermal comfort of the occupant as well as performing important energy savings.

5.5 Other applications

To confirm these previous results, two other applications of this control approach were executed on two different offices (1 & 2) in the same building A4 (figure 5.9). Same procedure of grey box modeling and parameters' identification was applied. Same methodology of control is used, but instead of 1500W initial heating, 1000W (max power heating of the radiator) was applied.

Same process is executed to define the response time of rooms in order to get the high-level heating period. Applying simple on/off control of 1000W heating revealed a needed period of 85min for the 2 offices. Figure 5.10 illustrates the results.

Figure 5.9: Modeled offices in building A4.

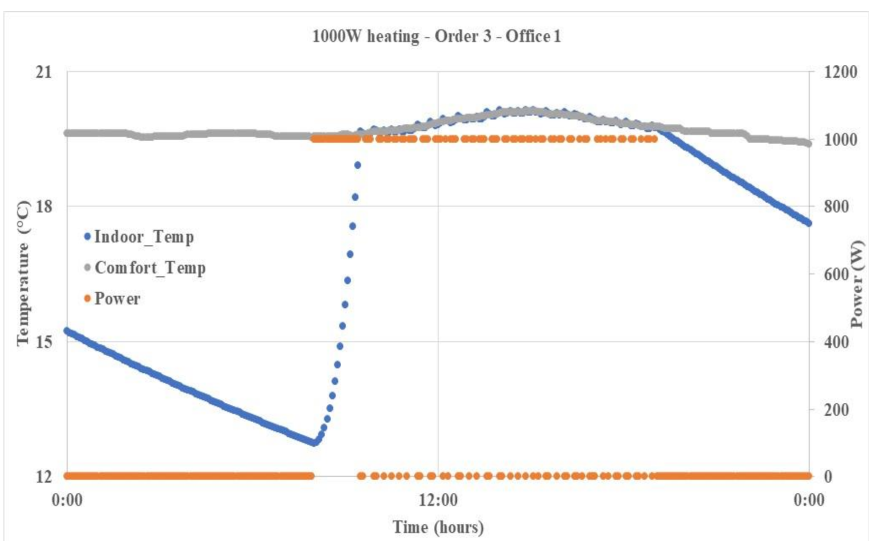

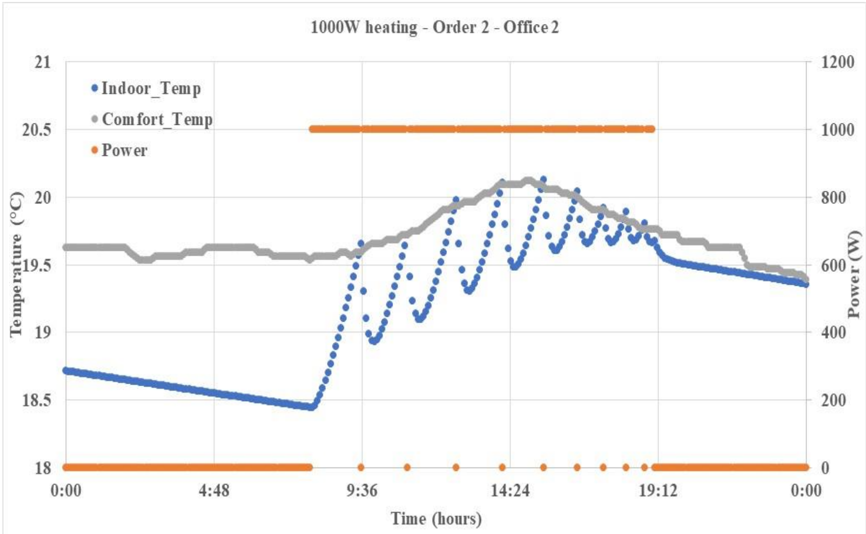

Figures 5.10: Indoor temperature variation with on/off 1000W heating for offices 1 and 2.

Thereby, the heating will be launched at 1000W for 85min before the occupation period for the two offices.

Like previous analysis, the occupation period for one week of December 2017 was known and the comfort temperature was determined for the same period for the two studied rooms.

After several attempts to find the most convenient heating power, it was noticed that 150W heating during occupation period was enough to provide the thermal comfort for models of order 3 for the two offices. While for order 2, office 1 needed 500W to reach the thermal comfort level, whereas for office 2, 350W was the convenient heating power. Figures 5.11 and 5.12 illustrate these results.

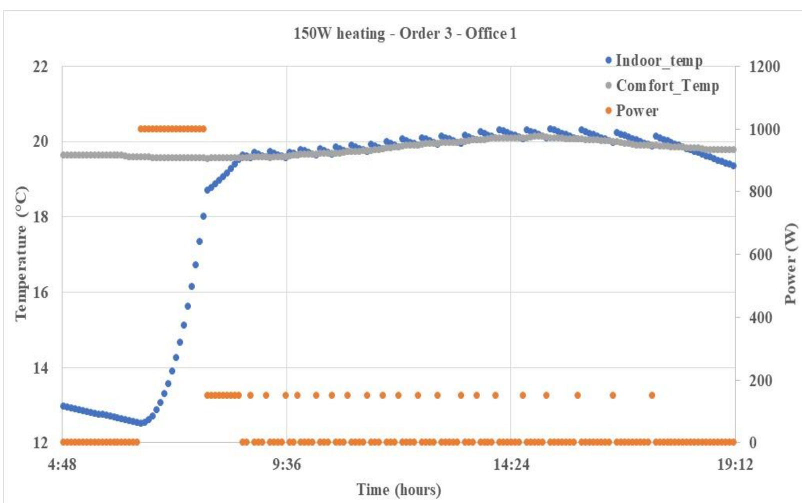

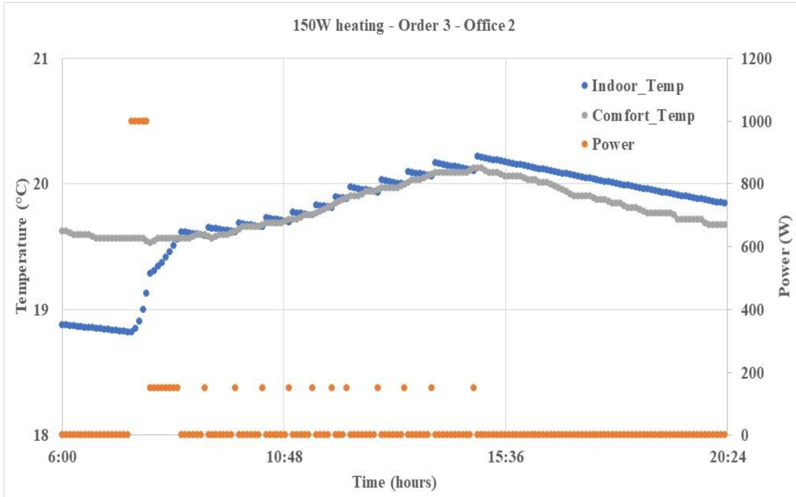

Figures 5.11: Empirical on/off control heating 150W – Model of order3 – Office 1 and 2.

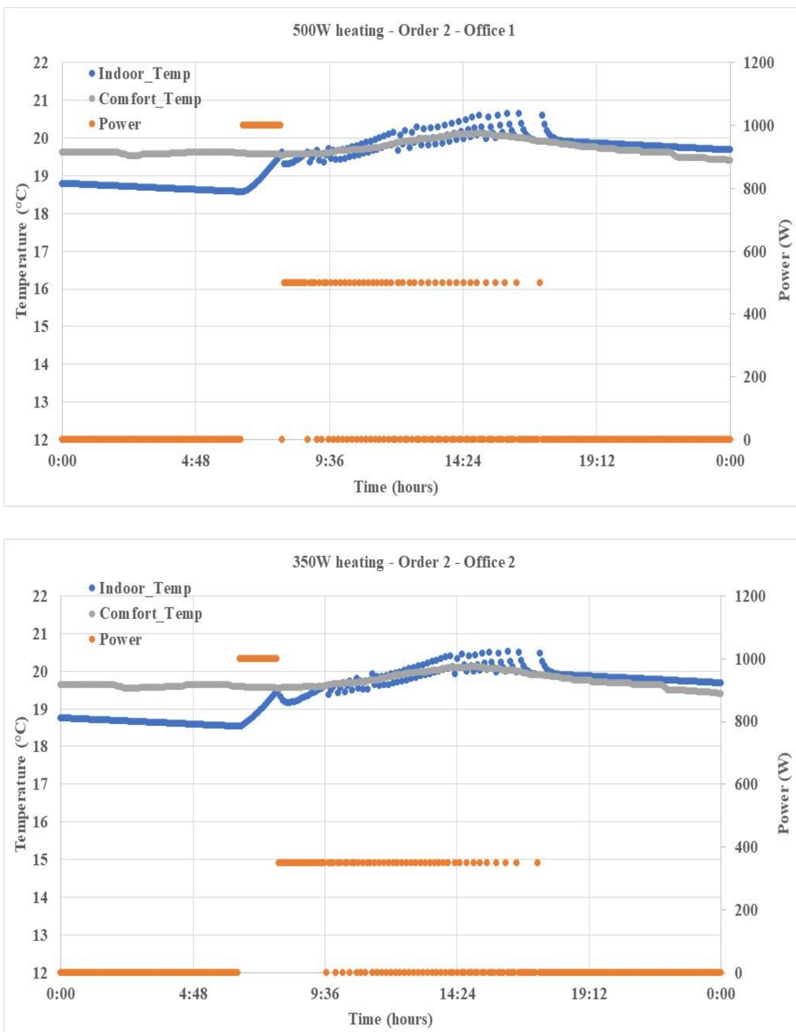

Figures 5.12: Empirical on/off control heating 150W – Model of order 2 – Office 1 and 2.

The error between the indoor temperature and the comfort one is less than 0.5℃ (figure 5.13). Thus, thermal comfort is well maintained.

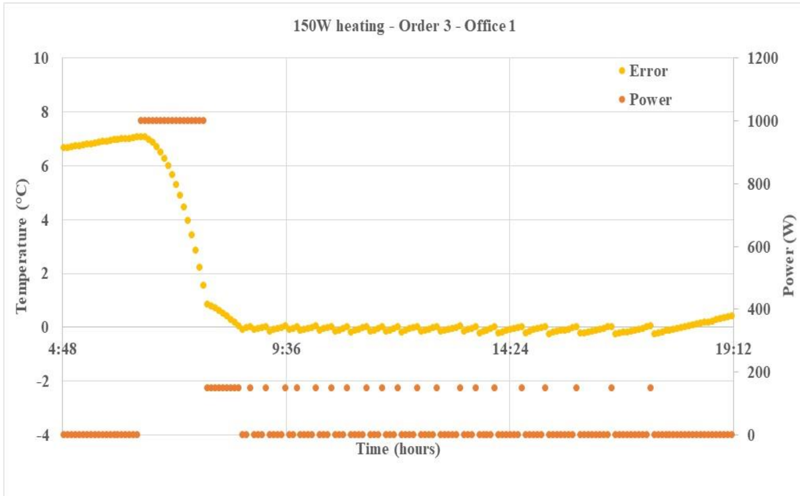

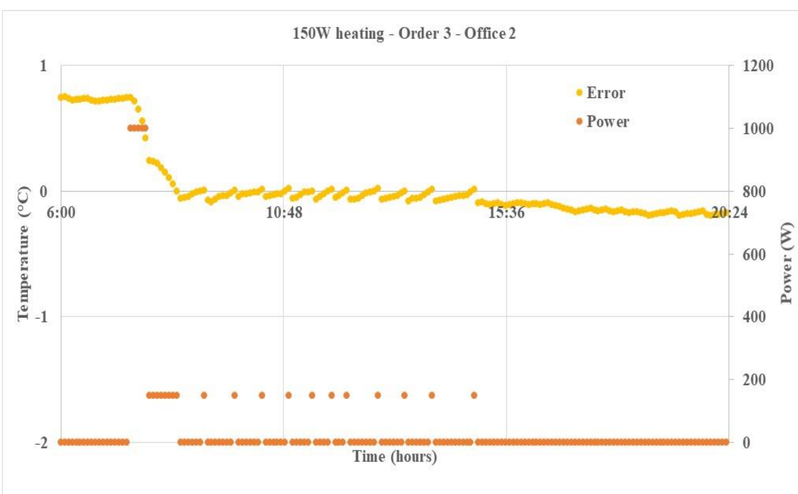

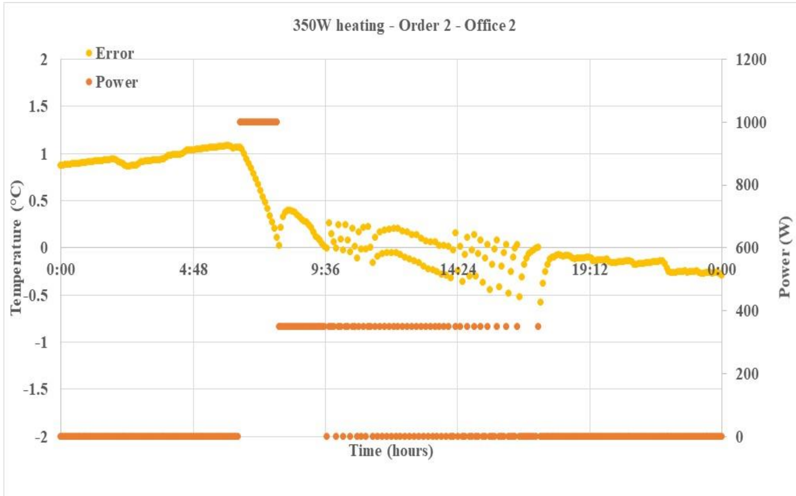

Figures 5.13: Error variation for orders 2 and 3 – Offices 1 and 2.

Furthermore, the energy consumption was analyzed for the studied rooms. The energy consumed by applying the empirical on/off control for the first office is about two times less than the energy consumed while applying a simple on/off control. Figures 5.14 and 5.15 illustrate a comparison of energy consumption and cost for 24h for different control methods for the first office. It indicates that for the two model's orders, the used control method is efficient and provides 2 to 3 times less energy consumption from a simple on/off control.

The energy consumed by applying the empirical on/off control for the second office is about two times less than the energy consumed for the second model's order while applying a simple on/off control. Whereas, the energy consumed by applying the empirical on/off control for the same office is about eight times less than the energy consumed for the third model's order while applying a simple on/off control. Figures 5.16 and 5.17 illustrate a comparison of energy consumption and cost for 24h for different control methods for the first office. It indicates that for the two model's orders, the used control method is efficient.
We should note that a simple on/off control can also contribute to an important energy saving in all the cases.

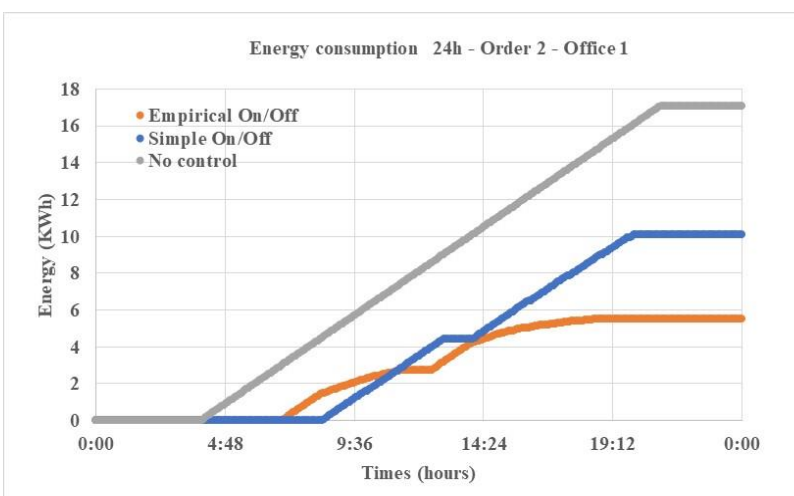

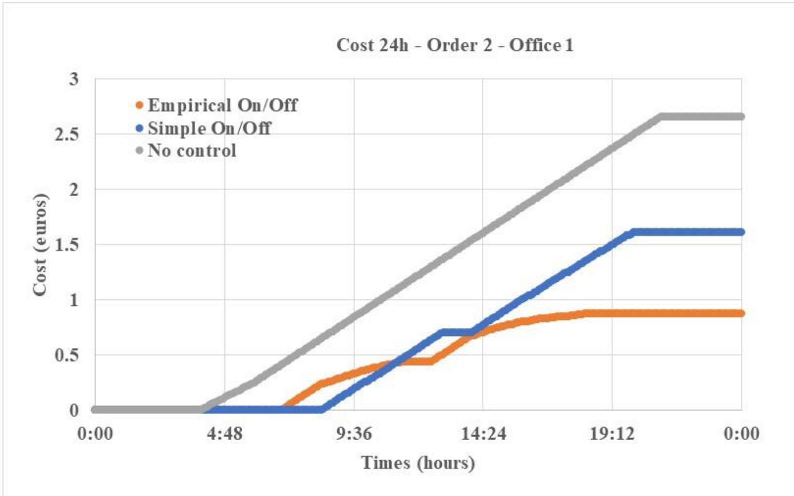

Figures 5.14: Comparison of energy consumption and cost for 24h for different control methods – Model of order 2 – Office 1.

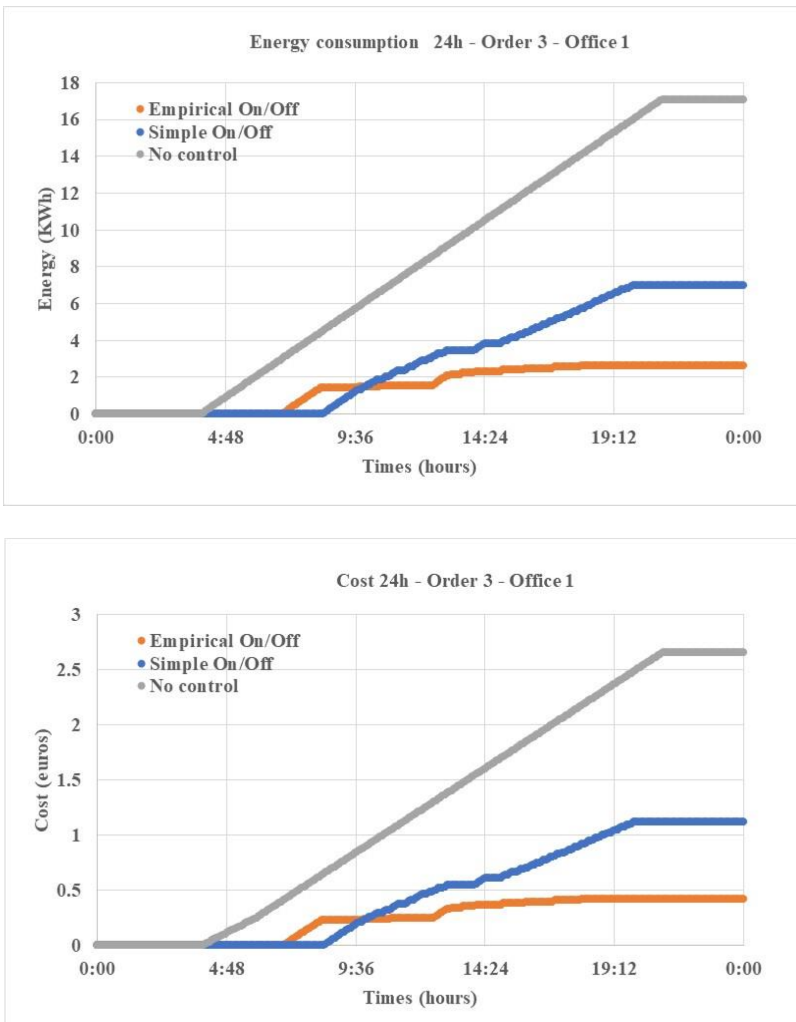

Figures 5.15: Comparison of energy consumption and cost for 24h for different control methods – Model of order 3 – Office 1.

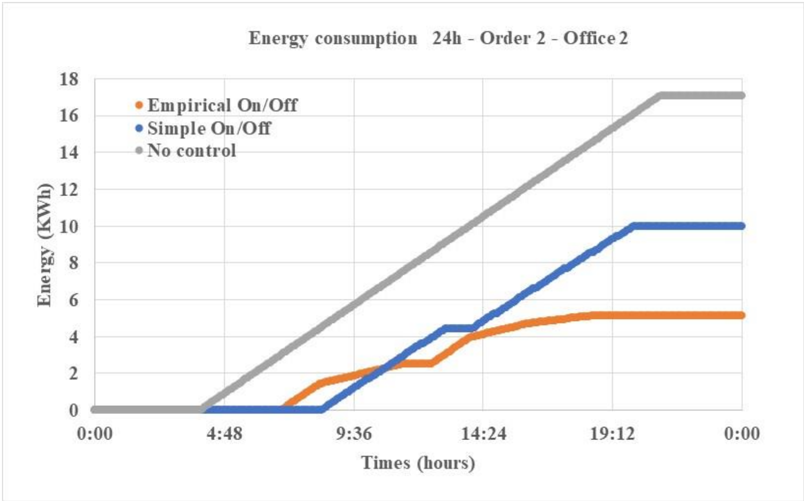

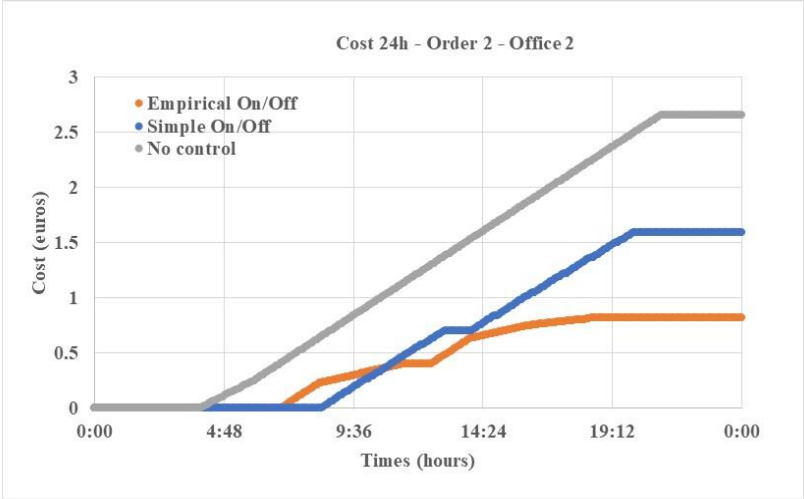

Figures 5.16: Comparison of energy consumption and cost for 24h for different control methods – Model of order 2 – Office 2.

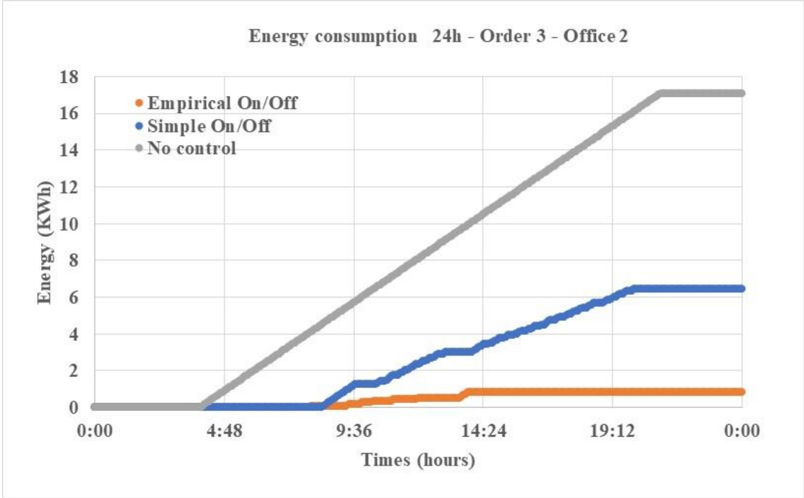

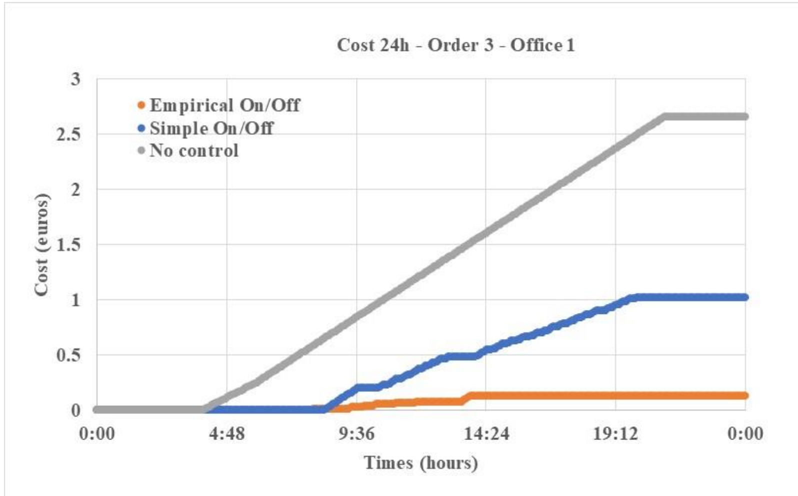

Figures 5.17: Comparison of energy consumption and cost for 24h for different control methods – Model of order 3 – Office 2.

This analysis confirms the effectivity of the proposed empirical on/off control method. These two applications complete the initial analysis and strengthen the previous results. The two main objectives of the control system were achieved: maintaining the thermal comfort of the occupant and performing important energy savings.

5.6 Conclusion

This chapter presented an empirical on/off control method to minimize the energy consumption. It was based on the previous grey box modeling and parameters identification. The most two performant model's orders were considered.

The research was conducted according to the following methodology. At first, a simple on/off control while heating at 1500W was applied to determine the response time needed to reach the comfort temperature. High level heating for the previous determined time was applied and followed by low-level power for the rest of the day considering the occupation period. The indoor temperature was predicted considering different heating powers and compared to the comfort one in order to optimize the energy consumption. 150W heating during occupation period was found enough to provide the thermal comfort for models of order 2 and 3.

This analysis indicates that this control method was effective. It maintains the thermal comfort of the occupant as well as performing important energy savings. Two other applications were conducted to confirm these results.

Conclusion and perspective

This work constitutes a part of Sunrise project, whose goal is to make the campus of Lille 1 university a demonstrator of a smart and durable city. The aim of this thesis is to introduce the smart concept in the building system to ensure occupant comfort, as well as for energy optimization. The use of this technology requires forecasting of the indoor temperature for the regulation of energy devices. Thus, the use of models for sustainability assessment of intelligent buildings was a key strategy to quantify the improvement of energy efficiency and occupants' satisfaction. The study is applied on tertiary buildings at the school of engineering 'Polytech'Lille' and at the research building 'A4' in Lille1 university in France. An advanced monitoring system was installed in many buildings for modeling purpose to study buildings' thermal behavior.

Firstly, a bibliographic analysis presented the problematic related to energy consumption and focused on thermal modeling for buildings. It showed that recent development in smart technology offers new opportunity to collect comprehensive data about the building environment and use. This study allows the selection of the appropriate classes of thermal models: 'Artificial Neural Network' which is a nonlinear application of the black box approach and Grey box models which is a hybrid approach located midway between the black box models and the white box models.

Thermal modeling required a preliminary analysis to determine the major factors influencing the indoor temperature for better forecasting and optimization of the heating energy in order to improve buildings performance. For this purpose, an experimental thermal investigation was conducted at three locations at the University of Lille Campus: One office in the first floor, 4 offices at the 4th floor and one open space in one level building. The study showed that indoor parameters' distribution is not uniform within the room. This analysis allowed the optimization of the monitoring system by focusing on monitoring the external wall for the fourth floor. The investigation indicates that indoor conditions are largely affected by the orientation of the room, the state of windows and users' behavior. Furthermore, the analysis of a central heating system for an open space showed that more significant energy savings can be done through regulation.

Afterwards, ANN prediction models for forecasting façade and indoor temperature for the 'polytech'Lille' building were presented. A methodology for the development of a simplified ANN-based model for forecasting indoor temperature was proposed. The methodology includes the forecasting of the indoor façade temperature considering outdoor and indoor conditions and the prediction of the temperature at the room center considering only the indoor façade temperature.

Relevance analysis of different parameters led to a simplified forecasting model with restricted input parameters. Analyses showed that two-hour façade temperature forecasting could be conducted with good precision using only the outdoor temperature and three-hour façade temperature history.

The proposed methodology could be used for other situations by using first only temperature sensors for measuring the outdoor and the indoor façade temperatures. Moreover, the ANN model gave good forecasting of the temperature at the room center in considering only the façade temperature.

The fourth chapter presented Grey Box models predicting indoor temperature of A4 building. Results showed that the most performant order for forecasting is not unique. It varies with the data dynamics. Reduced model of order 1 was sufficient to predict the indoor temperature without heating. For dynamic data, model of order 3 was the most performant for heating at 900W. Whereas, model of order 2 was the most performant for heating at 1500W. We noticed that, prediction models became more sensible for higher orders (order 4) for the first two experiments. It indicates that complexity and higher orders are always required for modelling buildings' characteristics and dynamics.
A sensitivity study showed that all the parameters of the three most performant models have a significant impact on model outputs (temperature). This validates the model architecture and ensure that all parameters are identifiable.

Finally, grey box modeling prediction was completed by the introduction of an empirical on/off control method. The proposed methodology aimed for reducing the initial high power and finding the most convenient one. Results showed that this method is effective and contributes to important energy savings. This was also confirmed by the application of two other models.

Several sequels to this work can be envisaged. This study can be developed to generate an automated process for model's training and identification to determine short term indoor temperature prediction and building characteristics based on grey-box modeling.
Application of the proposed methodology for ANN prediction should be investigated for long-term temperature forecasting.
As a follow-up to this study, it would be interesting to delve more deeply into general results.
Improvement tracks can be envisaged on the forecasting models and strategies on a more representative panel of tertiary building sector and for longer periods of heating and cooling.

References

[1] Costa, A.; Keane, M.; Torrens, J.; Edward, C. Building operation and energy performance: Monitoring, analysis and optimization toolkit. Appl Energy, 2013, 101, 310–316.

[2] http://www.statistiques.developpement-durable.gouv.fr

[3] Centre Scientifique et Technique du bâtiment. Comparaison international bâtiment et énergie.

[4] Maes, P. Labels d'efficacité énergétique. EYROLLES, 2010, ISBN :978-2- 212-12644-0.

[5] ADEME, consommation d'énergie dans les bâtiments – chiffre clés.

[6] Hensen, J.L.M. Simulation for performance-based building and systems design: some issues and solution direction, Proc. of 6th International Conference on Design and Decision Support Systems in Architecture and Urban Planning, 2002, 186-199.

[7] Richalet, V. Caractérisation énergétique des bâtiments sur site. Identification de modèles dynamiques. Méthodes de signature Energétique. Thèse de doctorat, INPG, 1991, Grenoble, France.

[8] Lacassagne, S.; and Schilken.P. Les outils de planification énergétique territoriale. Bonnes pratiques de villes européennes, 2003.

[9] Direction de la Climatologie MÉTÉO FRANCE : Fiche méthode degrés jours. Disponible sur internet à l'adresse http ://climatheque.meteo.fr/Docs/DJC-methode.pdf, 03 2005.

[10] Da silva, D. Analyse de la flexibilité des usages électriques résidentiels : application aux usages thermiques. Thèse de doctorat, 2011, MINES ParisTech, France.

[11] Bertagnolio, S. Evidence-based model calibration for efficient building energy services. 2012, University of Liège, France.

[12] Foucquier, A.; Robert, S.; Suard, F.; Stéphan, L.; Jay, A.; State of the art in building modelling and energy performances prediction: A review, Renew Sust Energ Rev. 2013, 23, 272–288.

[13] Fang, P.; Liu, T.; Liu, K.; Zhang, Y.; Zhao, J. A Simulation model to calculate temperature distribution of an air-conditioned room. In Proceedings of the 2016 8th International Conference on Intelligent Human-Machine Systems and Cybernetics, Hangzhou, China, 27–28 August 2006.

[14] Jigang, Z. Study on the Airflow & Temperature Field Characteristics in the Room with Wall Air Conditioner and on the Human Thermal Comfort; Shandong University: Jinan, China, 2007.

[15] Lawrence Berkeley Laboratory, "DOE-2 Engineering Manual Version 2.1C", Lawrence Berkeley Laboratory, Berkeley, 1982.

[16] Park, C.; Clark, D.R.; Kelly, G.E. HVACSIM+ building systems and equipment simulation program: building loads calculation, NBSIR 86-3331, National Bureau of Standards, February 1986.

[17] Klein, S.A. et al., TRNSYS 16 –A TRaNsient SYstem Simulation program, Solar Energy Laboratory, University of Wisconsin-Madison, Madison, USA, User Manual, 2004.

[18] Hittle, D.C. Building loads analysis and system thermodynamic (BLAST) programs. Version 2.0: Users' Manual", Technical Report E-153, US Army Construction Engineering Research Laboratory (USACERL), Champaign, IL, 1979.

[19] Crawley, D.B.; Lawrie, L. K.; Pedersen, C. O.; Winkelmann, F. C. EnergyPlus: energy simulation program, ASHRAE Journal, 2000, 42, 49-56. (http://apps1.eere.energy.gov/buildings/energy-plus/pdfs/bibliography/ashrae_journal_0400.pdf)

[20] Dodier, R. H; Henze, G. P. Statistical analysis of neural networks as applied to building energy prediction, Journal of Solar Energy Engineering, Transactions of the ASME, Feb 2004, 126, 592-600.

[21] Ruano, A. E.; Crispim, E. M.; Conceição, E. Z. E.; Lúcio, M. M. J. R. Prediction of building's temperature using neural networks models, Energy and Build. 2006, 38, 682-694.

[22] Soleimani-Mohseni, M.; Thomas, B.; Fahlén, P. Estimation of operative temperature in buildings using artificial neural networks. Energy and Build. 2006, 38, 635-640.

[23] Rabl, A.; Rialhe, A. Energy signature models for commercial buildings: test with measured data and interpretation. Energy and build. 1992, 19,143-154.

[24] Andersen, P. H. D.; Madsen, H.; Rode, C. Models for the energy performance of low-energy houses. Kgs. Lyngby: Technical University of Denmark (DTU), 2013.

[25] Afroz, Z.; Shafiullah, GM.; Urmee, T.; Higgins, G. Prediction of indoor temperature in an institutional building. 9th International Conference on Applied Energy, ICAE2017, 21-24 August 2017, Cardiff, UK

[26] Ahmad, M.; Mourshed, M.; Rezgui, Y. Trees vs Neurons: comparison between random forest and ANN for high-resolution prediction of building energy consumption. Energy and Build. 2017, 147, 77–89.

[27] Wang, Z.; Srinivasan, R.S. A review of artificial intelligence-based building energy use prediction: Contrasting the capabilities of single and ensemble prediction models. Renew Sust Energ Rev. 2017,75, 796–808.

[28] Deb, C.; Zhang, F.; Yang, J.; Lee, S. E; Shah, K.W. A review on time series forecasting techniques for building energy Consumption. Renew Sust Energ Rev. 2017, 74, 902–924.

[29] Laret, L. Contribution au développement de modèles mathématiques du comportement thermique transitoire de structures d'habitation. 1980, Université de Liège, France.

[30] Roux, J.-J. Proposition de modèles simplifies pour l'étude du comportement thermique des bâtiments. Thèse de doctorat, Institut national des sciences appliquées de Lyon, 1980, Lyon, France.

[31] Zayane, C. Identification d'un modèle de comportement thermique de bâtiment à partir de sa courbe de charge. PhD thesis, Ecole Nationale Superieure des Mines de Paris, 2011, Paris, France.

[32] Deng, K.; Barooah, P.; Mehta, P. G.; Meyn, S. P. Building thermal model reduction via aggregation of states. In American Control Conference (ACC), 2010, 5118–5123. IEEE, 2010.

[33] Janssens, A. Reliable building energy performance characterization based on full scale dynamic measurements. International Energy Agency, Technical report, EBC Annex 58.

[34] SEMTECH Advanced communications and sensing, www.semtech.com.

[35] Barbuiya S.; Barbuiya S. Thermal comfort and energy consumption in a UK educational building. Build Environ 2013; 68:1-11.

[36] Zhang, H.J.; Dai, L.; Xu, G.Q.; Li, Y.; Chen, W.; Tao, W.Q. Studies of air-flow and temperature fields inside a passenger compartment for improving thermal comfort and saving energy, part I: test/numerical model and validation, Appl Therm Eng. 2009, 29 (10), 2022–2027.

[37] Zingano, B.W. A discussion on thermal comfort with reference to bath water temperature to deduce a midpoint of the thermal comfort temperature zone, Renew Energ. 2001, 23 (1), 41–47.

[38] Manzan, M.; Saro, O. Numerical analysis of heat and mass transfer in a passive building component cooled by water evaporation, Energy and Build. 2002, 34 (4), 369–375.

[39] Chow, K.; Holdo, A. E. On the influence of boundary conditions and thermal radiation on predictive accuracy in numerical simulations of indoor ventilation, Build Enviro. 2010, 45, 437–444.

[40] Ding, G.L.; Qiao, H.T.; Lu, Z.L. Ways to improve thermal uniformity inside a refrigerator, Appl Therm Eng. 2004, 24, 1827–1840.

[41] Antonio, C.C.; Afonso, C.F. Air temperature fields inside refrigeration cabins: a comparison of results from CFD and ANN modelling, Appl Therm Eng. 2011, 31, 1244–1251.

[42] Liu, J.; Aizawa, Y.; Yoshino, H. Experimental and numerical study on indoor temperature and humidity with free water surface, Energy and Build. 2005, 37, 383–388.

[43] Sureshkumar, R.; Kale, S.R.; Dhar, P.L. Heat and mass transfer processes between a water spray and ambient air – I. Experimental data, Appl Therm Eng. 2008, 28, 349–360.

[44] Sureshkumar, R.; Kale, S.R.; Dhar, P.L. Heat and mass transfer processes between a water spray and ambient air – II. Experimental data, Appl Therm Eng. 2008, 28, 349–360.

[45] Autodesk. Ecotect. 2013.

[46] U.S. Department of Energy. Energy plus 8.0. 2013.

[47] Dias Pereira, L.; Raimondo, D.; Corgnari, S.P.; Gemairo da Silva, M. Assessment of indoor air quality and thermal comfort in Portuguese secondary classrooms: Build Environ 2014; 81, 69-80.

[48] Deb, C.; Eang, L. S.; Yang, J.; Santamouris, M. Forecasting diurnal cooling energy load for institutional buildings using Artificial Neural Networks. Energy and Build. 2016, 121, 284-297.

[49] Jovanovi´c, R.Z.; Sretenovi´c, A.A.; Zivkovi´c, B.D. Ensemble of various neural networks for prediction of heating energy consumption, Energy Build. 2015, 94, 189–199.

[50] Li, Q.; Meng, Q.; Cai, J.; Yoshino, H.; Mochida, A. Predicting hourly cooling load in the building: a comparison of support vector machine and different artificial neural networks, Energy Convers. Manage. 2009, 50, 90–96.

[51] Azadeh, A.; Ghaderi, S.; Tarverdian, S.; Saberi, M. Integration of artificial neural networks and genetic algorithm to predict electrical energy consumption, Appl. Math. Comput. 2007, 186, 1731–1741.

[52] Cybenko, G. Approximation by superposition of a sigmoidal function, Math. Control Signal Syst. 1989, 2, 303–314.

[53] Funahashi, K. On the approximate realization of continuous mappings by neural networks. Neural Netw. 1989, 2, 183–192.

[54] Hornik, K.; Stinchcombe, M.; White, H. Multilayer feed forward networks are universal approximators. Neural Netw. 1989, 2, 359–366.

[55] Girosi, F.; Poggio, T. Networks and the Best Approximation Property. Biol. Cybern. 1990, 63, 169–176.

[56] Thibault, J.; Grand jean, B.P.A. A neural network methodology for heat transfer data analysis. Int. J. Heat Mass Transfer 1991, 34, 2063–2070.

[57] Zdaniuk, G.J. Heat Transfer and Friction in Helically-finned Tubes Using Artificial Neural Networks. Ph.D. dissertation, 2006, Mississippi State University, USA.

[58] Yilmaz, S.; Atik, K. Modeling of a mechanical cooling system with variable cooling capacity by using artificial neural network, Appl. Therm. Eng. 2007, 27, 2308–2313.

[59] Kreider, J.F. Neural networks applied to building energy studies, in: H. Bloem (Ed.), Workshop on Parameter Identification, JRC Ispra, Ispra, 1995, 243–251.

[60] Subodh, K.S.; Manju, R.; Gayatri, P.K. M. Expression pattern analysis of different micro RNAs under nitrogen deprivation condition in root tissues of different wheat genotypes, Indo Global J. Pharm. Sci. 2014, 4 (3), 194.

[61] Njau, E.C. Prediction of meteorological parameters: I. Analytical method, Nuovo Cimento 14C, 1991, 473–488.

[62] Njau, E.C. Prediction of meteorological parameters: II. Methods based on an electronic system, in: Proceedings of the International Conference on Global Warming and Climate Change, Geneva, Switzerland, 1993.

[63] Gobakis, K.; Kolokotsa, D.; Synnefa, A.; Saliari, M.; Giannopoulou, K.; Santamouris, M.; Development of a model for urban heat island prediction using neural network techniques, Sustain. Cities Soc. 2011, 1, 104–115.

[64] Mihalakakou, G.; Santamouris, M.; Asimakopoulos, D.N. The total solar radiation time series simulation in Athens, using neural networks, Theor. Appl. Climatol. 2000, 66 (3–4), 185–197.

[65] Mihalakakou, G.; Santamouris, M.; Asimakopoulos, D. Modeling ambient air temperature time series using neural networks, J. Geophys. Res. 1998, 103, 509–517.

[66] Kolokotroni, M.; Davies, M.; Croxford, B.; Bhuiyan, S.; Mavrogianni, A. A validated methodology for the prediction of heating and cooling energy demand for buildings within the Urban Heat Island: case-study of London, Sol. Energy. 2010, 84 (12), 2246–2255.

[67] Parishwad, G.V.; Bhardwaj, R.K.; Nema, V.K. Prediction of monthly-mean hourly relative humidity, ambient temperature, and wind velocity for India, Renew. Energy. 1998, 13 (3), 363–380.

[68] Imran, T.; Shafiqur, R.; Khaled B. Application of neural networks for the prediction of hourly mean surface temperatures in Saudi Arabia, Renew. Energy. 2002, 25, 545–554.

[69] Lu, T.; Viljanen, M. Prediction of indoor temperature and relative humidity using neural network models: Model comparison. Neural Comput. Appl. 2009, 18, 345–357.

[70] Zabada, S.; Shahrour, I. Analysis of Heating Expenses in a Large Social Housing Stock Using Artificial Neural Networks. Energies 2017, 10, 2086.

[71] Khayatian, F.; Sarto, L.; Dall'O, G. Application of neural networks for evaluating energy performance certificates of residential buildings. Energy Build. 2006, 125, 45–54.

[72] P.J. Werbos, Beyond regression: new tools for prediction and analysis in the behavioral science, Harvard University, Cambridge, MA, 1974 (PhD thesis).

[73] Mba, L. Modélisation du Comportement Thermique du Bâtiment: Application d'une Méthode Neuronale; Université de Douala-Cameroun: Douala, Cameroon, 2009.

[74] Mba, L.; Kemajou, A.; Meukam, P. Application of artificial neural network for modeling the thermal behavior of building in humid region. Presented at the Actes des 3ème Rencontres EG@, Yaoundé, Cameroun, 14–16 Septembre 2010.

[75] Brano, V.L.; Ciulla, G.; Falco, M.D. Artificial neural networks to predict the power output of PV panel. Int. J. Photoenergy 2014, 2014, 193083.

[76] Kemajou, A.; Mba, L.; Meukam, P. Application of artificial neural network for predicting the indoor air temperature in modern building in humid region. Br. J. Appl. Sci. Technol. 2012, 2, 23–34.

[77] Manssouri, T.; Sahbi, H.; Manssouri, I.; Boudad, B. Utilisation d'un modèle hybride base sur la rlms et les rna-pmc pour la prédiction des paramètres indicateurs de la qualité des eaux souterraines cas de la nappe de Souss-Massa-Maroc. Eur. Sci. J. 2015, 11, 35–46.

[78] Paudel, S.; Elmtiri, M.; Kling, W.L.; Le Corre, O.; Lacarrière, B. Pseudo dynamic transitional modeling of building heating energy demand using artificial neural network. Energy Build. 2014, 70, 81–93.

[79] Said, S.M. Degree-day base temperature for residential building energy prediction in Saudia Arabia. ASHRAE Trans. 1992, 98, 346–353.

[80] Ding, Y.; Zhang, Q.; Yuan, T.; Yang, K. Model input selection for building heating load prediction: A case study for an office building in Tianjin. Energy Build. 2018, 159, 254–270.

[81] Ferrari, S. Building envelope and heat capacity: Re-discovering the thermal mass of winter energy savings. In Proceedings of the 28th AIVC Conference, Crete, Greece, 27–29 September 2007.

[82] Gagliano, A.; Patania, F.; Nocera, F.; Signorello, C. Assessment of the dynamic thermal performance of massive buildings. Energy Build. 2014, 72, 361–370.

[83] Ulgen, K. Experimental and theoretical investigation of effects of walls' thermos-physical properties on time lag and decrement factor. Energy Build. 2002, 34, 273–278.

[84] Strachan, P.A.; Vandaele, L. Case studies of outdoor testing and analysis of building components, Build. Environ. 2008, 43 (2), 129–142.

[85] Androutsopoulos, A.; Bloem, J.J.; Van Dijk, H.A.L.; Baker, P.H. Comparison of user performance when applying system identification for assessment of the energy performance of building components, Build. Environ. 2008, 43 (2), 189–196.

[86] Hazyuk, I.; Ghiaus, C.; Penhouet, D. Optimal temperature control of intermittently heated buildings using model predictive control: Part I –Building modeling, Build. Environ. 2012, 51, 379–387.

[87] Lee, K.-h.; Braun (Eds.), J.E. Development and Application of an Inverse Building Model for Demand Response in Small Commercial Buildings, Boulderand CO, 2004.

[88] Klaus, K.A.; Henrik, M.; Lars, H.H. Modelling the heat dynamics of a building using stochastic differential equations, Energy Build. 2000, 31 (1), 13 -24.

[89] Hudson, G.; Underwood, C.P. A simple building modelling procedure for matlab/simulink, in: Proceedings of 7th Conference of International Building Performance Simulation Association and Kyoto and Japan, 1999.

[90] Kramer, R.; Van Schijndel, J.; Schellen, H. Simplified thermal and hygric building models: a literature review, Front. Archit. Res. 2012, 1 (4), 318–325.

[91] Hedgaard, R.E.; Peterson, S. Evaluation of grey box model parameter estimates intended for thermal characterization of buildings. 11th Nordic Symposium on Building Physics, NSB2017, 11-14 June 2017, Trondheim, Norway.

[92] Bacher, P.; Madsen, H. Identifying suitable models for the heat dynamics of buildings, Energy Build. 2011, 43 (7), 1511–1522.

[93] Fux, S.F.; Ashouri, A.; Benz, M.J.; Guzzella, L. EKF based self-adaptive thermal model for a passive house, Energy Build. 2014,68 (Part C), 811–817.

[94] Harb, H.; Boyanov, N.; Hernandez, L.; Streblow, R.; Müller, D. Development and validation of grey-box models for forecasting the thermal response of occupied buildings. Energy Build. 2016,117, 199-207.

[95] Fonti, A.; Comodi, G.; Pizzuti, S.; Arteconi, A.; Helsen, L. Low order grey box models for short-term thermal behavior prediction in buildings. The 8th International Conference on Applied Energy – ICAE, 2016, China.

[96] Afram, A.; Janabi-Sharifi, F. Review of modeling methods for HVAC systems, Appl Therm Eng. 2014, 67, 507-519.

[97] K. K. Associates, Thermal Network Modeling Handbook, 2000.

[98] Floyd, T.L. Electronic devices. Upper Saddle River, N.J.: Prentice Hall, 2002.

[99] https://fr.mathworks.com/help/ident/ref/nlgreyestoptions.html.

[100] Berthou, T.; Stabat, P.; Salvazet, R.; Marchio, D. Development and validation of a gray box model to predict thermal behavior of occupied office buildings, Energy Build. 2014, 74, 91–100.

[101] CSTB, 2005. Réglementation Thermique 2005.

[102] CSTB, 2012. Réglementation Thermique 2012.

[103] https://fr.mathworks.com/help/ident/ref/goodnessoffit.html?s_tid=doc_ta.

[104] Keesman KJ. System Identification. 1st ed. London: Springer-Verlag; 2011.

[105] Reynders, G.; Nuytten, T.; Saelens, D. Robustness of reduced-order models for prediction and simulation of the thermal behavior of dwellings. 13th Conference of International Building Performance Simulation Association, Chambéry, France, August 26-28, 2013.

[106] Saltelli, A.; Annoni, P.; Azzini, I.; Campolongo, F.; Ratto, M.; Tarantola, S.; Variance based sensitivity analysis of model output. Design and estimator for the total sensitivity index, Computer Physics Communications 2010, 181, 259–270.

[107] Jansen, M.J. Analysis of variance designs for model output, Computer Physics Communications. 1999, 117, 35–43.

[108] M. Castilla, J.D. Alvarez, M. Berenguel, F. Rodriguez, J.L. Guzman, M. Perez, A comparison of thermal comfort predictive control strategies. Energy Build. 43(2011) 2737 – 2746.

[109] C. Dai, L. Lan, Z. Lian, Method for the determination of optimal work environment in office buildings considering energy consumption and human performance. Energy Build. 76 (2014) 278 – 283.

[110] Z. Vàn̂a, J. Cigler, J. Široky, E. Žačekova, L. Ferkl, Model based energy efficient control applied to an office building. Journal of Process Control, 24 (2014) 790 – 797.

[111] L. Peeters, J. Van der Veken, H. Hens, L. Helsen, W. D'haeseleer, Control of heating systems in residential buildings: Current practice. Energy Build. 40 (2008) 1446 – 1455.

[112] G. S. Brager, R. de Dear, Climate, comfort, & natural ventilation: a new adaptive comfort standard for ashrae standard 55, 2001.

[113] G. S. Brager, R. de Dear, Climate, comfort, & natural ventilation: a new adaptive comfort standard for ashrae standard 55. UC Berkeley: Center for the Built Environment, 2001.

[114] G. Ye, C. Yang, Y. Chen, Y. Li, A new approach for measuring predicted mean vote (pmv) and standard effective temperature (set). Building Env., 38 (2003) 33 – 44.

Appendix A Publication

energies

MDPI

Article

Smart Building: Use of the Artificial Neural Network Approach for Indoor Temperature Forecasting

Nivine Attoue [1], Isam Shahrour [1,2,*] and Rafic Younes [3]

[1] Laboratory of Civil Engineering and Geo-Environment, Lille University, 59650 Villeneuve d'Ascq, France; nivine.attoue@gmail.com

[2] School of Civil Engineering, Tongji University, Shanghai 200092, China

[3] Modeling Center, Lebanese University, Hadath 99000, Lebanon; ryounes@ul.edu.lb

* Correspondence: isam.shahrour@univ-lille1.fr; Tel.: +33-320434545

Received: 6 January 2018; Accepted: 7 February 2018; Published: 8 February 2018

Abstract: The smart building concept aims to use smart technology to reduce energy consumption, as well as to improve comfort conditions and users' satisfaction. It is based on the use of smart sensors and software to follow both outdoor and indoor conditions for the control of comfort, and security devices for the optimization of energy consumption. This paper presents a data-based model for indoor temperature forecasting, which could be used for the optimization of energy device use. The model is based on an artificial neural network (ANN), which is validated on data recorded in an old building. The novelty of this work consists of the methodology proposed for the development of a simplified model for indoor temperature forecasting. This methodology is based on the selection of pertinent input parameters after a relevance analysis of a large set of input parameters, including solar radiation outdoor temperature history, outdoor humidity, indoor facade temperature, and humidity. It shows that an ANN-based model using outdoor and facade temperature sensors provides good forecasting of indoor temperatures. This model can be easily used in the optimal regulation of buildings' energy devices.

Keywords: smart building; artificial neural network (ANN); indoor; temperature; facade; outdoor; forecasting; relevance; sensors; recorded data

1. Introduction

The smart building concept aims to use smart technology to reduce energy consumption, as well as to improve comfort and users' satisfaction. Forecasting of the indoor temperature is necessary for the regulation of energy devices to ensure occupant comfort, as well as for energy optimization [1,2]. This forecasting constitutes a complex task, because it is governed by complex physical and behavioral phenomena. It is affected by a multitude of parameters, which could be classified into three groups: outdoor conditions, building characteristics, and occupants' behavior [3–5]. In addition, investigations showed that the indoor temperature does not have uniform distribution [6].

Indoor temperature forecasting could be carried out using physical or data-driven approaches [7]. The physical approach is based on the use of numerical modelling [8,9], which requires detailed information about a building's characteristics, appliances, and occupant behavior.

The data-driven approach is based on the use of collected data for developing relationships (models) between 'input' parameters and 'output' parameters. These relationships could be established by learning from collected data. The artificial neural network (ANN) approach was used to build data-driven models [10–12]. Soleimani-Mohseni et al. [13] showed that the operative temperature could be well estimated by the ANN approach using the indoor air temperature, electrical power, outdoor temperature, time of day, wall temperature, and ventilation flow rate. Lu and Viljanen [14] used the ANN approach to predict air temperature and relative humidity in a test room using indoor and outdoor temperature and humidity. Recently, Zabada and Shahrour [15] used the ANN approach for the analysis of the heating expenses in social housing. In these works, the ANN model was used as a prediction tool for specific cases. This paper proposes a methodology, which could be followed for the use of the ANN approach for the indoor temperature forecasting in any type of building. This methodology is based on the use of a relevance analysis for the determination of pertinent input parameters and the optimal ANN architecture. The methodology is presented through its application on data recorded in an old building.

2. Data Collection

Data were collected using a smart monitoring of an old building of Polytech'Lille Engineering School in the north of France. Monitoring concerned indoor and outdoor temperature and humidity, as well as solar radiation [16,17]. Parameters were recorded at five-minute intervals and then sent to a local server. Figure 1 illustrates an example of recorded data on a summer day. Data concerns the outdoor temperature, as well as the indoor temperature at three locations in the office: facade, center of the lateral wall, and office center. The external temperature varied between 17.5 °C and 34 °C, while the facade indoor temperature varied between 21 °C and 25.5 °C. The temperatures at the center of the office and the center of the lateral wall varied between 22 °C and 24.2 °C.

Data were collected for two summer months (June and July) in different offices of the building.

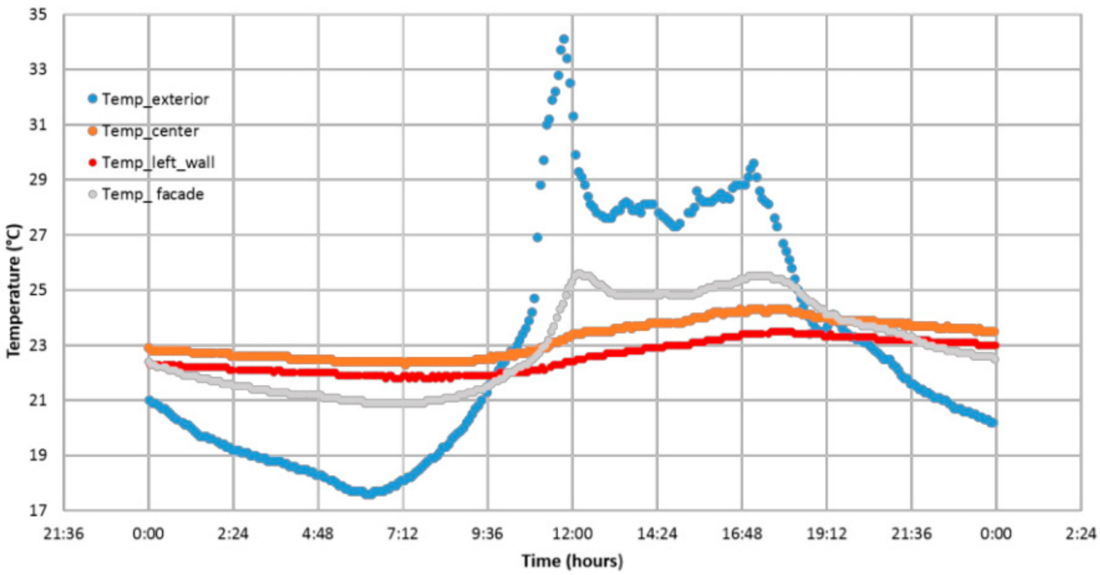

Figure 1. Temperature variation on a summer day.

3. Artificial Neural Network Approach

The ANN approach is inspired from the ability of the human brain to predict patterns based on learning and recalling processes. It allows the construction of relationships between input parameters and output parameters using artificial neurons, which are arranged in an input layer, an output layer and one or more hidden layers [18]. Analyses were conducted using the multilayer back-propagation neural network. We used a three-layer ANN with n, m, and k as the number of input, hidden, and output nodes, respectively, based on the equation:

$$Y_k = S(\sum_{j=1}^{m} W_{jk} \times S(\sum_{i=1}^{n} W_{ij} X_i)), \tag{1}$$

where Y_k stands for the output values and X_i denotes the input values; W_{ij} gives the weights of connection between the input layer and the hidden layer.

The ANN performances could be evaluated using the mean square error (MSE) and the coefficient of correlation (R)

$$MSE = \sum_{i=1}^{n} \left(\frac{e_i^2}{N}\right), \tag{2}$$

$$R = \pm\sqrt{\frac{\sum_{i=1}^{N} \left(Y_i - \overline{X}\right)^2}{\sum_{i=1}^{N} \left(X_i - \overline{X}\right)^2}} = \sqrt{1 - \frac{\sum_{i=1}^{N} \left(e_i\right)^2}{\sum_{i=1}^{N} \left(X_i - \overline{X}\right)^2}} \tag{3}$$

where e_i is the error between the ANN output (Y_i) and the experimental input (X_i), $\overline{X}$ represents the mean of the input target.

Different ANN architectures exist. The multilayer perception (MLP) structure is the most popular [19–24]. Its use with a single hidden layer and a sufficient number of neurons provided good accuracy for the approximated function [25,26]. This architecture is used in this work.

The use of ANN for temperature forecasting aims to predict the building indoor temperature for the optimal regulation of energy devices as well as for ensuring occupants' comfort. Indoor conditions of a building are highly affected by its age and thermal performance, which depends on its envelope and construction material. The input parameters concern the outdoor conditions, indoor conditions, as well as the occupants' behavior. The forecasting time depends on the building thermal inertia and energy regulation system. Each building is characterized by its time lag and the time of heat transmission delay [27–30]. The prediction time for ANN models ranged from 0.5 to 4 h to cover the phase of heating exchange through the facade and to investigate the effectiveness of this approach.

This paper proposes a methodology composed of two steps for the use of the ANN approach for indoor temperature forecasting. The first step concerns the indoor facade temperature forecasting considering outdoor and indoor conditions, while the second step concerns the prediction of the temperature at the room center considering the indoor facade temperature.

Analyses were conducted using MATLAB (Mathworks Inc., Natick, MA, USA—Group License) for ANN modeling and IBM SPSS statistics for input parameter ranking.

4. Facade Indoor Temperature Forecasting

4.1. Analysis of the Input Parameters' Relevance

The input parameters used in the global analysis are summarized in Table 1. They concern the outdoor conditions (temperature, humidity, and solar radiation), outdoor temperature history (input matrix for the last 3-h values having 30 min lag between its different columns: if the actual outdoor temperature was recorded at time t, the history matrix corresponds to t—0.5 h, t—1 h, t—1.5 h, t—2 h, t—2.5 h, and t—3 h, the indoor facade temperature history (similar matrix history as the outdoor temperature), and time (cumulative minutes of the day). The time range of history inputs was chosen with respect to the prediction time to cover the phase shift that will occur at the facade level. The impact of a larger range (t—5 h, t—6 h, etc.) for the history inputs did not affect the results. A 30 min lag was chosen to detect any sudden variation at the facade level.

Table 1. Input parameters for the facade temperature forecasting.

Input Parameters
Outdoor temperature
Outdoor humidity
Solar radiation
Outdoor temperature history
Time
Facade temperature history

The ANN optimal architecture (Figure 2) was fixed after several comparative analyses. It includes one hidden layer with four neurons. Table 2 provides the weights of neurons' connections obtained from MATLAB software. We can observe that the weight could be negative or positive providing excitatory or inhibitory influence on each input.

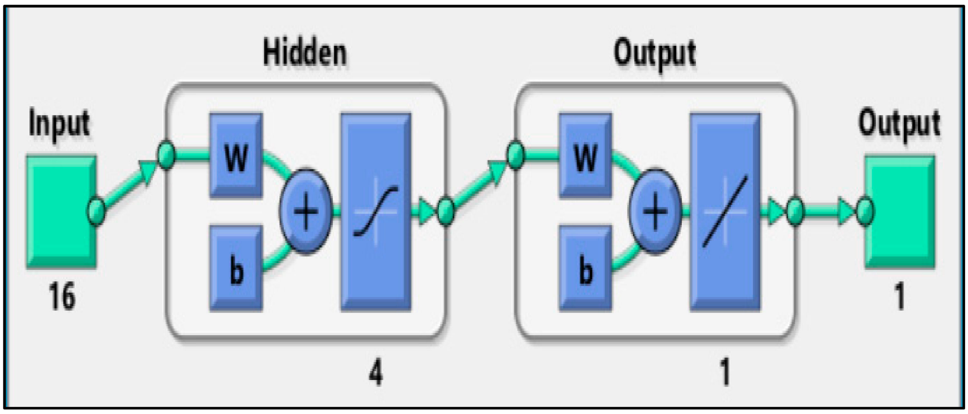

Figure 2. Artificial Neural Network (ANN) optimal architecture.

Table 2. Weight of neurons' connections.

Input Parameters	Neuron 1	Neuron 2	Neuron 3	Neuron 4
Time	2.59	0.02	1.46	–0.02
Outdoor temperature	1.13	–1.25	–0.05	1.32
History of outdoor temperature	2.55 1.79 2.67 –1.11 –1.21 0.86	1.65 –1.05 0.62 –0.95 0.21 –0.02	–0.93 –1.66 –2.02 0.17 –0.54 0.23	–1.60 0.93 –0.64 0.92 –0.27 0.06
History of facade temperature	–2.65 –3.00 –1.04 –0.26 0.50 –0.34	–0.72 0.90 0.50 0.61 –0.31 0.07	–2.76 –1.58 –1.20 –1.18 –0.13 –1.10	1.43 –1.12 –0.38 –0.57 0.33 –0.12
Solar radiation	1.27	0.23	3.52	–0.22
Outdoor humidity	0.01	–0.10	–0.43	0.09

Figure 3 shows comparison of 'predicted' and 'recorded' facade temperatures. We observe a good agreement between these values with $R = 0.9967$ and $MSE = 0.0277$. This result shows that the ANN model predicts well the facade indoor temperature. The determination of input parameters requires two temperature sensors (outdoor and indoor), an external humidity sensor, and a solar radiation sensor.

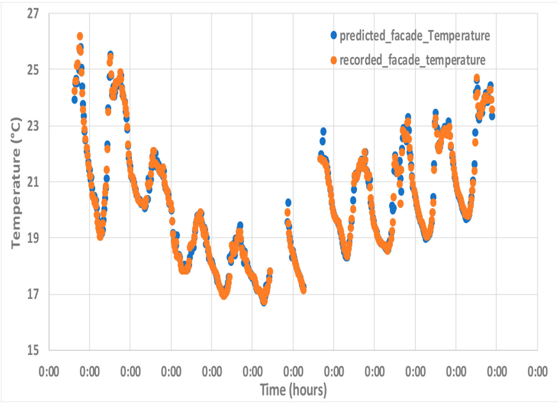

(**a**)

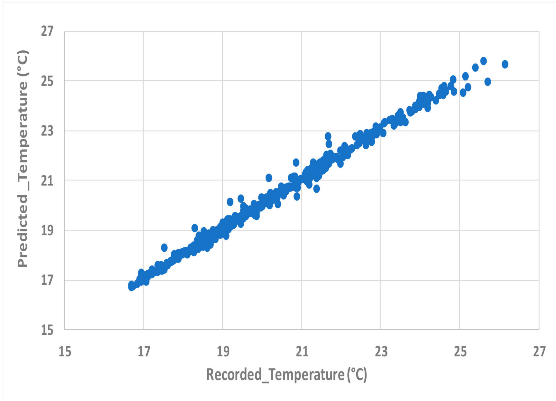

(**b**)

Figure 3. Predicted and recorded facade temperatures: (**a**) variation of both temperatures in time domain; and (**b**) the predicted facade temperature with the recorded facade temperature.

In order to determine the most important input parameters in the ANN model, IBM SPSS statistical software was used to analyze the 'importance' of these parameters. This software is based on inferential statistics. It uses recorded data to perform a sensitivity analysis for the determination of the importance of each input parameter. Table 3 summarizes the obtained results. It shows that the solar radiation, time and humidity have a low role in the forecasting model, with an importance factor lower than 5.1%. The outdoor temperature has the highest importance (Importance Factor = 42%), followed by the historical facade temperature (Importance Factor = 31.9%). The historical outdoor temperature has an intermediate influence with an Importance Factor = 12.8%.

Table 3. Analysis of the relevance of input parameters.

Parameter	Importance Factor (%)
Solar radiation	3.7
Time	4.5
Humidity	5.1
Historic outdoor temperature	12.8
Historic facade temperature	31.9
Outdoor temperature	42.0

Since the role of some input parameters in the ANN model is very weak (with reference to the SPSS classification), analyses were conducted by neglecting these parameters. Table 4 summarizes the results of these analyses. It shows clearly that the neglect of solar radiation, humidity, and historical outdoor temperature (Model 5) does not significantly deteriorate the quality of the ANN model: the mean square error (*MSE*) increases from 0.0277 to 0.0365, while the coefficient of correlation (*R*) decreases from 0.9967 to 0.9959. The additional neglect of the historical data of the facade temperature (Model 6) has a higher influence: *MSE* increases from 0.0277 to 0.4922, while R decreases from 0.9967 to 0.946. Figure 4 illustrates the results of Models 1, 5, and 6. As expected and according to the physics of the heat transfer in transient conditions, this result shows that the facade temperature could be effectively predicted in considering only the outdoor temperature and the historical data of the facade indoor temperature.

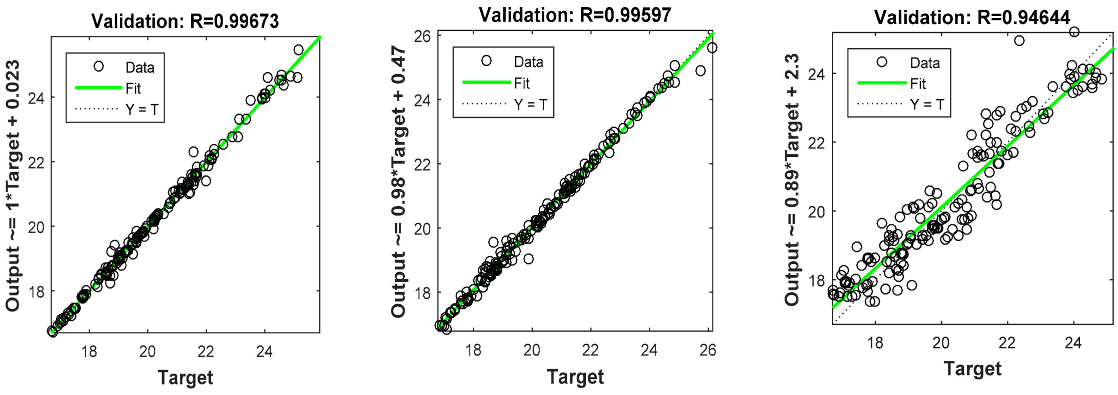

(**a**) (**b**) (**c**)

Figure 4. *R* results for different models: (**a**) Model 1; (**b**) Model 5; and (**c**) Model 6.

Table 4. Degraded model results.

Model	Input Parameter	R	*MSE*
1	Outdoor temperature and history, outdoor humidity, sun radiation, time, facade history	0.9967	0.0277
2	Outdoor temperature, historic, outdoor humidity, time, facade history	0.99687	0.03
3	Outdoor temperature, historic, outdoor humidity, facade history	0.9969	0.0269
4	Outdoor temperature, historic, facade history	0.9975	0.0199
5	Outdoor temperature, facade history	0.9959	0.0365
6	Outdoor temperature	0.946	0.4922

4.2. Facade Temperature Forecasting Model

4.2.1. Use of the Outdoor Temperature as Input Parameter

Considering the results of the previous section, the outdoor temperature is first used as the input parameter for forecasting the facade indoor temperature. The forecasting model provides the temperature at 0.5, 1, 2, and 4 h.

Figures 5 and 6 show the forecasting results at 0.5 and 1.0 h. We observe that the ANN model reproduces well the recorded temperature. For 0.5-h forecasting, R is equal to 0.956 and MSE is equal to 0.4369; while for one-hour forecasting, $R = 0.928$ and $MSE = 0.48454$. Figure 7 shows the forecasting error distribution for 0.5 and one hour. It shows that about 90% of the forecasting error are less than 1 °C.

Figures 8 and 9 shows the forecasting results at two and four hours. We observe a deterioration in the quality of forecasting regarding those obtained at 0.5 and one hour. For two-hour forecasting, $R = 0.9109$ and $MSE = 0.89078$, while for four-hour forecasting, $R = 0.8370$ and $MSE = 1.23783$. Figure 10 shows the forecasting error distribution for two and four hours. It shows that for the former, about 70% of the forecasting error are less than 1 °C, while for the latter about 64% of the forecasting error are less than 1 °C. Table 5 summarizes the forecasting results.

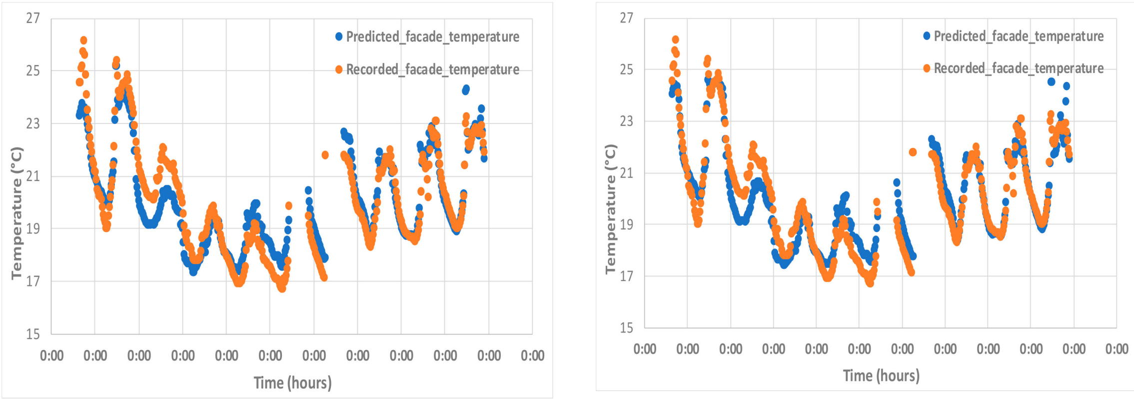

(**a**) (**b**)

Figure 5. Recorded and predicted facade temperature variation in the time domain: (**a**) prediction for 0.5 h; and (**b**) prediction for 1 h.

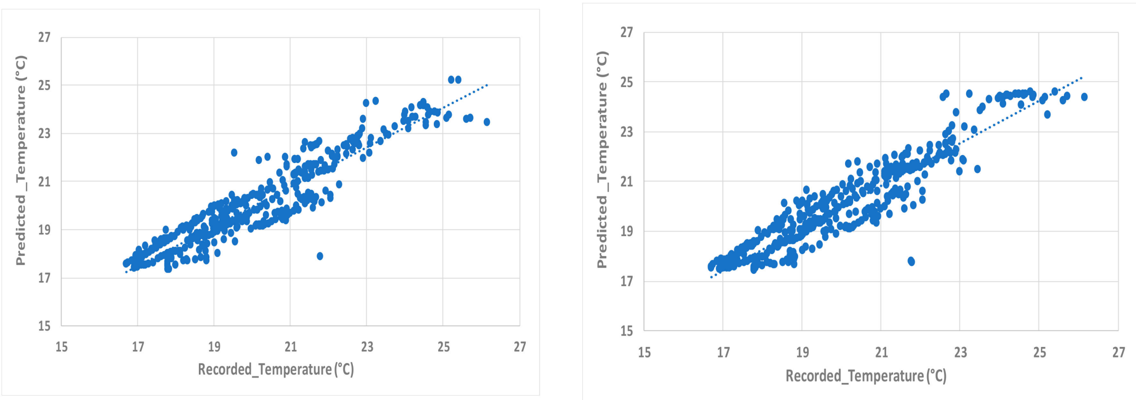

(**a**) (**b**)

Figure 6. Predicted facade temperature with the recorded facade temperature (input parameter = outdoor temperature): (**a**) prediction for 0.5 h; and (**b**) prediction for 1 h.

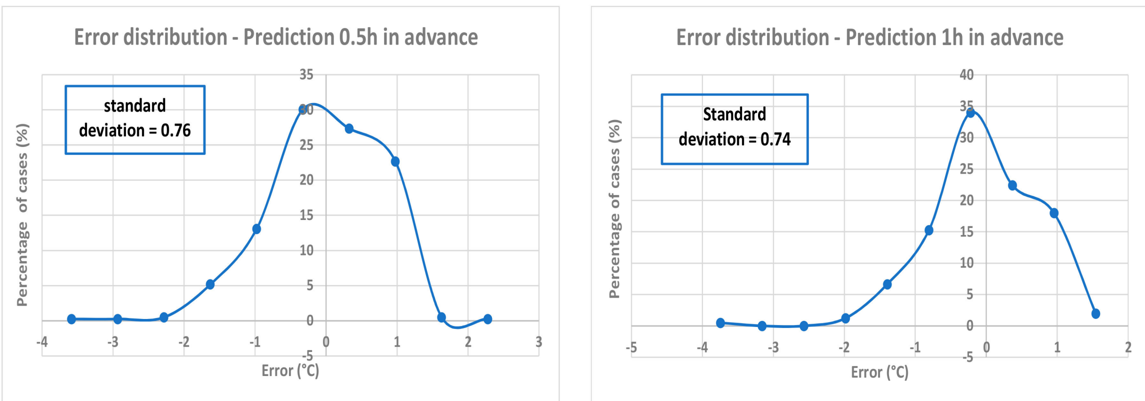

(**a**) (**b**)

Figure 7. Distribution of the error forecasting (input parameter = outdoor temperature): (**a**) prediction for 0.5 h; and (**b**) prediction for 1 h.

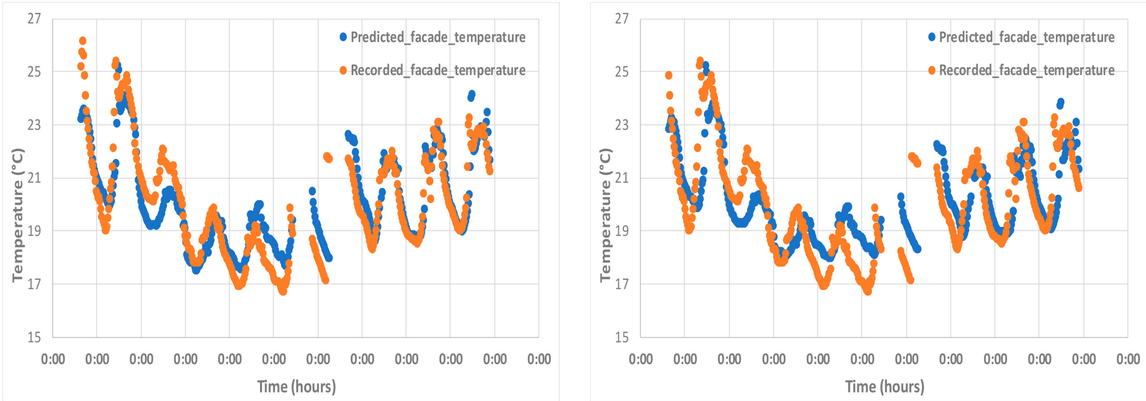

(**a**) (**b**)

Figure 8. Recorded and predicted facade temperature variation in the time domain: (**a**) prediction for 2 h; (**b**) prediction for 4 h.

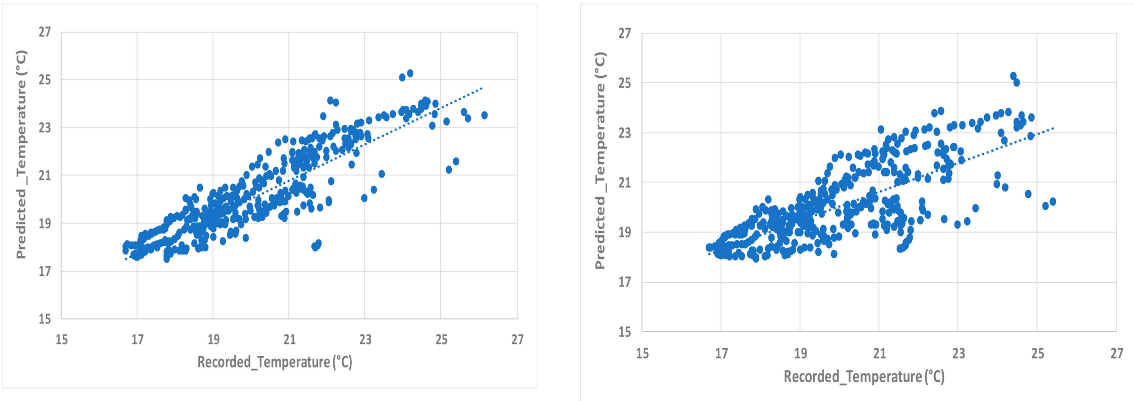

(**a**) (**b**)

Figure 9. Predicted facade temperature with the recorded facade temperature (input parameter = outdoor temperature): (**a**) prediction for 2 h; and (**b**) prediction for 4 h.

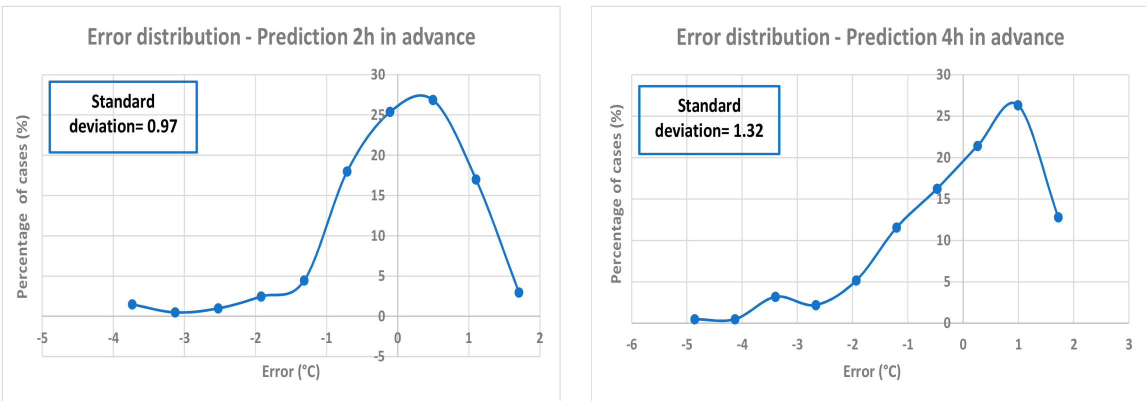

(**a**) (**b**)

Figure 10. Distribution of error forecasting (input parameter = outdoor temperature): (**a**) prediction for 2 h; and (**b**) prediction for 4 h.

Table 5. Performances of the forecasting models (input parameter = outdoor temperature)

Model	Time	*R*	*MSE*
1	+0.5 h	0.9560	0.436900
2	+1 h	0.9528	0.484594
3	+2 h	0.9109	0.89078
4	+4 h	0.8370	1.23783

4.2.2. Use of the Outdoor Temperature and the History of the Facade Temperature as Input Parameters

In this section, both outdoor temperature and three-hour facade temperature history are used as input parameters in the forecasting model. The forecasting model provides the temperature at 0.5, 1, 2, and 4 h. Table 6 summarizes the obtained results. The temperature forecasting is improved regarding the forecasting model using the outdoor temperature as input. This result is particularly interesting for the temperature foresting at two hours: $R = 0.957$ and $MSE = 0.3299$ to be compared with $R = 0.9109$ and $MSE = 0.89078$ obtained with the outdoor temperature as input parameter. Figure 11 shows the forecasting error distribution for two hours. It shows that about 88% of the forecasting error are less than 1 °C to be compared with 70% obtained with the previous model.

The four-hour foresting is still weak with $R = 0.852$; $MSE = 1.0533$. About 68% of the forecasting error are less than 1 °C (Figure 11).

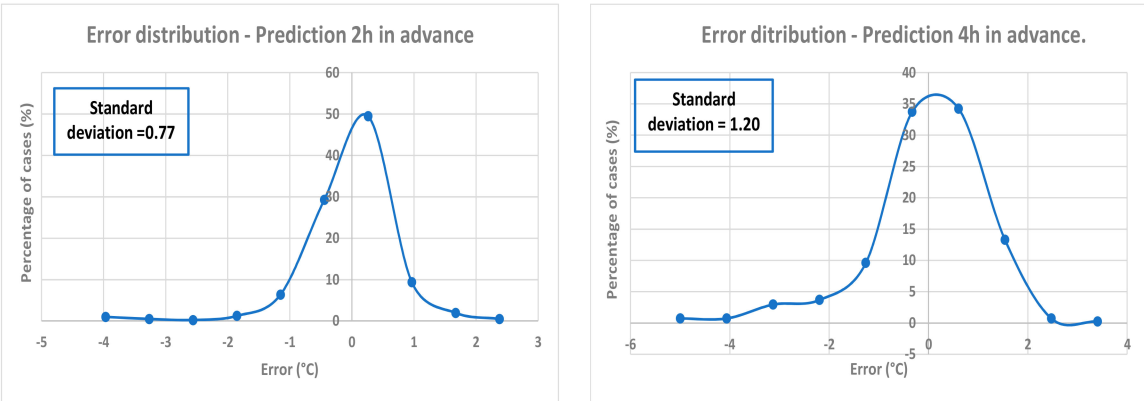

(**a**) (**b**)

Figure 11. Distribution of error forecasting (input parameter = outdoor temperature and 3-h facade temperature): (**a**) prediction for 2 h; and (**b**) prediction for 4 h.

Table 6. Performances of the forecasting models (input parameters = outdoor temperature and three-hour facade temperature)

Model	Time	*R*	*MSE*
1	+0.5 h	0.992	0.0701
2	+1 h	0.982	0.1515
3	+2 h	0.957	0.3299
4	+4 h	0.852	1.0533

4.3. Indoor Temperature Forecasting (Room Center)

The ANN approach is used for forecasting the temperature at the room center considering only the facade temperature as input parameter. Figure 12 shows a comparison of 'predicted' and 'recorded' indoor temperatures. A good agreement is observed between recorded temperature and ANN prediction with $R = 0.951$; $MSE = 0.1679$. Only 1% of data has an error greater than 1 °C (Figure 13).

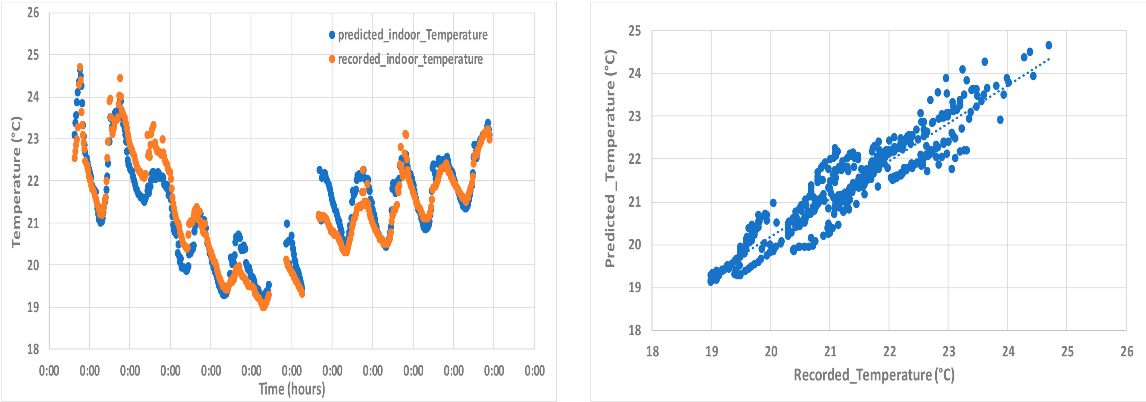

(**a**) (**b**)

Figure 12. Predicted and recorded indoor temperatures: (**a**) the variation of both temperatures in time domain; and (**b**) the predicted indoor temperature with the recorded indoor temperature.

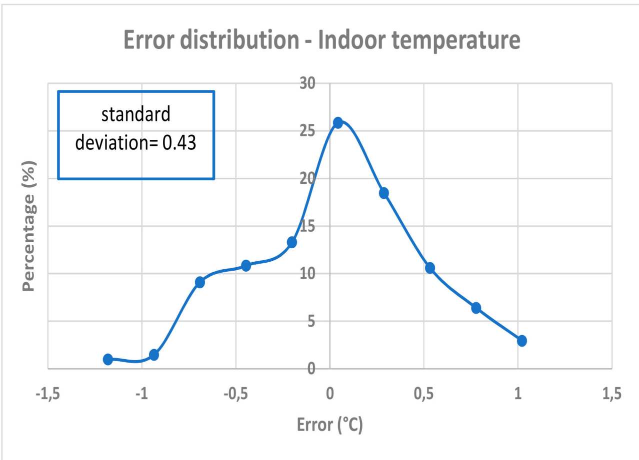

Figure 13. Distribution of error forecasting for indoor temperature (input parameters = facade temperature).

5. Discussion of Results

Relevance analysis and ANN modeling using different sets of input parameters showed that the indoor temperature forecasting could be conducted with good precision considering only outdoor temperature and indoor facade temperature history. Indeed, the influence of solar radiation, humidity, and outdoor temperature history in the forecasting model could be neglected. The prediction of the facade temperature was conducted with different inputs parameters and for different forecasting times. In the example presented in this paper, predictions were good up to two hours. The four-hour prediction gave unsatisfactory results with $R = 0.852$; $MSE = 1.0533$.

Indoor temperature forecasting was successfully conducted using the facade temperature. Available data did not include indoor activities. The presence of significant indoor activities—such as meetings, use of energy consuming devices, as well as opening doors and windows—could significantly affect the energy balance in the room. If these activities are significant, they should be monitored and included in the forecasting model.

6. Conclusions

This paper proposed a methodology for the development of a simplified ANN-based model for forecasting indoor temperature. The methodology includes two steps. The first step concerns the forecasting of the indoor facade temperature considering outdoor and indoor conditions, while the second step concerns the prediction of the temperature at the room center considering only the indoor facade temperature.

This paper shows that both relevance analysis and the use of different sets of input parameters could lead to a simplified forecasting model with restricted input parameters. This methodology was illustrated through its application to data collected in an old building. Data included outdoor and indoor temperature and humidity, as well as solar radiation. Analyses showed that two-hour facade temperature forecasting could be conducted with good precision using only the outdoor temperature and three-hour facade temperature history. This result could not be generalized. However, the proposed methodology could be used for other situations by using first only temperature sensors for measuring the outdoor and the indoor facade temperatures. Concerning the second step, the ANN model gave good forecasting of the temperature at the room center in considering only the facade temperature. Available data did not include indoor activities. The presence of significant indoor activities should be considered in the forecasting model.

Acknowledgments: This research received funding by the University of Lille, the French University Agency (AUF) and the Lebanese National Council for Scientific Research CNRS-L.

Author Contributions: Nivine Attoue and Isam Shahrour conceived and designed the experiments; Nivine Attoue performed the experiments; Nivine Attoue, Isam Shahrour and Rafic Younes analyzed the data; Nivine Attoue and Isam Shahrour wrote the paper.

Conflicts of Interest: The authors declare no conflict of interest.

References

1. Holz, R.; Hourigan, A.; Sloop, R.; Monkman, P.; Krarti, M. Effects of standard energy conserving measures on thermal comfort. *Build. Environ.* **1997**, *32*, 31–43. [CrossRef]
2. Tham, K.W.; Ullah, M.B. Building energy performance and thermal comfort in Singapore. *ASHRAE Trans.* **1993**, *99*, 308–321.
3. Huebner, G.M.; McMichael, M.; Shipworth, D.; Shipworth, M.; Durand-Daubin, M.; Summerfield, A. The reality of English living rooms, a comparison of internal temperatures against common model assumptions. *Energy Build.* **2013**, *66*, 688–696. [CrossRef]
4. Nguyen, J.L.; Schwartz, J.; Dockery, D.W. The relationship between indoor and outdoor temperature, apparent temperature, relative humidity and absolute humidity. *Indoor Air* **2014**, *24*, 103–112. [CrossRef] [PubMed]
5. Hens, H.; Parijs, W.; Deurinck, M. Energy consumption for heating and rebound effects. *Energy Build.* **2010**, *42*, 105–110. [CrossRef]
6. Shao, X.; Ma, X.; Li, X.; Liang, C. Fast prediction of non-uniform temperature distribution: A concise expression and reliability analysis. *Energy Build.* **2017**, *141*, 295–307. [CrossRef]
7. Ruano, A.E.; Crispim, E.M.; Conceição, E.Z.E.; Lucio, M.M.J.R. Prediction of building's temperature using neural networks models. *Energy Build.* **2006**, *38*, 682–694. [CrossRef]
8. Fang, P.; Liu, T.; Liu, K.; Zhang, Y.; Zhao, J. A Simulation model to calculate temperature distribution of an air-conditioned room. In Proceedings of the 2016 8th International Conference on Intelligent Human-Machine Systems and Cybernetics, Hangzhou, China, 27–28 August 2006.
9. Jigang, Z. *Study on the Airflow & Temperature Field Characteristics in the Room with Wall Air Conditioner and on the Human Thermal Comfort*; Shandong University: Jinan, China, 2007.
10. Funahashi, K. On the approximate realization of continuous mappings by neural networks. *Neural Netw.* **1989**, *2*, 183–192. [CrossRef]
11. Hornik, K.; Stinchcombe, M.; White, H. Multilayer feed forward networks are universal approximators. *Neural Netw.* **1989**, *2*, 359–366. [CrossRef]
12. Girosi, F.; Poggio, T. Networks and the Best Approximation Property. *Biol. Cybern.* **1990**, *63*, 169–176. [CrossRef]
13. Soleimani-Mohseni, M.; Thomas, B.; Fahlén, P. Estimation of operative temperature in buildings using artificial neural network. *Energy Build.* **2006**, *38*, 635–640. [CrossRef]

14. Lu, T.; Viljanen, M. Prediction of indoor temperature and relative humidity using neural network models: Model comparison. *Neural Comput. Appl.* **2009**, *18*, 345–357. [CrossRef]
15. Zabada, S.; Shahrour, I. Analysis of Heating Expenses in a Large Social Housing Stock Using Artificial Neural Networks. *Energies* **2017**, *10*, 2086. [CrossRef]
16. Aljer, A.; Loriot, M.; Shahrour, I.; Benyahya, A. Smart system for social housing monitoring. In Proceedings of the 2017 Sensors Networks Smart and Emerging Technologies (SENSET), Beirut, Lebanon, 12–14 September 2017; IEEE: Piscataway, NJ, USA, 2017. [CrossRef]
17. Attoue, N.; Shahrour, I.; Younes, R.; Aljer, A.; Loriot, M. Analysis of Buildings Energy Losses Using Smart Monitoring. In Proceedings of the International Work-Conference on Time Series (ITISE 2017), Granada, Spain, 18–20 September 2017.
18. Khayatian, F.; Sarto, L.; Dall'O, G. Application of neural networks for evaluating energy performance certificates of residential buildings. *Energy Build.* **2016**, *125*, 45–54. [CrossRef]
19. Mba, L. *Modélisation du Comportement Thermique du Bâtiment: Application d'une Méthode Neuronale*; Université de Douala-Cameroun: Douala, Cameroon, 2009.
20. Mba, L.; Kemajou, A.; Meukam, P. Application of artificial neural network for modeling the thermal behavior of building in humid region. Presented at the Actes des 3ème Rencontres EG@, Yaoundé, Cameroun, 14–16 Septembre 2010.
21. Brano, V.L.; Ciulla, G.; Falco, M.D. Artificial neural networks to predict the power output of PV panel. *Int. J. Photoenergy* **2014**, *2014*, 193083. [CrossRef]
22. Kemajou, A.; Mba, L.; Meukam, P. Application of artificial neural network for predicting the indoor air temperature in modern building in humid region. *Br. J. Appl. Sci. Technol.* **2012**, *2*, 23–34. [CrossRef]
23. Manssouri, T.; Sahbi, H.; Manssouri, I.; Boudad, B. Utilisation d'un modèle hybride base sur la rlms et les rna-pmc pour la prédiction des paramètres indicateurs de la qualité des eaux souterraines cas de la nappe de Souss-Massa-Maroc. *Eur. Sci. J.* **2015**, *11*, 35–46.
24. Paudel, S.; Elmtiri, M.; Kling, W.L.; Le Corre, O.; Lacarrière, B. Pseudo dynamic transitional modeling of building heating energy demand using artificial neural network. *Energy Build.* **2014**, *70*, 81–93. [CrossRef]
25. Tasadduq, I.; Rehman, S.; Bubshait, K. Application of neural networks for the prediction of hourly mean surface temperatures in Saudi Arabia. *Renew. Energy* **2002**, *25*, 545–554. [CrossRef]
26. Said, S.M. Degree-day base temperature for residential building energy prediction in Saudia Arabia. *ASHRAE Trans.* **1992**, *98*, 346–353.
27. Ding, Y.; Zhang, Q.; Yuan, T.; Yang, K. Model input selection for building heating load prediction: A case study for an office building in Tianjin. *Energy Build.* **2018**, *159*, 254–270. [CrossRef]
28. Ferrari, S. Building envelope and heat capacity: Re-discovering the thermal mass of winter energy savings. In Proceedings of the 28th AIVC Conference, Crete, Greece, 27–29 September 2007.
29. Gagliano, A.; Patania, F.; Nocera, F.; Signorello, C. Assessment of the dynamic thermal performance of massive buildings. *Energy Build.* **2014**, *72*, 361–370. [CrossRef]
30. Ulgen, K. Experimental and theoretical investigation of effects of walls' thermos-physical properties on time lag and decrement factor. *Energy Build.* **2002**, *34*, 273–278. [CrossRef]